



Schulich
MEDICINE & DENTISTRY

ONCOLOGY RESEARCH AND EDUCATION DAY 2024

Categories: Fundamental Cancer Research, Cancer Imaging & Medical Physics, Clinical Oncology (Medical, Radiation, Surgical, Hematology, Gynecological Oncology)



Plenary Speaker
Dr. Charles Gawad
Stanford University

13
JUNE
2024
08:30 - 5:30PM
LAMPLIGHTER INN, LONDON

Oncology Talks by:

Dr. Danilo Giffoni, Dr. Joelle Helou,
Dr. Saman Maleki, Dr. Armen Parsyan,
Dr. Jason Vickress



Registration
Link



20th Annual Oncology Research & Education Day

Co-Chairs: Ana Lohmann MD. PhD. and Vanessa Dumeaux PhD.

Thursday, June 13, 2024 8:30 AM – 5:30 PM

(Breakfast starts at 7:45 am)

Best Western Lamplighter Inn, Crystal Ballroom, Regency Room, Chelsea Room, and Atrium
591 Wellington Rd. S., London, Ontario, N6C4R3

AGENDA

Overall Learning Objectives:

By the end of this program, participants will be able to:

1. To review contributions from different oncology disciplines, including medical oncology, radiation oncology, surgery, and medical biophysics, to a comprehensive cancer treatment approach;
2. Discuss and assess cutting-edge research in oncology, including novel methodologies for studying cancer at the cellular level and the implications for treatment resistance and patient care;
3. Appraise research findings and demonstrate how collaboration bridge clinical and basic science research in oncology.

7:45 – 9:00	REGISTRATION AND OPENING REMARKS <i>Atrium & Crystal Ballroom</i>
 7:45	Registration and Breakfast Please register and enjoy a light breakfast while networking with colleagues.
8:30	Welcome and Opening Remarks Ana Lohmann MD. PhD. and Vanessa Dumeaux, PhD. - Conference Co-Chairs Michael Ott MD. FRCS(C). - Chair/Chief, Department of Oncology Kirk Baines – Philanthropist & Founder of the Baines Centre for Translational Cancer Research
9:00 – 9:30	ONCOLOGY TALKS <i>Crystal Ballroom</i>
9:00	Experimental Oncology: Translating Science into Survival Division of Experimental Oncology – Saman Maleki PhD. Learning Objectives: 1. To describe how to transform immune cold tumors to immune hot via induction of DNA repair damage in tumor cells; 2. The describe the role of gut microbiome in anti-tumor immune response; 3. To describe how modifying the gut microbiome to increase the effectiveness of immunotherapy in patients.
9:15	Is Anthracycline Chemotherapy Essential in the Treatment of Women with Breast Cancer? Division of Medical Oncology - Danilo Giffoni MD. FRCP(C). Learning Objectives: 1. Compare efficacy between anthracycline vs. non-anthracycline chemotherapy in early breast cancer; 2. Introduce treatment strategies for high-risk breast cancer; 3. Present cardiotoxicity risks induced by anthracycline.
9:30 – 10:10	MORNING ORAL PRESENTATIONS Judges: Drs. Gabriel DiMattia, Charles Gawad, and Michael Ott <i>Crystal Ballroom</i>
9:30	1. The role of immunotherapy in head and neck cancer – Mushfiq Shaikh, PhD
9:40	2. Mice deficient in RanBP9 and p53 display increased tumourigenesis – Brianna Gongga-Cave, PhD Candidate
9:50	3. Body Composition and Melanoma Outcomes in Patients on Immunotherapy or Targeted Therapy – an analysis from Canadian Melanoma Research Network - Sanji Ali, MO PGY5
10:00	4. Exploring the mutational landscape of pure ductal carcinoma in situ and its association with disease progression and response to radiotherapy – Noor Rizvi, MSc. Candidate
10:10 – 11:45 	POSTER AND NETWORKING SESSION (Odd Numbers) <i>Regency and Chelsea Conference Rooms & Atrium</i>
10:10 - 11:45	Poster Viewing and Judging (Regency and Chelsea Conference Rooms) Please enjoy refreshments and light snack (Atrium)
11:45 – 12:45	KEYNOTE LECTURE – Crystal Ballroom “Dissecting Tissue Genomes at Single-Cell Resolution” Charles Gawad MD. PhD.

	<p>Objectives: Define somatic mutation and explain how those genetic changes can contribute to diseases; Describe the tools used for single-cell sequencing and the unique information obtained from this approach compared to standard tissue-level sequencing; Define single-cell multiomics and discuss the insights into cancer biology that can be gained by studying the genome and transcriptome of the same cancer cell.</p>
12:45 – 1:45 	<p>LUNCH <i>Crystal Ballroom & Atrium</i></p>
1:45 – 2:30	<p>ONCOLOGY TALKS</p>
1:45	<p>Introducing a New Paradigm with Real-Time Adaptive Radiotherapy in London Division of Medical Biophysics – Jason Vickress PhD. MCCPM. Learning Objectives: Define Adaptive Radiotherapy in the current clinical context; 2. Examine new technologies enabling Real-Time Adaptive Radiotherapy in London; 3. Formulate future research projects for Real-Time Adaptive Radiotherapy.</p>
2:00	<p>Adapting to Changing Ideals and Evolving Essentials in Radiation Oncology Division of Radiation Oncology – Joelle Helou MD. FRCPC. Learning Objectives: 1. To review recent paradigm changes in metastatic cancer; 2. To integrate advanced technology in the changing landscape of systemic treatments and precision medicine; 3. To integrate patient values and preferences in our decision-making</p>
2:15	<p>Modern Approaches in Translational Breast Cancer Research Division of Surgery – Armen Parsyan MD. PhD. FRCSC. Learning Objectives: 1. To provide an overview describing some cutting-edge methodologies in translational breast cancer research; 2. To describe how these technologies are utilized in translational breast cancer research; 3. At the end of this session, participants will be able to describe how newly identified target molecules can potentially be utilized in breast cancer management in the future.</p>
2:30 – 3:10	<p>AFTERNOON ORAL PRESENTATIONS Judges: Drs. Gabriel DiMattia, Charles Gawad, and Michael Ott <i>Crystal Ballroom</i></p>
2:30	<p>5. Impact of macrophages on immune checkpoint inhibitor response in DNA mismatch repair-deficient neuroblastoma tumours – Megan Hong, PhD Candidate</p>
2:40	<p>6. DNA methylation profiles define new epigenetic-based pancreatic ductal adenocarcinoma subtypes – Joana Ribeiro Pinto, PhD Candidate</p>
2:50	<p>7. Analyzing the effect of neoadjuvant stereotactic ablative radiotherapy (SABR) on pancreatic tumour perfusion using computed tomography perfusion (CTP) – Jin-Young Bang, MSc. Candidate</p>
3:00	<p>8. Exploring Principles of the Interplay Between Tumour-Initiating Cells and the Tumour Microenvironment in Glioblastoma"– Alan Cieslukowski, MSc. Candidate</p>
3:10 – 4:45 	<p>POSTER & NETWORKING SESSION – (Even Numbers) <i>Regency & Chelsea Conference Rooms & Atrium</i></p>
3:10 – 4:45	<p>Poster Viewing and Judging (Regency and Chelsea Conference Rooms) Please enjoy refreshments and light snack (Atrium)</p>
4:45 – 5:30	<p>Award Ceremony</p>
4:45	<p>Presentation of Awards Michael Ott - <i>Department of Oncology, Excellence in Academic and Teaching Awards (5)</i> Morgan Black - <i>Denise Power Cancer Research Staff Award of Excellence</i> Ana Lohmann and Vanessa Dumeaux - <i>Oral and Poster Presentation Awards</i></p>
5:30	<p>Concluding Remarks and Adjournment Ana Lohmann and Vanessa Dumeaux</p>

*25% of this program is dedicated to participant interaction.

* This event is an Accredited Group Learning Activity (Section 1) as defined by the Maintenance of Certification Program of the Royal College of Physicians and Surgeons of Canada, and approved by Continuing Professional Development, Schulich School of Medicine & Dentistry, Western University. You may claim a maximum of **XX** hours (credits are automatically calculated).

*This program has received an educational grant or in-kind support from; Silver Sponsors: AbbVie, Agendia, AstraZeneca, Astella, Eisai, EMD Sereno, GSK, Ipsen, Janssen, Jazz Pharmaceuticals, Knight Therapeutics, Lilly, Merck, Novartis, Pfizer, Roche. Bronze Sponsors: BeiGene, Gilead, Takeda



Charles Gawad

Associate Professor of Pediatrics (Hematology/Oncology)

Pediatrics - Hematology & Oncology

CLINICAL OFFICES

- **Pediatric Hematology and Oncology**

725 Welch Rd

MC 5798

Palo Alto, CA 94304

Tel (650) 497-8953

Fax (650) 497-8959

Bio

BIO

Our lab works at the interface of biotechnology, computational biology, cellular biology, and clinical medicine to develop and apply new tools for characterizing genetic variation across single cells within a tissue with unparalleled sensitivity and accuracy. We are focused on applying these technologies to study cancer clonal evolution while patients are undergoing treatment with the aim of identifying cancer clonotypes that are associated with resistance to specific drugs so as to better understand and predict treatment response. We are also applying these methods to understand how more virulent pathogens emerge from a population of bacteria or viruses with an emphasis on developing a deeper understanding of how antibiotic resistance develops.

CLINICAL FOCUS

- Pediatric Hematology-Oncology
- Hematologic Malignancies

ACADEMIC APPOINTMENTS

- Associate Professor, Pediatrics - Hematology & Oncology
- Faculty Fellow, Sarafan ChEM-H
- Member, Stanford Cancer Institute

HONORS AND AWARDS

- Investigator, Chan Zuckerberg Biohub (2019-2024)
- Taube Distinguished Scholar for Pediatric Oncology, Stanford (2019-2024)
- New Innovator Award, Office of Director, National Institutes of Health (2018-2023)
- Career Award for Medical Scientists, Burroughs Wellcome Fund (2015-2020)
- Special Fellow, Leukemia and Lymphoma Society (2013-2016)
- Fellow Basic Research Scholar, American Society of Hematology (2013-2015)
- Advanced Residency Training Program, Stanford (2011-present)

- Fellowship for Medical Students Continued Support Award, HHMI (2003-2005)
- Cloister Scholar, HHMI-NIH (2002-2003)

BOARDS, ADVISORY COMMITTEES, PROFESSIONAL ORGANIZATIONS

- Co-Founder, Board Director, BioSkryb, Inc. (2018 - present)
- Editorial Board Member, Nucleic Acids Research Cancer (2019 - present)

PROFESSIONAL EDUCATION

- Board Certification: Pediatrics, American Board of Pediatrics (2017)
- Board Certification: Pediatric Hematology-Oncology, American Board of Pediatrics (2017)
- Residency: UCLA Pediatric Residency (2009) CA
- PhD Training: Stanford University School of Medicine - Office of Graduate Affairs - Postdoctoral Affairs (2015) CA
- Fellowship: Stanford University Pediatric Hematology Oncology Fellowship (2012) CA
- Medical Education: University of Arizona College of Medicine Office of the Registrar (2006) AZ
- PhD, Stanford University , Cancer Biology (2015)
- MD, University of Arizona , Medicine (2006)
- BS, Arizona State University , Chemistry and Microbiology (2001)

PATENTS

- Charles Gawad, Veronica Gonzalez-Pena, Robert Carter, Sivaraman Natarajan, Jason West. "United States Patent 62/881,180 Genetic Mutation Analysis"
- Charles Gawad, Jason West. "United States Patent 62/881,183 Single Cell Analysis"
- Charles Gawad, Jason West, Paul McEwan. "United States Patent 62/972,557 Phi29 Mutants and Use Thereof"
- Charles Gawad, Veronica Gonzalez-Pena, John Easton. "United States Patent WO2019148119A1 Method for Nucleic Acid Amplification"
- Charles Gawad, Siddhartha Kadia, Jason West. "United States Detection of Low Abundance Nucleic Acids", Apr 28, 2020
- Charles Gawad, Jason West, Jon Zawistowski. "United States Patent 55461-706.101 Detection of Low Abundance Viruses", Mar 31, 2020

LINKS

- Gawad Lab Website: <http://www.gawadlab.org/>

Research & Scholarship

CLINICAL TRIALS

- Genome, Proteome and Tissue Microarray in Childhood Acute Leukemia, Not Recruiting

Teaching

GRADUATE AND FELLOWSHIP PROGRAM AFFILIATIONS

- Cancer Biology (Phd Program)

Publications

PUBLICATIONS

- **Single-cell RNA sequencing distinctly characterizes the wide heterogeneity in pediatric mixed phenotype acute leukemia.** *Genome medicine* Mumme, H. L., Raikar, S. S., Bhasin, S. S., Thomas, B. E., Lawrence, T., Weinzierl, E. P., Pang, Y., DeRyckere, D., Gawad, C., Wechsler, D. S., Porter, C. C., Castellino, S. M., Graham, et al
2023; 15 (1): 83

- **Single-cell Retrieval from Clinical Cytology Slides Under Morphologic Guidance Facilitates Future Comprehensive Genomic Profiling from Paucicellular Samples**
Zhu, Y., Aragon, A., Wang, A., Gonzalez-pena, V., Gawad, C., Lowe, A.
ELSEVIER SCIENCE INC.2023: S388
- **Duplex Sequencing Uncovers Recurrent Low-frequency Cancer-associated Mutations in Infant and Childhood KMT2A-rearranged Acute Leukemia.** *HemaSphere*
Pilheden, M., Ahlgren, L., Hyrenius-Wittsten, A., Gonzalez-Pena, V., Sturesson, H., Hansen Marquart, H. V., Lausen, B., Castor, A., Pronk, C. J., Barbany, G., Pokrovskaja Tamm, K., Fogelstrand, L., Lohi, et al
2022; 6 (10): e785
- **Single-cell genome sequencing of human neurons identifies somatic point mutation and indel enrichment in regulatory elements.** *Nature genetics*
Luquette, L. J., Miller, M. B., Zhou, Z., Bohrsen, C. L., Zhao, Y., Jin, H., Gulhan, D., Ganz, J., Bizzotto, S., Kirkham, S., Hochepped, T., Libert, C., Galor, et al
2022
- **Simultaneous monitoring of disease and microbe dynamics through plasma DNA sequencing in pediatric patients with acute lymphoblastic leukemia.** *Science advances*
Barsan, V., Xia, Y., Klein, D., Gonzalez-Pena, V., Youssef, S., Inaba, Y., Mahmud, O., Natarajan, S., Agarwal, V., Pang, Y., Autry, R., Pui, C. H., Inaba, et al
2022; 8 (16): eabj1360
- **Bringing precision oncology to cellular resolution with single-cell genomics.** *Clinical & experimental metastasis*
Xia, Y., Gawad, C.
2021
- **Accurate genomic variant detection in single cells with primary template-directed amplification.** *Proceedings of the National Academy of Sciences of the United States of America*
Gonzalez-Pena, V., Natarajan, S., Xia, Y., Klein, D., Carter, R., Pang, Y., Shaner, B., Annu, K., Putnam, D., Chen, W., Connelly, J., Pruett-Miller, S., Chen, et al
2021; 118 (24)
- **Integrative genomic analyses reveal mechanisms of glucocorticoid resistance in acute lymphoblastic leukemia.** *Nature cancer*
Autry, R. J., Paugh, S. W., Carter, R. n., Shi, L. n., Liu, J. n., Ferguson, D. C., Lau, C. E., Bonten, E. J., Yang, W. n., McCorkle, J. R., Beard, J. A., Panetta, J. C., Diedrich, et al
2020; 1 (3): 329–44
- **Evaluation of Plasma Microbial Cell-Free DNA Sequencing to Predict Bloodstream Infection in Pediatric Patients With Relapsed or Refractory Cancer.** *JAMA oncology*
Goggin, K. P., Gonzalez-Pena, V. n., Inaba, Y. n., Allison, K. J., Hong, D. K., Ahmed, A. A., Hollemon, D. n., Natarajan, S. n., Mahmud, O. n., Kuenzinger, W. n., Youssef, S. n., Brenner, A. n., Maron, et al
2019
- **Sequencing the Genomes of Single Cells.** *Methods in molecular biology (Clifton, N.J.)*
Gonzalez-Pena, V. n., Gawad, C. n.
2019; 1979: 227–34
- **Single-cell RNA sequencing reveals the impact of chromosomal instability on glioblastoma cancer stem cells.** *BMC medical genomics*
Zhao, Y. n., Carter, R. n., Natarajan, S. n., Varn, F. S., Compton, D. A., Gawad, C. n., Cheng, C. n., Godek, K. M.
2019; 12 (1): 79
- **Resolving medulloblastoma cellular architecture by single-cell genomics.** *Nature*
Hovestadt, V. n., Smith, K. S., Bihannic, L. n., Filbin, M. G., Shaw, M. L., Baumgartner, A. n., DeWitt, J. C., Groves, A. n., Mayr, L. n., Weisman, H. R., Richman, A. R., Shore, M. E., Goumnerova, et al
2019; 572 (7767): 74–79
- **Murine hematopoietic stem cell activity is derived from pre-circulation embryos but not yolk sacs.** *Nature communications*
Ganuza, M. n., Chabot, A. n., Tang, X. n., Bi, W. n., Natarajan, S. n., Carter, R. n., Gawad, C. n., Kang, G. n., Cheng, Y. n., McKinney-Freeman, S. n.
2018; 9 (1): 5405
- **Measurable residual disease detection by high-throughput sequencing improves risk stratification for pediatric B-ALL.** *Blood*
Wood, B. n., Wu, D. n., Crossley, B. n., Dai, Y. n., Williamson, D. n., Gawad, C. n., Borowitz, M. J., Devidas, M. n., Maloney, K. W., Larsen, E. n., Winick, N. n., Raetz, E. n., Carroll, et al
2018; 131 (12): 1350–59

- **Pan-cancer genome and transcriptome analyses of 1,699 paediatric leukaemias and solid tumours.** *Nature*
Ma, X. n., Liu, Y. n., Liu, Y. n., Alexandrov, L. B., Edmonson, M. N., Gawad, C. n., Zhou, X. n., Li, Y. n., Rusch, M. C., Easton, J. n., Huether, R. n., Gonzalez-Pena, V. n., Wilkinson, et al
2018; 555 (7696): 371–76
- **High-resolution transcriptional dissection of in vivo Atoh1-mediated hair cell conversion in mature cochleae identifies Isl1 as a co-reprogramming factor.** *PLoS genetics*
Yamashita, T. n., Zheng, F. n., Finkelstein, D. n., Kellard, Z. n., Carter, R. n., Rosencrance, C. D., Sugino, K. n., Easton, J. n., Gawad, C. n., Zuo, J. n.
2018; 14 (7): e1007552
- **A Single-Cell Transcriptional Atlas of the Developing Murine Cerebellum.** *Current biology : CB*
Carter, R. A., Bihannic, L. n., Rosencrance, C. n., Hadley, J. L., Tong, Y. n., Phoenix, T. N., Natarajan, S. n., Easton, J. n., Northcott, P. A., Gawad, C. n.
2018; 28 (18): 2910–20.e2
- **LC3-Associated Phagocytosis in Myeloid Cells Promotes Tumor Immune Tolerance.** *Cell*
Cunha, L. D., Yang, M. n., Carter, R. n., Guy, C. n., Harris, L. n., Crawford, J. C., Quarato, G. n., Boada-Romero, E. n., Kalkavan, H. n., Johnson, M. D., Natarajan, S. n., Turnis, M. E., Finkelstein, et al
2018; 175 (2): 429–41.e16
- **Genome-wide segregation of single nucleotide and structural variants into single cancer cells.** *BMC genomics*
Easton, J. n., Gonzalez-Pena, V. n., Yergeau, D. n., Ma, X. n., Gawad, C. n.
2017; 18 (1): 906
- **Early somatic mosaicism is a rare cause of long-QT syndrome** *PROCEEDINGS OF THE NATIONAL ACADEMY OF SCIENCES OF THE UNITED STATES OF AMERICA*
Priest, J. R., Gawad, C., Kahlig, K. M., Yu, J. K., O'Hara, T., Boyle, P. M., Rajamani, S., Clark, M. J., Garcia, S. T., Ceresnak, S., Harris, J., Boyle, S., Dewey, et al
2016; 113 (41): 11555-11560
- **Single-cell genome sequencing: current state of the science** *NATURE REVIEWS GENETICS*
Gawad, C., Koh, W., Quake, S. R.
2016; 17 (3): 175-188
- **Dynamic ASXL1 Exon Skipping and Alternative Circular Splicing in Single Human Cells.** *PloS one*
Koh, W., Gonzalez, V., Natarajan, S., Carter, R., Brown, P. O., Gawad, C.
2016; 11 (10)
- **Dissecting the clonal origins of childhood acute lymphoblastic leukemia by single-cell genomics.** *Proceedings of the National Academy of Sciences of the United States of America*
Gawad, C., Koh, W., Quake, S. R.
2014; 111 (50): 17947-17952
- **Noninvasive in vivo monitoring of tissue-specific global gene expression in humans.** *Proceedings of the National Academy of Sciences of the United States of America*
Koh, W., Pan, W., Gawad, C., Fan, H. C., Kerchner, G. A., Wyss-Coray, T., Blumenfeld, Y. J., El-Sayed, Y. Y., Quake, S. R.
2014; 111 (20): 7361-7366
- **A quantitative comparison of single-cell whole genome amplification methods.** *PloS one*
de Bourcy, C. F., De Vlaminck, I., Kanbar, J. N., Wang, J., Gawad, C., Quake, S. R.
2014; 9 (8)
- **Massive evolution of the immunoglobulin heavy chain locus in children with B precursor acute lymphoblastic leukemia** *BLOOD*
Gawad, C., Pepin, F., Carlton, V. E., Klinger, M., Logan, A. C., Miklos, D. B., Faham, M., Dahl, G., Lacayo, N.
2012; 120 (22): 4407-4417
- **Circular RNAs Are the Predominant Transcript Isoform from Hundreds of Human Genes in Diverse Cell Types** *PLOS ONE*
Salzman, J., Gawad, C., Wang, P. L., Lacayo, N., Brown, P. O.
2012; 7 (2)
- **Gene Expression Arrays in Pancreatic Cancer Drug Discovery Research** *DRUG DISCOVERY IN PANCREATIC CANCER: MODELS AND TECHNIQUES*
Gawad, C., Han, H., Grippo, P.

2010: 113-134

- **Towards molecular medicine - A case for a biological periodic table** *AMERICAN JOURNAL OF PHARMACOGENOMICS*
Gawad, C.
2005; 5 (4): 207-211

Exploring the Role of Gut Microbiota on Immunologically Active Neuroblastoma Tumours

Hasti Gholami¹, Kait F. Al^{2,3}, Rene Figueredo⁴, Megan Hong¹, Jeremy P. Burton^{2,3,5}, and Saman Maleki Vareki^{1,4,6,7}

¹ Department of Pathology and Laboratory Medicine, Western University, London, ON, Canada

² Department of Microbiology and Immunology, Western University, London, ON, Canada

³ Canadian Research and Development Centre for Probiotics, Lawson Research Health Research Institute, London, ON, Canada

⁴ London Regional Cancer Program, Lawson Health Research Institute, London, ON, Canada

⁵ Division of Urology, Department of Surgery, Western University, London, ON, Canada

⁶ Department of Oncology, Western University, London, ON, Canada

⁷ Department of Medical Biophysics, Western University, London, ON, Canada

Introduction: Anti-cytotoxic-lymphocyte-associated protein-4 (anti-CTLA-4) therapy has shown promise in enhancing anti-tumour immune responses, particularly in neuroblastoma tumours made immunologically active through induced DNA mismatch repair (MMR) deficiency. Our laboratory has previously demonstrated that inducing MMR deficiency in immunologically cold neuroblastoma tumours renders them more immunogenic than their parental counterparts and promotes enhanced T-cell infiltration and diminished growth in immunocompetent mice. Recent data highlights the substantial role of host-specific factors, particularly the gut microbiota, in shaping therapeutic outcomes. This extends beyond tumour genomics, with preclinical and clinical evidence suggesting that the gut microbiota can modulate anti-tumour immunity and the efficacy of immunotherapies. Therefore, this study elucidates the complex interplay between the gut microbiota and the immune landscape of immunologically hot neuroblastoma tumours, offering insights into their interactions in the context of induced MMR deficiency (idMMR).

Methods: To investigate the role of the gut microbiota in idMMR neuro-2a (N2a) tumour progression and immune phenotype of tumours, immunocompetent 6-8-week-old female A/J mice were either administered phosphate-buffered saline (PBS) or an antibiotic cocktail (ABX) comprising ampicillin, metronidazole, vancomycin, and neomycin consecutively for ten days. Subsequently, mice were subcutaneously inoculated with N2a cells. Once tumours were palpable, both PBS- and ABX-treated groups were intraperitoneally administered 200µg of anti-CTLA-4 every three days for a total of three injections. Control mice from both PBS- and ABX-treated groups received 200µg of Syrian Hamster IgG. Tumour volumes were monitored at 2–3-day intervals. Flow cytometry was used to assess the immunophenotypes of tumour-infiltrating lymphocytes (TILs), while 16S rRNA gene sequencing was used to analyze gut microbial composition.

Results: ABX treatment led to notable gut microbiome alterations, characterized by reduced microbial diversity and evenness, within four days following the ten-day treatment period ($p < 0.005$). Furthermore, the gut microbial composition of ABX-treated hosts was significantly

altered, showing a decrease in the relative abundance of bacterial species commonly present in hosts with intact gut microbiota (permanova, $p < 0.005$). A depleted gut microbiota further promoted idMMR neuroblastoma tumour progression, evidenced by larger tumour volumes (figure 1). ABX treatment significantly reduced the presence of CD3⁺CD45⁺TILs, including both CD4⁺ and CD8⁺ subtypes. These TILs exhibited an increase in dysfunctional and exhausted CD8⁺ TIL phenotypes, as indicated by elevated expressions of PD1⁺CD38⁺ as well as PD1⁺CD39⁺, PD1⁺LAG3⁺, PD1⁺TIM3⁺, TIM3⁺CD39⁺, and TIM3⁺LAG3⁺ cells, respectively. Interestingly, treatment with anti-CTLA-4 therapy not only counteracted the detrimental effects of microbiota depletion on tumour size, but also fostered immune memory in responsive hosts, irrespective of previous PBS or ABX treatment (figure 1).

Conclusions: This study underscores the critical influence of gut microbiota on the progression and immune response of idMMR N2a tumours, highlighting the interaction between microbiota depletion and enhanced tumour growth alongside diminished efficacy of tumour-specific T-cell populations. These alterations contribute to increased T-cell exhaustion and dysfunctionality and suggest a significant modulation of the tumour immune microenvironment by the gut microbiota, potentially affecting the sensitivity to immunotherapy. Our findings advance the understanding of gut microbiota's complex role in shaping the tumour immune microenvironment and potential effects on cancer immunotherapy.

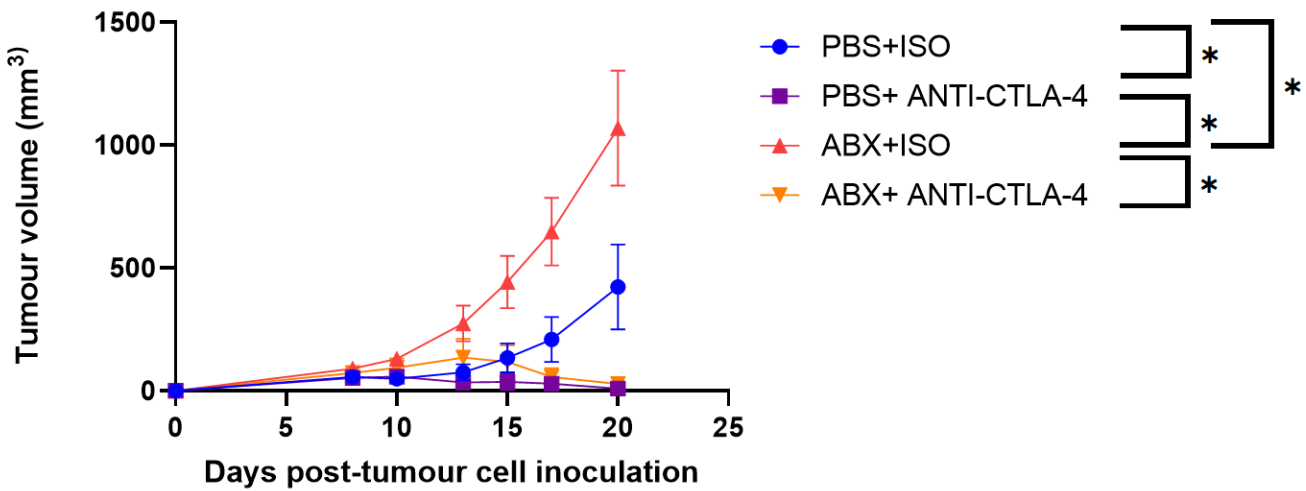


Figure 1. A depleted gut microbiota promotes idMMR neuroblastoma (N2a) tumour progression, but anti-CTLA-4 overcomes this effect. A/J mice were administered an antibiotic cocktail consisting of 1 mg/mL ampicillin, 1 mg/mL neomycin, 0.5 mg/mL vancomycin, and 1 mg/mL metronidazole to modulate their gut microbiota ($n=12$) or phosphate-buffered saline (PBS) ($n=12$). A four-day ABX withdrawal period was given, after which idMMR N2a cells (5×10^5) were inoculated. Once tumours were palpable, PBS- and ABX-treated mice received three intraperitoneal doses of 200 μ g of Syrian Hamster isotype IgG (ISO) or Anti-cytotoxic-lymphocyte-associated protein-4 (CTLA-4) every three days ($n=6$ for each paired treatment). Tumour volumes in idMMR N2a-mice across PBS+ISO-, PBS+Anti-CTLA-4-, ABX+ISO-, and ABX+Anti-CTLA-4-treated groups were monitored every 2-3 days upon palpable tumour detection.

Mice deficient in RanBP9 and p53 display increased tumorigenesis

Brianna C. Gongga-Cavé^{1,2}, Gabriel Onea^{1,2}, Patti Kaiser³, Xu Wang¹, Caroline Schild-Poulter^{1,2,*}

¹Robarts Research Institute, University of Western Ontario, London, ON N6A 5B7, Canada, ²Department of Biochemistry, Schulich School of Medicine and Dentistry, University of Western Ontario, London, ON N6G 2V4, ³Department of Pathology, Schulich School of Medicine and Dentistry, University of Western Ontario, London, ON N6G 2V4

Introduction: RAN binding protein 9 (RanBP9) is a scaffolding protein best known for its role as a core member within a multi-subunit E3 ubiquitin ligase termed the C-terminal to Lis-1 homology (CTLH) complex. Multiple groups have identified the CTLH complex in regulating a broad range of biological processes including cell cycle, cell proliferation, and metabolism. Various studies have demonstrated that RanBP9 functions as a tumour suppressor, but none have shown whether the loss of RanBP9 can initiate spontaneous tumour formation. Here, we investigated the tumour-suppressive role of RanBP9 in mice.

Methods: We initially conducted an observational study in C57BL/6 mice with *RanBP9*^{+/-} and *RanBP9*^{-/-} genotype. In addition, bulk RNA sequencing (RNA-seq) analysis of 1-month-old *RanBP9*^{-/-} mice liver was performed. We conducted a second observational study in C57BL/6 mice with *RanBP9*^{+/-}: *Trp53*^{+/-} (DKO^{+/-}) and *RanBP9*^{-/-}: *Trp53*^{-/-} (DKO^{-/-}) genotypes. These mice were monitored over 17 months for the development of spontaneous tumours. The primary endpoint was defined as the development of a visible mass (>1.5 cm) or symptoms of cancer. Tumour biopsies were collected and subjected to immunohistopathological analysis. Samples were assessed by a pathologist to classify tumours and evaluate tumour burden.

Results: A total of 19 *RanBP9*^{+/-} and 29 *RanBP9*^{-/-} mice were generated for the initial observational study. RNA-seq analysis identified an upregulation of several oncogenic signalling genes. *RanBP9*^{-/-} mice displayed a shortened lifespan, but never developed spontaneous tumours. DKO^{+/-} mice (n=23) developed sarcomas at an earlier time compared to control *Trp53*^{+/-} mice (n=18; p<0.05). DKO^{-/-} mice (n=5) had a shorter median survival of 28 weeks compared with 36.5 weeks for control *Trp53*^{-/-} mice (n=6). Both DKO^{+/-} and DKO^{-/-} mice displayed altered tumour spectrum compared to control mice with increased frequency in hemangiosarcoma development.

Discussion: Our data indicates that the ablation of RanBP9 alone is insufficient to initiate tumour development. However, the combination of RanBP9 and p53 loss led to increased sarcoma development. Ongoing efforts are to further characterize DKO^{+/-} and DKO^{-/-} tumours and elucidate the mechanism to understand how the loss of RanBP9 contributes to sarcoma development in the absence of p53. Together, our findings may support the development of anti-cancer therapeutics that target RanBP9-CTLH complex activity.

Body Composition and Melanoma Outcomes in Patients on Immunotherapy or Targeted Therapy – an analysis from Canadian Melanoma Research Network

Sanji Ali¹, Thiago Muniz², Samir Fasih¹, Margeurite Ennis³, Scott Ernst^{1,4} & Ana Elisa Lohmann¹

1- London Health Sciences Center (LHSC), University of Western Ontario (UWO)

2- Princess Margaret Cancer Center (PMCC)

3- Biostatistician, Markham, Ontario, Canada

4- Canadian Melanoma Research Network

Funding: Catalyst

Introduction: Obesity, measured by body mass index (BMI), is associated with better outcomes in metastatic melanoma patients treated with immunotherapy and targeted therapy¹. Since BMI does not differentiate between adipose tissue and lean mass, other methods need to be utilized to understand the relationship between body composition and treatment outcomes in melanoma¹⁻⁷. This study aimed to analyze the association between body composition and outcomes in patients with advanced melanoma by measuring adiposity from computed tomography (CT) done prior to initiation of systemic treatment.

Methods: This is a retrospective population-based cohort study including patients diagnosed with unresectable loco-regional or metastatic melanoma registered in the Canadian Melanoma Research Network registry. CT scans were examined via a validated software (AUTOMATICA) to assess visceral adipose tissue (VAT), subcutaneous adipose tissue (SAT), intermuscular adipose tissue (IMAT) and skeletal muscle index (SMI). Kaplan-Meier estimates of the probability of survival outcomes were plotted. Log-rank tests were used to test for differences in survival by different categories. Analyses were performed using the R software (R core team 2023).

Results: In total, 170 patients treated at PMCC and LHSC between 2020 and 2022 met the eligibility criteria and were included in the study. Overall, there were 110 (64.7%) male and 60 (35.3%) females. 62.4% (106) patients were treated with either single agent or combination immunotherapy and 37.6% (64) were treated with targeted therapy. Most of the patients (152, 89.4%) were ECOG 0 or 1. Most patients (120, 70.6%) had a BMI of less than 30 and mean BMI was 28.1 with SD of ± 6.5 . VAT surface area mean was 165.9 cm². Low VAT (<86.7cm²) was associated with better progression free survival (p-value 0.083) and overall survival (p-value 0.03). Survival outcomes for low SAT did not indicate a significant difference, with a p-value of 0.57 for progression free survival and a p-value of 0.45 for overall survival.

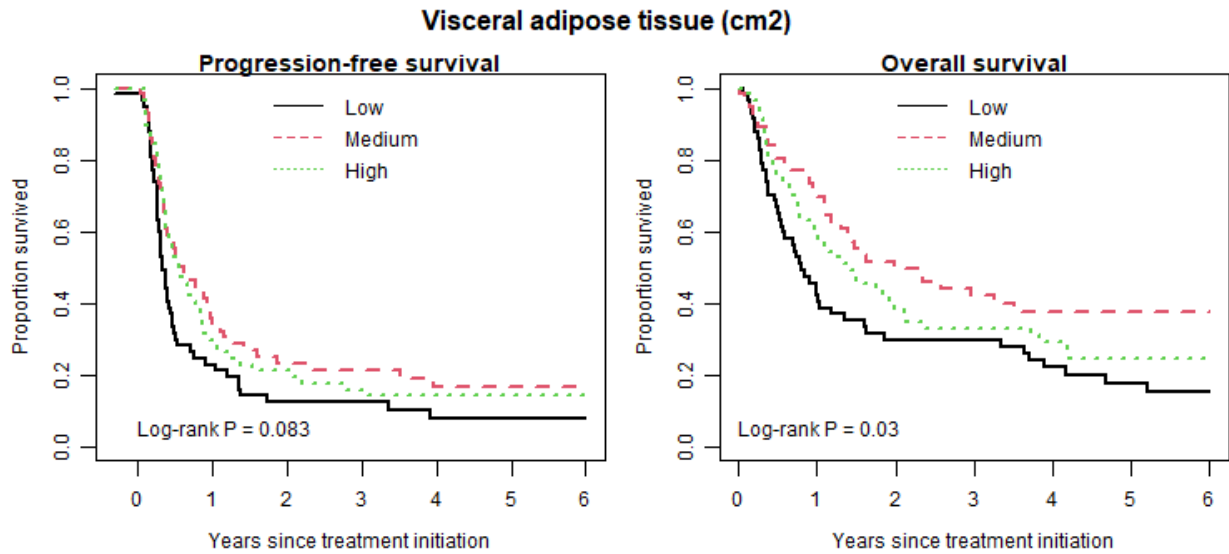


Figure 1. Progression free survival and overall survival Kaplan-Meier curves for low, medium and high visceral adipose tissue distribution.

Conclusions: On initial analysis, lower VAT was associated with better survival outcomes in patients treated with immunotherapy or targeted therapy. SAT and IMAT were not associated with any statistically improved outcomes. However, additional results and analyses will be available on Research & Education day.

Exploring the mutational landscape of pure ductal carcinoma in situ and its association with disease progression and response to radiotherapy

Noor Rizvi¹, Eliseos J. Mucaki^{1,2}, Emily L. Salmini¹, Sharon Nofech-Mozes³, Michael Hallett^{1,4,5}, Eileen Rakovitch³, Vanessa Dumeaux^{1,2,4,5}

¹Department of Biochemistry, Western University; ²Department of Anatomy and Cell Biology, Western University; ³Sunnybrook Health Sciences Centre, Odette Cancer Centre, Toronto ON; ⁴Department of Oncology, Western University, ⁵Centre for Translational Cancer Research, Western University.

Background: Ductal Carcinoma in Situ (DCIS) poses significant challenges in breast cancer management due to the absence of reliable markers for predicting progression to invasive disease. Although the typical treatment involves breast-conserving surgery followed by radiation therapy (RT), this approach often leads to overtreatment, as not all DCIS cases advance to an invasive stage. Our study aims to use genetic information from DCIS tumors to predict disease progression and RT response, thereby refining clinical decision-making and enhancing patient outcomes.

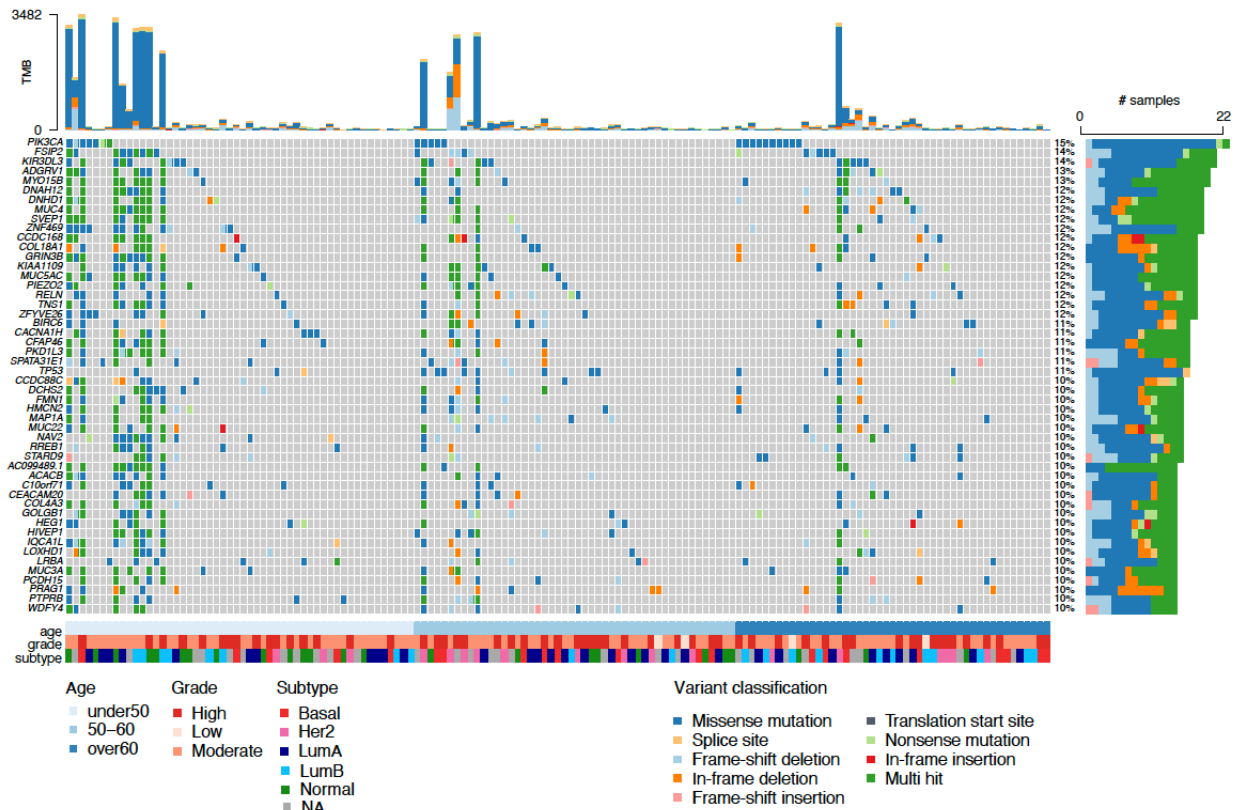
Methods: We established an Ontario population-based cohort of women diagnosed with pure DCIS from 1994-2003, treated with surgery with or without RT and followed for 10 years. DNA was extracted from tumor and matched normal FFPE tissue blocks for whole-exome sequencing (n=174 patients). A deep learning approach was used for variant identification, leveraging results from six distinct variant callers and facilitating driver gene discovery.

Results: Initial analysis identified the most frequently mutated genes in our cohort, such as *PIK3CA* and *TP53*, which are prevalent in invasive breast cancer but less so in this cohort of pure DCIS tumors (approximately 10%, **Figure 1**). We also found mutations commonly affecting genes related to cell polarity, adhesion, glycosylation, and extracellular matrix structure (**Figure 1**). Specific variants showed strong correlations with certain clinical-pathological features: younger patients (*FILP1L*, *CFAP61*, *FREM1*), high-grade tumors (*TP53*), and HER2-enriched molecular subtype (*ASH1L*, *NAGPA*, *DMD*) (p<0.001). A significant increase in mutational load and a characteristic mutational signature associated with impaired mismatch repair and microsatellite instability were found in patients under 50. Importantly, we identified 13 variants associated with poorer outcomes in RT-treated patients (log-rank test p<0.0001). These variants, frequently co-occurring, were linked to genes involved in cell polarity, migration, extracellular matrix adhesion, and immune response, highlighting their potential impact on treatment responses. Additionally, while no variants significantly predicted recurrence within 10 years in untreated patients, five variants were associated with local-recurrence free survival, regardless of treatment status.

Discussion: Our findings emphasize the importance of molecular profiling in refining DCIS treatment strategies to tailor therapies to individual patient needs. Tumors in younger patients (under 50 years) may undergo distinct mutational processes, possibly related to deficient mismatch repair, influencing the early onset of DCIS. We identified specific DNA mutations suggesting resistance to RT and associated with early recurrence post-treatment. Factors such

as cell polarity, migration, extracellular matrix adhesion, and immune responses are crucial in determining disease behavior and response to RT. Overall, these insights have the potential to significantly enhance the precision of clinical management for patients with non-invasive breast cancer.

Figure1. The top 50 most frequent non-synonymous small variants identified in pure DCIS lesions. Samples are in columns and variants are color-coded based on their classification. The tumor mutational burden of each lesion is displayed on top. The samples are organized according to the age of diagnosis. Grade and subtype of each lesion are also depicted at the bottom.



Title: Impact of macrophages on immune checkpoint inhibitor response in DNA mismatch repair-deficient neuroblastoma tumours

Megan M Y Hong¹, Rene Figueredo³, Saman Maleki Vareki¹⁻⁴

¹Department of Pathology and Laboratory Medicine, University of Western Ontario, London, Ontario, Canada

²Verspeeten Family Cancer Centre, Lawson Health Research Institute, London, Ontario, Canada

³Department of Oncology, University of Western Ontario, London, Ontario, Canada

⁴Department of Medical Biophysics, University of Western Ontario, London, Ontario, Canada

Introduction: Immune checkpoint inhibitors (ICIs) such as anti-PD1 and anti-CTLA-4 have revolutionized cancer treatment by potentiating patients' anti-tumour immune responses. The DNA mismatch repair (MMR) pathway corrects mismatched base pairs that occur during DNA replication. Notably, patients with MMR-deficient (dMMR) tumours respond better to anti-PD1 therapy compared to patients with MMR-proficient (pMMR) tumours regardless of cancer type. Although anti-PD1 monotherapy is approved for these patients, more than half do not respond, highlighting the need to understand mechanisms of resistance to provide alternative therapeutic approaches. Previously, we have shown that inducing MMR deficiency in an ICI-refractory and MMR-proficient (pMMR) neuroblastoma model renders tumours sensitive to anti-CTLA-4 therapy, but they remain unresponsive to anti-PD1 therapy. This study investigates how MMR deficiency modulates the tumour immune microenvironment and examines mechanisms driving anti-PD1 resistance and anti-CTLA-4 sensitivity in these tumours.

Methods: MMR repair deficiency was induced in the murine neuro-2a cell line by knocking out *Mlh1* expression using CRISPR/Cas9. pMMR or dMMR tumours were grown in immunocompetent syngeneic A/J mice and were treated with anti-CTLA-4 or anti-PD1. Targeted immune cell populations were depleted to assess their effects on ICI response. Tumour growth was measured followed by immunophenotyping of tumours and spleens by flow cytometry.

Results: Induced MMR deficiency in neuro-2a tumours significantly increased the presence of macrophages compared to pMMR tumours. Preliminary data suggest that depletion of macrophages in dMMR tumours can sensitize them to anti-PD1 therapy and improve overall survival. In contrast, anti-CTLA-4 efficacy in dMMR tumours depended on the presence of Ly6c^{High} macrophages that depleted regulatory T-cells through Fc-dependent mechanisms.

Conclusions: These results suggest that while the presence of macrophages in dMMR tumours can render tumours resistant to anti-PD1 therapy, they can be leveraged to improve the efficacy of Fc-dependent therapeutics such as anti-CTLA-4. In conclusion, understanding tumour immune microenvironment features that facilitate response to ICIs will enable us to choose therapeutics strategically, ultimately optimizing patient outcomes.

DNA methylation profiles define new epigenetic-based pancreatic ductal adenocarcinoma subtypes

Joana Ribeiro Pinto¹, Gun Ho Jang⁶, Brian Yan⁴, Michael Sey⁴, Nadeem Hussain⁴, Faiyaz Notta⁶, Emilie Jaune-Pons^{1,5} and Christopher Pin¹⁻³

Departments of Physiology and Pharmacology¹, Oncology², Paediatrics³, and Medicine⁴, Schulich School of Medicine & Dentistry at Western University⁵; Princess Margaret Cancer Centre⁶, Toronto ON and Baker Centre for Pancreatic Cancer Research, London ON, Canada

Introduction: Pancreatic Ductal Adenocarcinoma (PDAC) is predicted to become the second leading cause of cancer-related deaths by 2040 with a 5-year survival rate of ~12%. This dismal outcome is mostly attributed to patients being diagnosed at later disease stages decreasing surgery eligibility to 20%. Extensive genomic analysis has been performed on PDAC and identified activating KRAS mutations in >90% of patients, along with mutations in CDKN2A, p53 and SMAD4. However, these known driver mutations are not predictive of patient response and recent attempts at transcriptomic-based tumor stratification are discordant based on the technique used. The mostly accepted subtypes are “classical” and “basal” which are characterized by the expression of either GATA6 or KRT17 respectively. Even though basal tumors are classified as being more aggressive than classical tumors, these stratifications do not shed any light on PDAC adaptability mechanisms. The rapid acquired resistance is thought to involve epigenetic reprogramming leading to the repression of pathways involved in chemosensitivity. Therefore, identifying epigenetic profiles that correlate to tumor subtypes and therapeutic sensitivity may allow for the better predictive value in how PDAC tumors will respond. We hypothesize that DNA methylation profiles provide a more stable definition of tumor subtypes, which are linked to clinical characteristics and chemosensitivity.

Methods: DNA was isolated from Patient Derived Organoids (PDOs) derived either from the COMPASS cohort (n=24) or locally from endoscopic ultrasound biopsies. DNA methylation enrichment was assessed using the Illumina BeadChip EPIC array, which includes 900k regulatory sites of gene expression. DNA methylation profiles were identified using SEnSible Step-wise Analysis of DNA Methylation (SeSAME) for processing and differentially methylated regions (DMRs) were identified using the DMRich and LOLA packages for a deeper understanding of regulatory regions enrichment. The subsequent methylation profiles were then compared to corresponding transcriptomic profiles identified using whole transcriptome sequencing and DESeq2 analysis.

Results: Preliminary results showed samples could be segregated based on global DNA methylation patterns by hierarchical clustering in groups reflective of PDAC subtypes. Furthermore, transcriptomic-classification associated biomarkers were found to be targeted by DNA methylation, namely the “classical” biomarker GATA6 was found hypermethylated in “basal-like” organoids suggesting gene repression on these samples. The clustering was coherent when compared to transcriptomic-based subtyping further supporting the involvement of DNA methylation in the regulation of tumor phenotype.

Conclusions : Patient derived organoids have been established as a reliable model for targeted therapeutic studies as they consistently maintain patient characteristics. Using this model in our study identifies a more stable categorization of cancerous cells compared to transcriptomic data and epigenetic profiles that may be linked to specific clinical features. These results support the hypothesis that PDAC epigenetic programs are stable and used to identify additional therapeutic targets delivered in a patient-specific fashion.

Analyzing the effect of neoadjuvant stereotactic ablative radiotherapy (SABR) on pancreatic tumour perfusion using computed tomography perfusion (CTP)

Jin-Young Bang^{1,2}, Ting-Yim Lee^{1,3}, Stewart Gaede^{1,2}

¹Department of Medical Biophysics, Western University; ²London Regional Cancer Program, Victoria Hospital; ³Robarts Research Institute, London, ON.

Introduction: Currently, surgical resection is the sole curative option for pancreatic cancer. Unfortunately, surgery is only feasible if a patient is deemed resectable, which means that the cancer is nonmetastatic, well-localized, and has minimal involvement of the critical blood vessels around the primary tumour. Eligible patients with poor surgical prognosis due to the involvement of the surrounding vasculature, also known as the borderline resectable patients, often undergo presurgical or neoadjuvant therapy (NAT), such as neoadjuvant chemotherapy, to help reduce the tumour volume and downstage the tumour conditions for better surgical outcome. However, the highly limited blood perfusion to the pancreatic tumour still poses a significant challenge as it restricts the delivery of systemic cancer drugs to the tumour site. Therefore, the objective of this preliminary study was to assess the feasibility of administering neoadjuvant stereotactic ablative radiotherapy (SABR) to increase pancreatic tumour perfusion.

Methods: Patients with resectable (RPC) (n=1) and borderline resectable pancreatic cancer (BRPC) (n=5) underwent neoadjuvant SABR with a prescription dose to the planning target volume (PTV) ranging between 27-30 Gy in 3 fractions. A dose boost of up to 45 Gy was also given to the metabolically active areas of the tumour site indicated by positron emission tomography (PET). For each patient, computed tomography perfusion (CTP) images were acquired at baseline, 6 hours after delivering the first fraction (post-1st-fx), and 3-4 weeks post-SABR using the GE HealthCare Revolution CT scanner (GE HealthCare, Waukesha, USA). For the BRPC patients, images were also obtained after neoadjuvant chemotherapy preceding SABR. From the acquired images, a prototype deconvolution-based CTP software (GE Healthcare) was used to generate perfusion maps of hemodynamic parameters including blood flow (BF), blood volume (BV), and the permeability surface area product (PS).

Results: Relative to baseline, the average increase in the mean tumour BF observed post-1st-fx was 115% in the BRPC group, followed by a general decline at 3-4 weeks post-SABR (89%). The post-1st-fx increase in tumour BF was also observed in the RPC patient (131% relative to baseline), and it was maintained at 3-4 weeks post-SABR (129%). For PS, the BRPC patients showed an average decline of 17% post-1st-fx relative to post-chemotherapy, but no such change could be observed in the RPC patient. No general pattern could be established for BV.

Discussion: While these observations have yet to be verified with additional patient accrual, preliminary evidence from the patients enrolled to date demonstrates that neoadjuvant SABR may be a feasible option to induce a transient increase in pancreatic tumour perfusion; thus, opening a window of opportunity to overcome tumour chemoresistance by enhancing the systemic delivery of cancer drugs to the tumour site.

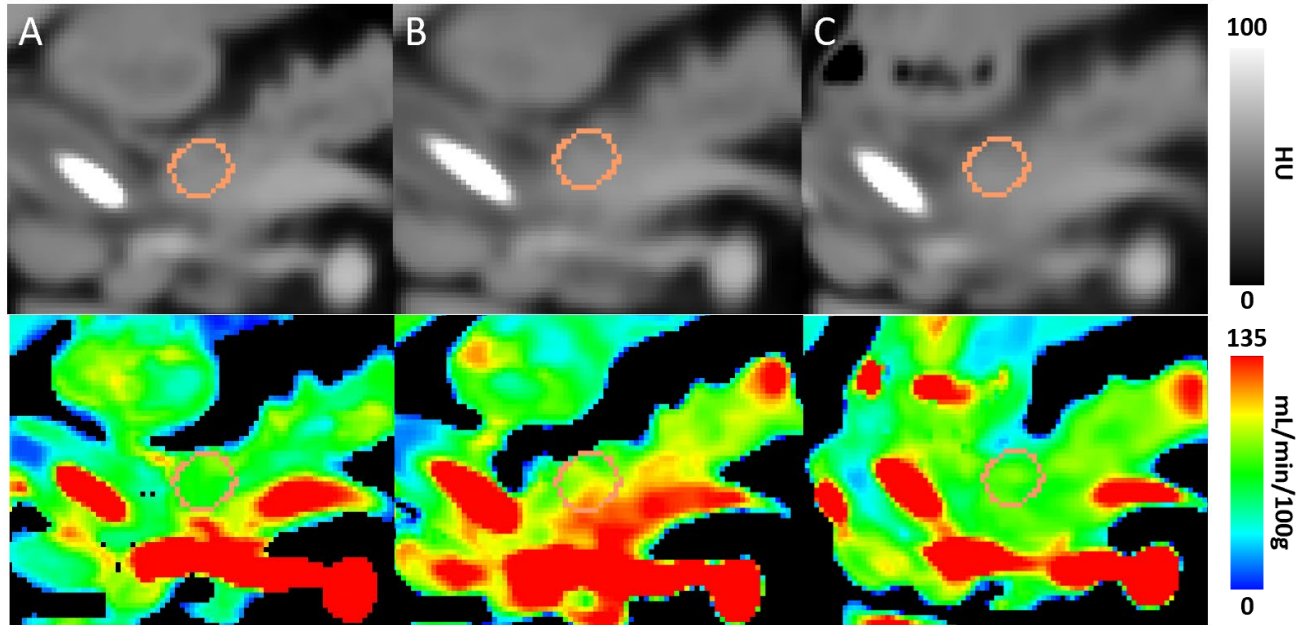


Figure 1. The top row shows the average CT scans of a resectable pancreatic cancer (RPC) patient acquired at A) baseline, B) 6 hours after the first fraction of neoadjuvant SABR, and C) 3-4 weeks post-SABR. The scans were non-rigidly registered to the baseline. The orange ROI was drawn within the gross tumour volume (GTV). The bottom row illustrates the corresponding blood flow (BF) maps generated by the CTP software at each study instance.

Exploring principles of the interplay between tumour-initiating cells and the endothelial component in glioblastoma.

Alan Cieslukowski¹, Dorota Lubanska¹, Elizabeth Fidalgo da Silva¹, Mohamed AR Soliman^{2,3}, Abdalla Shamisa⁴, Ana deCarvalho⁵, Swati Kulkarni⁴, Lisa A. Porter¹

¹ Department of Biomedical Sciences, University of Windsor, Windsor, ON, Canada; ² Department of Neurosurgery, Faculty of Medicine, Cairo University, Cairo, Egypt; ³ Department of Neurosurgery, Jacobs School of Medicine and Biomedical Sciences, University at Buffalo, Buffalo, NY, USA ; ⁴ Schulich School of Medicine and Dentistry, Western University, Windsor, ON, Canada; ⁵ Department of Neurosurgery, Henry Ford Hospital, Detroit, MI, 48202, USA

Introduction: Efficient targeting of multiple components of a tumour might be a successful strategy in aggressive types of cancer such as glioblastoma (GBM), which for decades now, remains the most common and malignant primary brain tumour with an extremely poor patient survival of less than 15 months¹. The significant therapeutic challenge posed by GBM stems from its genetic and phenotypic heterogeneity fueled by multiple components of the tumour biology including aggressive and treatment-resistant populations of Tumour Initiating Cells (TICs) and high levels of angiogenesis contributing to tumour evolution, evasion of therapy and recurrence. TICs, which are at the source of GBM patient relapse, thrive in the niches close to the blood vessels where they interact with endothelial cells (ECs), exit the cell cycle, and evade therapies². TICs can be identified by the presence of two well-established cell surface markers- CD133 and CD44. Targeted antiangiogenic drugs, preventing the recruitment of new blood vessels by GBM cells, only display efficacy in 50% of patients and hold temporary effectiveness due to acquired secondary resistance by the tumour suggesting there is an urgent need for new and effective therapeutic strategies². This project will explore the TIC-EC interplay and its role in propagating tumour aggressiveness and therapy resistance.

Methods: This project investigates the impact of ECs on the aggressive characteristics of individual, specific populations of TICs using GBM patient-derived systems, including 3D organoid models and zebrafish patient-derived xenografts (PDXs). Cell cycle dynamics of TICs cocultured with specific populations of TICs will be studied using the Fucci cell cycle reporter system in conjunction with continuous live-cell imaging.

Results: The specific subpopulation of TICs marked by the presence of CD44 only demonstrates enhanced recruitment of surrounding ECs in the tumour microenvironment resulting in changes within the TICs associated with a differentiation phenotype and decreased progression through the cell cycle. This appears to contribute to the enhanced therapy resistance displayed by this subpopulation.

Discussion: Elucidating the details of cell cycle signaling in specific cellular populations of aggressive TICs of predominant dependence on the EC component will contribute to the identification of novel and improved therapeutic targets for the prevention of tumour angiogenesis and generalized personalized approaches for the treatment of patients with GBM in the future.

References: 1. CCS Canadian Cancer Statistics <http://www.cancer.ca> (2012). 2. Akil, A et al. Front Cell Dev. Biol. 9(642352), (2021).

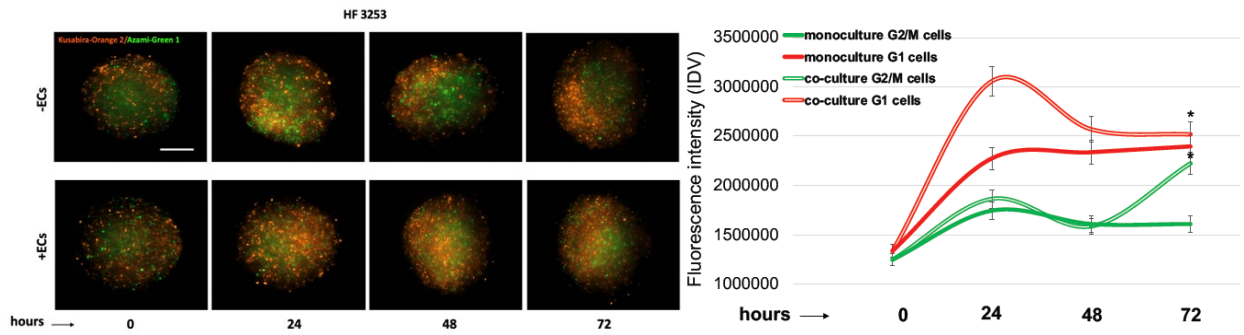


Figure 1. HF3253-FUCCI reporter stable patient cell line was used to generate organoids which were cultured using a Boyden chamber over a monolayer of HUVECs (+ECs) or no monolayer (-ECs) for 72 hours. The expression of Kusabira-Orange 2 indicated cells residing in G1 phase of the cell cycle while Azami-Green 1 indicated cells in G2/M. Fluorescence was measured every 24 hours and the fluorescence intensity was scored using ImageJ. Higher proportion of non-mitotic TICs was seen in the presence of ECs. The mm bar = 200. All data are shown as mean \pm SEM, * $p < 0.05$, ** $p < 0.01$, *** $p < 0.001$; $n=3$, Student's *t*-Test.

Title:**Myelodysplastic Neoplasms (MDS) with Ring Sideroblasts or SF3B1 Mutations: The Improved Clinical Utility of World Health Organization and International Consensus Classification 2022 Definitions, A Single Centre Retrospective Chart Review**

Shamim Mortuza^{1,†}, MD, Benjamin Chin-Yee^{1,†}, MD, FRCPC, Tyler E. James³, MD, FRCPC, Ian H. Chin-Yee^{1,2}, MD, FRCPC, Benjamin D. Hedley², PhD, Jenny M. Ho¹, MD, FRCPC, Lalit Saini¹, MD, FRCPC, Alejandro Lazo-Langner¹, MD, FRCPC, Laila Schenkel², PhD, Pratibha Bhai², PhD, Bekim Sadikovic², PhD, Jonathan Keow⁴, MD, FRCPC, Nikhil Sangal², MD, FRCPC, Cyrus C. Hsia^{1,*}, MD, FRCPC

¹Department of Medicine, Division of Hematology, London Health Sciences Centre, London, Ontario

²Department of Pathology and Laboratory Medicine, London Health Sciences Centre, London, Ontario

³Department of Medicine, Division of Hematology, University of Ottawa, Ottawa, Ontario

⁴Edmonton Base Lab, Alberta Precision Laboratories, Edmonton, Alberta

*Correspondence: cyrus.hsia@lhsc.on.ca; tel: 1-519-685-8500 x 56060

Abstract:**Introduction:**

Myelodysplastic neoplasms (MDS) with ring sideroblasts (RS) is diagnosed on bone marrow aspirate in the presence of either i) $\geq 15\%$ RS or ii) 5-14% RS and an *SF3B1* mutation. Based on the evidence from recent randomized clinical trials, lower risk MDS-RS patients demonstrated decreased transfusion dependency with luspatercept. Thus, MDS patients with $< 15\%$ RS with *SF3B1* mutations may still benefit from luspatercept. We performed a retrospective study to identify and to estimate the proportion of patients with *SF3B1* defined MDS-RS who would be excluded based on morphologic criteria alone.

Methods:

A total of 6817 patients with suspected hematologic malignancy underwent molecular testing using a next generation sequencing based genetic assay and 395 MDS patients seen at our centre from January 1, 2018 to May 31, 2023 were reviewed.

Results and Discussion:

There were 39 lower risk MDS with *SF3B1* mutations, 20 (51.3%) males and 19 (48.7%) females, with median age 77 years (range 57-92). Nineteen (48.7%) patients had an isolated *SF3B1* mutation with mean variant allele frequency 35.2% +/- 8.1% ranging from 7.4% to 46.0%. There were 29 (74.4%) patients with $\geq 15\%$ RS, 6 (15.4%) with 5 to 14% RS, one (2.6%) with 1% RS, and 3 (7.7%) with no RS. Our study suggests that approximately 25% of patients would be missed based on morphologic criterion of $\geq 15\%$ RS only and support the revised 2022 World Health Organization (WHO) and International Consensus Classification (ICC) definitions which shift toward this molecularly defined subtype of MDS and appropriate testing.

Marginalization and Factors Associated with Early Mortality among Patients Diagnosed with de novo Metastatic Breast Cancer in Ontario, Canada

Priya Thomas¹, Brooke Carter², Craig C. Earle^{2,3}, Salimah Shariff², Jacques Raphael^{2,4,5}, Alyson Mahar⁶, Sarah Knowles⁷, Muriel Brackstone⁷, Michael Lock⁸, Andrea Eisen³ and Phillip S. Blanchette^{2,4,5}

¹Schulich School of Medicine, Western University, London, Ontario, Canada, ²ICES, Ontario, Canada, ³Division of Medical Oncology, Sunnybrook Odette Cancer Centre, University of Toronto, Toronto, Ontario, Canada, ⁴Division of Medical Oncology, London Health Sciences Centre, Western University, London, Ontario, Canada, ⁵Department of Epidemiology and Biostatistics, Western University, London, Ontario, Canada, ⁶ Division of Cancer Care and Epidemiology, Cancer Research Institute, Queen's University, Ontario, Canada, ⁷ Division of Surgery, London Health Sciences Centre and St. Joseph Hospital, Western University, London, Ontario, Canada, ⁸Division of Radiation Oncology, London Health Sciences Centre, Western University, London, Ontario, Canada

Introduction: Breast cancer is a common disease in Ontario affecting 1 in 9 women during their lifetime, and 2000 women die from breast cancer in the province annually. Early death from breast cancer is uncommon and may be influenced by disease biology and sociodemographic factors such as age, marginalization, socioeconomic status, and rurality. The objective of this study was to investigate factors associated with early mortality from advanced de novo metastatic breast cancer in a publicly funded health care system.

Methods: We used linked healthcare administrative data from 2010-2019 to determine the frequency of early mortality, defined as death within 6 months of cancer diagnosis, from de novo metastatic breast cancer. A multivariable logistic regression model was used to determine which patient, cancer, and provider characteristics may be associated with early mortality. The Ontario Marginalization Index, a census and geographically based tool evaluating economic, ethno-racial, age-based and social marginalization, was used.

Results: We identified 4,004 patients with de novo metastatic breast cancer, of whom 22.9% (N=918) experienced early mortality (death within 6 months). Multivariable regression revealed that advanced age and a high marginalization index score (HMIS) were significantly associated with early mortality. [HMIS odd ratio vs low marginalization index score (LMIS) (OR)=1.48, 95% confidence interval (CI)=1.17-1.88, p-value=0.001]. Registration with a family physician was associated with significant decreased risk of early mortality (OR=0.74, 95%CI=0.62-0.89, p-value<0.001). There was variability in early mortality across geographic regions of the province and rurality did not affect early mortality until patients received treatment. Treatment with chemotherapy alone (typically used in triple-negative breast cancer) had higher odds of early mortality. Provider characteristics and acuity of the cancer center were not associated with early mortality.

Discussion: The results of this study suggest that factors such as marginalization, access to a family physician, and geography play a role in early mortality from breast cancer in the setting of a publicly funded health care system. Improving access to a family physician may help to reduce early breast cancer mortality.

Stereotactic Ablative Radiotherapy (SABR) for Oligoprogressive Solid Tumours: A Systematic Review and Meta-analysis

Vivian S Tan¹, Jerusha Padayachee², George B Rodrigues¹, Inmaculada Navarro², Prakesh S Shah³, David A Palma¹, Aisling Barry⁴, Rouhi Fazelzad⁵, Jacques Raphael⁶, Joelle Helou¹

¹Department of Radiation Oncology, London Regional Cancer Center, ²Department of Radiation Oncology, Princess Margaret Cancer Center, ³Departments of Paediatrics, Mount Sinai Hospital, ⁴Department of Radiation Oncology, Cork University Hospital, ⁵Library and Information Services, Princess Margaret Cancer Centre, ⁶Department of Medical Oncology, London Regional Cancer Center

Introduction: Randomized trials have supported the role of SABR in the treatment of oligometastatic disease and more recently there has been an increased interest in exploring its role in the “oligoprogressive state”. The aim of this systematic review and meta-analysis was to assess the quality evidence and pool outcomes to assess the effectiveness of SABR in patients treated for oligoprogressive metastases.

Methods: MEDLINE ALL, Cochrane Central, Cochrane Database of Systematic Reviews, EMBASE, and Web of Science were searched from January 2010 to January 2023 for studies with oligoprogressive disease treated with SABR. The CURB trial was published on December 14, 2023 and was added thereafter. Studies must have reported progression-free survival (PFS), overall survival (OS) or time to change to next-line of systemic therapy (ST). Descriptive statistics were used to summarize the data collected including counts and percentages for categorical variables. Risk of bias among included studies was assessed using Newcastle-Ottawa Scale. Pooled analyses of proportions were conducted for sub-groups as applicable using the binary random effects model. Between studies heterogeneity was quantified using I^2 values.

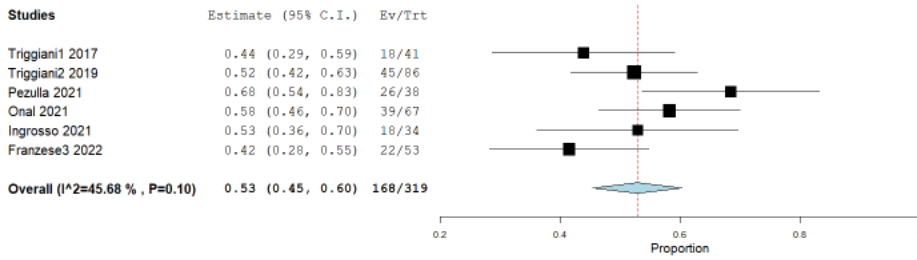
Results: Of the 12,366 titles/abstracts screened, 25 met eligibility criteria and were included in the review. All studies were published after 2017 with approximately 80% of the publications in 2021 and 2022. Twenty-one studies (84%) were retrospective design, three (12%) were prospective and one (4%) was a randomized controlled trial. Ninety-two percent (n=23) of studies had a moderate risk of bias and two studies (8%) had a low risk of bias. Eighteen studies (72%) used a threshold of 5 or fewer progressing lesions to define oligoprogression, while 5 studies (20%) used 3 or fewer lesions. The tumour primary was prostate (n=8, 32%), kidney (n=6, 24%), colorectal (n=4, 16%), breast (n=3, 12%), lung (n=2, 8%) and other (n=3, 12%).

At 1 year, the pooled PFS was 44% in all histologies (95% confidence interval [CI]: 34-53%, $I^2=91%$), 53% in prostate (95%CI: 45-60%, $I^2=46%$), 49% (95%CI: 33-65%, $I^2=88%$) in kidney, 62% (95%CI: 11-113%, $I^2=96%$) in lung, 13% (95%CI: 3-24%, $I^2=39%$) in breast and 30% (95%CI: 19-41%, $I^2=59%$) in other. The pooled OS at 1-year was 87% in all histologies (95%CI: 83-91%, $I^2=73%$), 95% (95%CI: 92-97% $I^2=1%$) in prostate, 89% (95%CI: 86-93%, $I^2=0%$) in kidney, 78% (95%CI: 64-91%, $I^2=0%$) in colorectal, 84% (95%CI: 54-113%, $I^2=91.4%$) in lung, 77% (95% CI: 66-87% $I^2=0%$) in breast and 76% (95%CI: 65-86%, $I^2=70%$) in other. A median time to change ST of 15.2 to 22.0 months was reported in prostate cancer (n=6), 12.6 to 18.2 months in kidney cancer (n=3), 4.9 to 5.2 months in colorectal (n=2), 8.0 months in breast cancer (n=1) and 8.1-11.0 months in mixed histology (n=3).

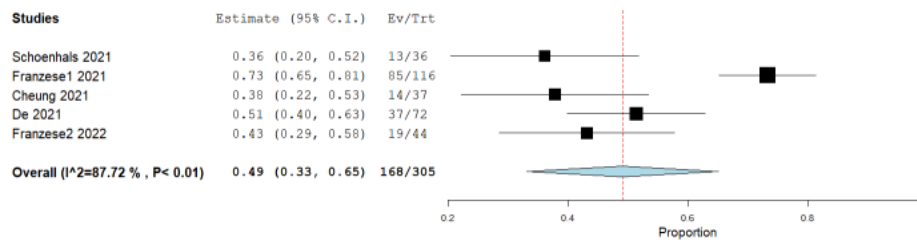
Conclusions: There has been a surge in publications describing the use of SABR in oligoprogressive tumours. Published studies are mostly retrospective and have frequently included small sample sizes. Promising outcomes have been reported in prostate and kidney cancers, with limited evidence in other sites. Universal definitions and guidelines are strongly recommended to ensure consistency in reporting and comparability of future studies.

Figure 1 Pooled 1-year Progression Free Survival (PFS1) for stereotactic ablative radiotherapy (SABR) to oligoprogressive metastases stratified

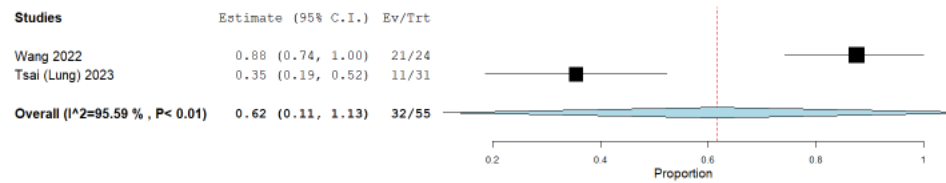
A Prostate



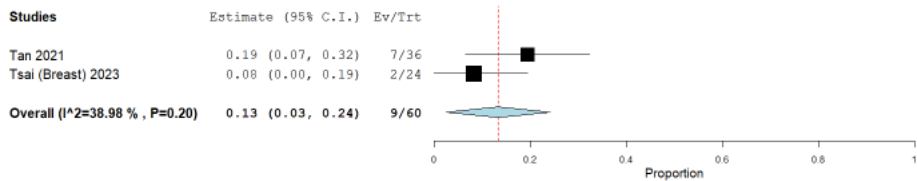
B Kidney



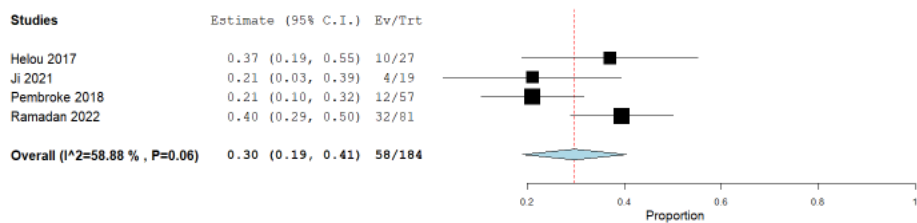
C Lung



D Breast



E Other



Pseudoprogession Following Liver SBRT in a Patient with Oligometastatic Leiomyosarcoma: A Case Report

Mohamed Aly¹, Shaheer Shahhat^{1,2}, and Timothy K. Nguyen^{1,2}

¹Schulich School of Medicine and Dentistry, Western University, London, Canada, ²London Regional Cancer Program, London Health Sciences Centre, London, Canada

Introduction: Uterine leiomyosarcoma is a rare, aggressive malignancy diagnosed most often in postmenopausal individuals with an incidence of less than 1%. The liver is a common site of metastases from leiomyosarcoma. Stereotactic Body Radiation Therapy (SBRT) is a non-invasive form of radiation that has been utilized for oligometastatic malignancies. However, pseudoprogession is a common radiological occurrence following this treatment, which presents with an increase in tumour size before its reduction. Additionally, the literature surrounding the use of SBRT for liver metastases in leiomyosarcoma is limited.

Methods: We present a case of a 58-year-old female diagnosed with leiomyosarcoma with a solitary liver metastasis demonstrating pseudoprogession following SBRT.

Results: Following surgery and post-operative radiation, the patient was later found to have a solitary liver metastasis after three years of surveillance, which was managed by SBRT. However, on short-term follow-up, the lesion had increased in size, prompting discussion regarding whether the growth was progession of disease or a secondary effect of treatment. After close follow-up, the tumour continued to shrink until it was no longer visible on imaging.

Discussion: This is the first case report discussing pseudoprogession following SBRT for a leiomyosarcoma patient. This serves as a reminder for clinicians to consider the possibility of pseudoprogession before failure of therapy.

Neoadjuvant Immuno-chemotherapy in Resectable Non-Small Cell Lung Cancer - A Retrospective Cohort Study

Authors

S. Verma, M.D. Vincent, M. Black, R. Nayak, M. Cecchini, R. Malthaner, J. Raphael, R. Inculet, D. Fortin, P. Blanchette, S. Kuruvilla, M. Qiabi, J. Younus, D.A. Breadner

Affiliation

London Regional Cancer Program, Schulich School of Medicine and Dentistry, Western University, London/ON/CA

Abstract:

Introduction: Neoadjuvant (NA) nivolumab-chemotherapy (nivo-chemo) has shown an improved survival and pathological complete response (pCR) rate, vs chemo alone, in early-stage, resectable non-small cell lung cancer (NSCLC). Nevertheless, there is a paucity of real-world data.

Methods: We performed a real-world, retrospective analysis of outcomes and toxicities in patients with resectable NSCLC (stage IB-IIIa; EGFR/ALK alterations excluded) treated with three cycles of NA nivo-chemo followed by surgery at a single, tertiary-level Canadian cancer centre from September 2022 to March 2024.

Results: Eighteen consecutive patients were treated with NA nivo-chemo. The median age was 69.5 years (range, 58 to 79) and 66% were males. 39% (n-7/18) and 11% (n-2/18) had N1 and N2 nodes, respectively. All patients completed three cycles of NA nivo-chemo. Objective response rate was 77% (n-14/18), as per RECIST1.1 (including two complete responses). Progression was noted in two patients (the CT predated initiation of treatment by more than 8 weeks in these patients). The median time to surgery was 10.6 weeks (range, 6-17.6). 83% patients (n-15/18) had a surgery (2 pneumonectomy, 13 lobectomies); and of these, 86% (n-13/15) are on surveillance while two patients had an event (death or progression). All (n-14/15) had R0 resection except one. 33% patients (n-6/18) had a pCR, including two with stage IIIa disease (PD-L1 TPS < 1% in four patients, PD-L1 TPS ≥ 50% in two patients). 61% (n-11/18) patients were started at a reduced chemo dose in cycle 1. 44% patients required further dose reduction in cycle 2. Grade 3 or 4 toxicities were seen in 22% patients (n-4/18), (neutropenia (n-2), febrile neutropenia (n-1) and pneumonitis (n-1, unresolved, grade 3 and resulting in decreased pulmonary reserve precluding surgery; patient is on close surveillance). Peri-operative (within 7 days) complications unrelated to systemic treatment were seen in 66% patients (n-10/15). One patient died on post-operative day 2 due to postoperative intra-thoracic bleed from pulmonary artery stump.

Table. Disease and treatment characteristics	
<i>Variable</i>	<i>N (%)</i>
Chemotherapy backbone	
Carboplatin-paclitaxel	11 (61)
Carboplatin-pemetrexed	4 (22)
Cisplatin-pemetrexed	2 (11)
Cisplatin-gemcitabine	1 (6)
Stage	
IB	3 (17)
IIA	2 (11)
IIB	7 (39)
IIIA	6 (33)

Histology	
Squamous	8 (44)
Adenocarcinoma	7 (38)
Adeno-squamous	1 (6)
Carcinosarcoma	1 (6)
NSCLC-NOS	1 (6)
PD-L1 (Tumor proportion score)	
< 1%	8 (44)
1 to 49%	6 (34)
≥ 50%	4 (22)

Conclusions: NA nivo-chemo in resectable NSCLC is safe and associated with improved pCR rate. A few patients may progress on NA treatment or have a grade 3-5 toxicity precluding curative surgery. Hence, individualized informed decisions should be made. There is an unmet need of biomarkers/models that can predict pCR/toxicity for better patient selection.

Contrast enhanced mammogram in the diagnosis and treatment of breast cancer in Ontario

Javadzadeh, Y^{1.}, Eltayeb, N^{1.}, Huhtala, M^{1.}, Pundaky, G^{1.}, Knowles, S^{1,2,3.}, Brackstone, M^{1,2,3.}

¹Schulich School of Medicine and Dentistry, Western University, London, Ontario, Canada

²London Health Sciences Center, London, Ontario, Canada

³Department of Surgery, University of Western Ontario, London, Ontario, Canada

Introduction: In Ontario, breast cancer diagnosis to treatment is a lengthy process associated with tremendous patient anxiety. Contrast enhanced mammography (CEM) is a modality with potential to detect early stages of breast cancer with greater accuracy and sensitivity in comparison to current imaging standards. Additionally, CEM is well tolerated and can be easily implemented in communities across Ontario, making its use more appealing. Our study aims to investigate how introduction of CEM impacts the timeliness of breast cancer treatment and streamlines the investigative work-up process.

Methods: A retrospective case-control study of breast cancer patients seen at London Health Sciences Centre (LHSC) was conducted using a locally maintained contrast imaging database and Breast Cancer Ontario database. Descriptive statistics were computed, and t-tests were used for comparative analysis of mean time to surgery and mean total number of investigations among women with breast cancer who received standard mammograms alone (prior to widespread CEM use) in 2016 versus those who also received CEM in 2019 at LHSC. Rates of breast conservation operative techniques as well as rates of positive margin re-excision surgery post operatively were compared.

Results: The total sample size was 331 patients, with 164 patients in the 2019 cohort compared to 167 patients in the 2016 cohort. Similar rates between both cohorts met provincial targets from identification of suspicious lesion to surgery. On preliminary analysis, introducing CEM reduced the number of additional tests required prior to surgery. A greater proportion of patients underwent breast conserving operative management in the post-CEM cohort. We anticipate completing our analysis by the end of April 2024.

Conclusions: The results of this study will contribute to current literature on benefits associated with CEM as a diagnostic tool in breast cancer management. CEM is an opportunity to improve wait times and reduce patient anxiety while reducing associated healthcare costs.

Incorporating Patient Perspectives into Oncology Education: A Scoping Review and Pilot Study at Western University

Rayyan Syed Kamal¹, Hanna Dutt¹, Arleigh Dean¹, and Dr. Alison Allan^{1,2}

¹London Regional Cancer Program, London Health Sciences Centre, London, Ontario, Canada

²Department of Anatomy & Cell Biology, and Department of Oncology, Schulich School of Medicine & Dentistry, Western University, London, Ontario, Canada

Introduction: “Rational human beings should be treated as an end in themselves”. The shift towards person-centred care (PCC) in oncology presents the need for parallel evolution of oncology education programs to prepare the next generation of health professionals to deliver PCC. These programs should be designed utilizing perspectives from individuals who have lived experience with cancer to ensure that changes to education curricula translate to improved PCC in the clinic. This study assesses (1) current oncology education programs integrating patient perspectives to identify effective strategies for learning transferable skills and understanding PCC; and (2) the experiences of cancer patients and caregivers with multidisciplinary healthcare teams, and oncology trainees and program directors regarding their preparedness for providing PCC, to develop strategies to integrate patient perspectives specifically into Western University’s oncology training programs. These include postgraduate Medical and Radiation Oncology (PGME-O); Bachelor of Nursing, oncology elective (BScN-O); and Undergraduate Medical Education clerkship and electives in Oncology (UME-O) programs.

Methods: Keywords were agreed upon and searched across 4 databases and included articles describing methods for involving cancer patients in developing/delivering oncology-focused education programs. Partnering with the LRCP Patient and Family Advisory Council, we developed a mixed methods study with an explanatory sequential design involving 4 participant cohorts including Cancer Patients, Caregivers, Learners, and Program/Course Directors (N=100 total). Programs include PGME-O, BScN-O, and UME-O. Quantitative data (via online questionnaires) and qualitative data (via follow-up semi-structured interviews) are being collected to explore cancer care and training experiences. Quantitative data will be analyzed to identify generalizable insights about lived experiences with PCC during care and training. Qualitative data will be analyzed using an inductive approach to reveal themes and to contextualize/enrich the quantitative findings.

Results: 12 unique oncology education programs (including CME, UME, PGME, nursing, and radiation therapy) across 7 countries were identified. The programs were summarized into 3 pedagogical approaches (classroom-based learning, clinical skills learning, and asynchronous online modules). The integration of cancer patients' perspectives and narratives in the design and delivery of these programs enhanced learners' empathy, communication skills, and understanding of PCC. All can feasibly be created with the integration of patient perspectives/narratives. Therefore, involving cancer patients directly in the design/delivery of these programs may contribute to improved patient experiences. The pilot study is open to accrual, with N=37 participants recruited to date, N=17 have been interviewed, and N=4 have been coded.

Discussion: Including the perspectives of cancer patients in oncology curriculum development/delivery can improve established pedagogical approaches and enhance learner confidence and competency in delivering PCC. This study pioneers a new paradigm for the integration of patient perspectives into education programs by assessing and integrating the experiences of cancer patients, caregivers, trainees and program directors to develop strategies to meaningfully incorporate patient perspectives and lived experiences into the formal curriculum of oncology training and education. By understanding the experience of patients and the gaps in training of cancer care students, we hope to make recommendations to improve oncology education programs at Western University to better prepare students to provide PCC.

Adjuvant treatment of stage I-II serous endometrial carcinoma: a 20-year institutional experience

Aquila Akingbade¹, François Fabi², Rodrigo Cartes³, James M. G. Tsui³, Joanne Alfieri³

¹ Division of Radiation Oncology, London Health Sciences Center, Western University, London, ON N6A 5W9, Canada

² Faculty of Medicine and Health Sciences, McGill University, Montreal, QC, Canada

³ Division of Radiation Oncology, McGill University Health Center, Montreal, QC, H4A 3J1, Canada

Introduction: Serous endometrial carcinoma (SEC) is a rare but aggressive histologic variant of endometrial cancer. Historically, different combinations of adjuvant chemotherapy (CT), external beam radiotherapy (EBRT), vaginal vault brachytherapy, and concurrent chemoradiotherapy (CCRT) have been investigated for disease control, but optimal management of early-stage SEC remains unclear. We evaluated outcomes, toxicities, and recurrence patterns associated with various adjuvant treatment modalities.

Methods: A comprehensive retrospective search of the pathology database of the McGill University Health Center (MUHC) identified all treated cases of FIGO 2009 stage I-II SEC between 2002-2019. Demographic, pathologic, adjuvant treatment, recurrence characteristics, and acute and late toxicity data according to the CTCAE v4.0 were collected until September 2023. Overall Survival (OS) and Disease-Free Survival (DFS) were calculated with Kaplan-Meier estimates and log-rank test for statistical significance. Analyses were conducted using the lifelines library version 0.27.8 in Python v3.10.12. Descriptive statistics were used for other variables.

Results: We identified 50 patients who underwent total hysterectomy, bilateral salpingo-oophorectomy, omentectomy; most (90%) had nodal sampling. FIGO 2009 stages were IA (60%), IB (24%), II (16%). Patients analyzed received adjuvant CCRT (n=36, 72%), CT alone (n=6, 12%), RT alone (n=6, 12%). Two patients were observed and excluded from further analyses. Median follow-up was 90.9 months for the cohort (CCRT-group 97.6 months, CT-group 28.3 months, RT-group 141.9 months). At the time of analyses, 17 patients had died. OS and DFS, respectively, at 3 years, were 81% and 78% for the entire cohort, 91% and 83% for the CCRT-group, 33% and 50% for the CT-group, and 67% and 80% for the RT-group. Patients treated with CCRT had significantly better OS (HR 0.14, 95% CI 0.04-0.52, p<0.005) and DFS (HR 0.25, 95% CI 0.07-0.97, p=0.05) than patients with CT alone. There were no OS or DFS differences for RT-alone vs CT/CCRT. There were recurrences in 14 (29%) patients: 2 locoregional (CT-group), 9 distant (1 CT-group, 8 CCRT-group), and 3 combined locoregional and distant (2 RT-group, 1 CCRT-group) recurrences. Eleven of the 14 patients (79%) had died at time of analyses. Sites of distant metastases included the lungs (5 patients), distant lymph nodes (5 patients), liver (2 patients), peritoneum (3 patients), and brain (1 patient). Acute G3+ toxicities: hematologic (n=12, 4 CT-group, 8 CCRT-group), gastrointestinal (n=2, CCRT-group), genitourinary (n=1, CT-group). Late G3+ toxicities: hematologic (n=2, CCRT-group), genitourinary (n=1, CT-group). No patients experienced late G3+ gastrointestinal toxicity.

Conclusions: Our results emphasize the high recurrence rate of stage I-II SEC despite adjuvant treatment. Chemoradiotherapy demonstrates better survival outcomes versus chemotherapy alone, but not RT alone, with acceptable toxicity profile. Most recurrences were distant, underscoring the need for more efficacious systemic agents.

A Rare Occurrence of an Ependymoma with an SDHB Mutation: A Case Report

Renee-Marie Ragguett¹, Seth A. Climans², Gabe Boldt³, Vivian S Tan³

¹Schulich School of Medicine and Dentistry, Western University, London, Ontario, Canada,

²Departments of Neurology and Medical Oncology, Western University, London, Ontario,

Canada, ³Department of Radiation Oncology, Western University, London, Ontario, Canada

Introduction: Mutations in the SDHB gene generally present with a characteristic syndrome that includes paragangliomas (PGL) and pheochromocytomas (PCC). Herein we present a rare case of an ependymoma occurring alongside an SDHB mutation.

Methods: A thorough chart review of a patient with an *SDHB* mutation and ependymoma was conducted. Additionally, we completed a literature review to identify reports of other similar occurrences.

Results: A 41-year-old man with a positive family history of PGL/PCC syndrome was found to have the familial *SDHB* mutation. Upon screening, he was found to have a presumed ependymoma originating from the fourth ventricle. He was followed with serial imaging to assess for progression of the lesion. Due to substantial growth of the tumor (Figure 1), and increasing symptoms which included diplopia, unsteadiness, and wide-based gait, he underwent a resection 5 years after its identification. Unfortunately, on day 26 post-operatively he had a pulmonary embolism and died. His family consented to autopsy and autopsy revealed the presence of a pituitary adenoma.

Conclusion: Though ependymomas are not commonly seen in PGL/PCC syndrome, they can occur. This case represents the first molecularly characterized ependymal tumor described in this tumor predisposition syndrome. Clinicians ought to be aware of the risk of ependymoma in patients with PGL/PCC syndrome.

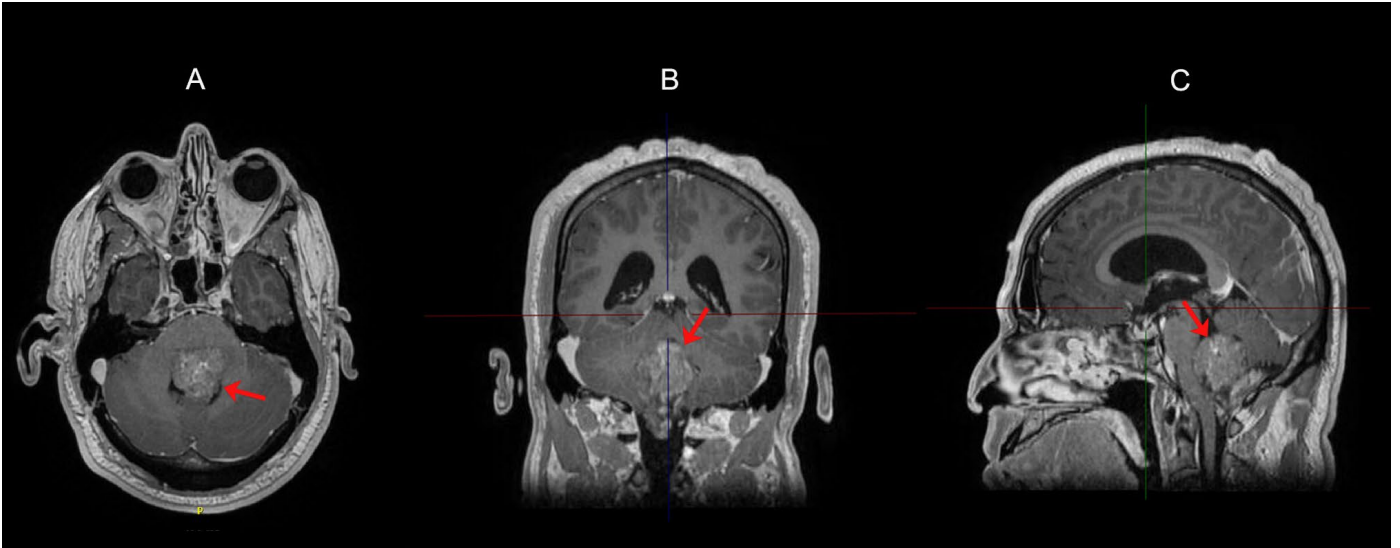


Figure 1. Final preoperative T1 MRI imaging of the head in a) axial, b) coronal and c) sagittal orientations. Ependymoma filling the fourth ventricle is indicated by the red arrow.

A Study Evaluating Drug Interactions in Prostate Cancer: the Impact of androgen receptor antagonists on direct oral AntiCoagulant Therapy (INTRACT) substudy

David Maj^{1,2}, Samantha Medwid¹, Steven Gryn¹, Cameron Ross¹, Morgan Black², Britney Messam², Eric Winquist², Scott Ernst², Ricardo Fernandes², Richard Kim^{1,2}, and Kylea Potvin²

¹Department of Medicine, University of Western Ontario, London, Canada

²Department of Oncology, University of Western Ontario, London, Canada

Introduction: Introduction of androgen receptor axis-targeted (ARAT) therapeutics have markedly improved prostate cancer disease progression and survival. However, ARATs are well known to interact with many widely prescribed medications through induction of drug metabolizing enzymes and transporters. Atrial fibrillation, a common cardiovascular disease often present in older adults, is often treated using oral anticoagulants known as direct oral anticoagulants (DOACs) to reduce the risk of stroke. Patients who are on ARAT therapy are potentially at risk for suboptimal response to DOACs due to the inducing effects of ARATs on DOAC metabolism pathways. The LHSC Anticoagulation Clinic (AC Clinic-University Hospital) utilizes a state-of-the-art liquid chromatography tandem mass spectrometry (LC-MS/MS) system to directly measure serum DOAC concentrations to aid in management decisions. Our study aims to assess the significance of ARAT (Enzalutamide, Apalutamide, Darolutamide) drug interaction upon DOACs (Apixaban, Edoxaban, Rivaroxaban) in patients starting ARAT treatment for prostate cancer.

Methods: This study is a prospective, non-randomized, self-controlled, observational trial evaluating the interactions of ARAT therapy upon DOAC drug concentrations. A 3 x 3 factorial design will be implemented to assess each ARAT-DOAC pair. Patients starting ARAT therapy for metastatic prostate cancer who are currently receiving DOAC therapy for atrial fibrillation will be recruited. Patients will have serum DOAC concentrations measured at time of enrolment and at 1, 3, and 6 months of ARAT therapy. DOAC concentrations will be measured by LC-MS/MS and plotted on a nomogram by time since last dose. Physicians at the AC clinic will modify patients' DOAC therapy as necessary. Primary outcome will be median change in serum DOAC concentration from baseline. Secondary outcomes include proportion of patients maintaining DOAC concentrations within therapeutic range, and composite of bleed, stroke, and VTE.

Discussion: Trial recruitment commenced in December 2023. To our knowledge this is the first trial that will assess the clinical significance of these predicted drug interactions in a real-world population. Results will provide important new insights on optimal DOAC selection and dosing for prostate cancer patients that will minimize the risk of stroke or bleed.

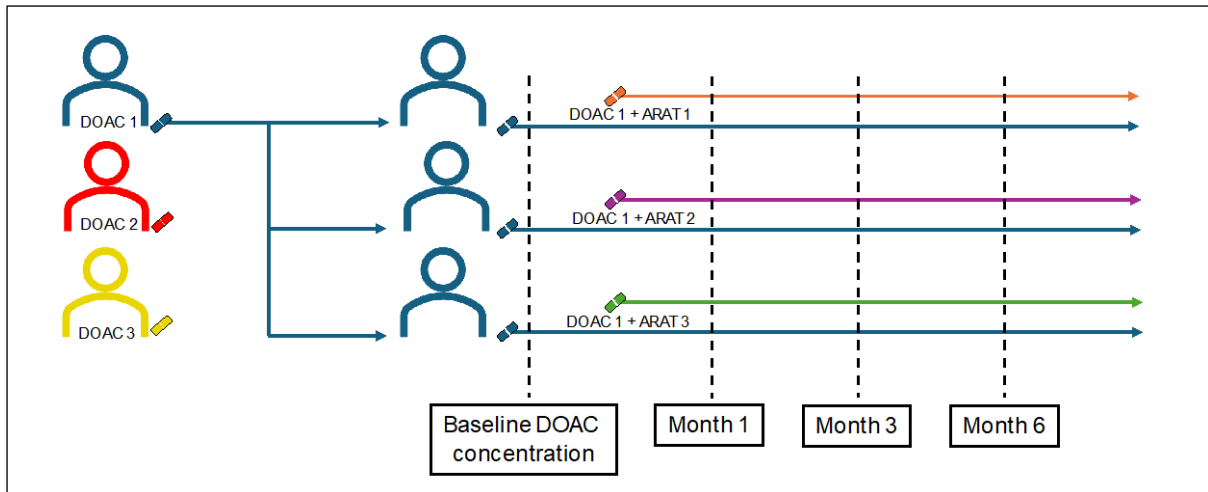


Figure 1: Patients will be recruited to one of 9 cohorts based upon DOAC-ARAT pair. DOAC concentrations will be measured by LC-MS/MS at 1, 3, and 6 months to measure change from pre-ARAT baseline and assess if DOAC concentrations remain in therapeutic range.

Association between immune-related side effects (irAEs) and Clinical Outcomes in patients with advanced renal cell carcinoma (RCC) treated with immunotherapy

Meh Noor¹, Prathana Nathan¹, Adnan Rajeh², Gabriel Boldt³, Saman Maleki^{3,4}, Ricardo Fernandes^{2,4}

¹ Department of Internal Medicine, Schulich School of Medicine & Dentistry, Western University, London, ON, CA

² Division of Medical Oncology, Department of Oncology, Schulich School of Medicine & Dentistry, Western University, London, ON, CA

³ London Regional Cancer Program, Victoria Hospital, LHSC, London, ON, CA

⁴ Cancer Research Laboratory Program, Lawson Health Research Institute, London, ON, Canada

⁵ Department of Pathology and Laboratory Medicine, Western University, London, ON, Canada

Introduction: Treatment for RCC has significantly evolved over the last decade, including the historic use of cytokine therapies such as interleukin-2 or interferon- α , and tyrosine kinase inhibitors (TKI), which remains a mainstay targeted therapy. More recently, immune checkpoint inhibition (ICI) is being studied and its targeted programmed death-1 (PD-1) or programmed death ligand-1 (PD-L1) pathways, and cytotoxic T lymphocyte antigen 4 (CTLA4). ICI can induce various immune-related adverse events (irAEs), potentially limiting their use in clinical settings. We aimed to better understand the relationship between irAEs and clinical outcomes.

Methods: This was a retrospective study of patients treated at the Verspeeten Family Cancer Centre in London, Ontario, Canada. Eligible patients had metastatic or advanced RCC and were treated with immunotherapy between xxx and xxx. Demographic data and clinical variables were collected and used to generate descriptive statistics using Cox's regression model. Patients with clinical benefit were compared to those with and without irAEs. Primary outcomes included incidence and severity of irAEs, and clinical outcomes in both groups. Secondary outcomes included progression free survival (PFS) and overall survival (OS).

Results: There were no statistically significant differences in the following variables of interest between the two groups: average age at diagnosis, sex, ECOG performance, smoking history as pack-years, previous therapies (radiation, TKI and chemotherapy), baseline neutrophil-lymphocyte ratio, prevalence of nephrectomy, presence of metastatic disease at beginning of immunotherapy, number of immunotherapy cycles, progression of disease, additional therapies, mortality, PFS or and OS. There was insufficient data to compare ethnicity and PDL1 status. There were significant effects of the following on both PFS and OS in both groups: baseline neutrophil-lymphocyte ratio (NLR), number of immunotherapy cycles, and smoking history. The overall incidence of irAE was 40.7% and the most common irAE in the clinical-benefit group was rash, 56.25%, compared to 20% in the overall population. Colitis and pneumonitis were 12.5% and 18.75% in the clinical-benefit group respectively, and 5% and 6.67% in the overall population respectively.

Conclusions: There was no observed difference in clinical outcomes, PFS, or OS in patients with clinical benefit from ICI treatment with or without irAEs.

A semi-automated computerized approach to quantifying tumor infiltrating lymphocytes in breast cancer

Natalie Grindrod¹, Matthew Cecchini², and Muriel Brackstone³

¹ Department of Pathology and Laboratory Medicine, Schulich School of Medicine & Dentistry, Western University, Canada, ² Department of Pathology and Laboratory Medicine, London Health Sciences Centre, Canada, ³ Department of Surgical Oncology, London Health Sciences Centre, Canada

Introduction: Breast cancer (BC) is the 2nd leading cause of cancer deaths for women worldwide, and 1 in 8 Canadian women will be diagnosed with BC. Tumour infiltrating lymphocytes (TILs) in BC is a prognostic and predictive biomarker. Good prognostic outcomes have been seen with high TILs in chemotherapy, but has not been fully explored with radiotherapy. Utilizing digital pathology allows TILs quantification to be more efficient. Local SIGNAL study slides previously collected were used, where patients underwent neoadjuvant chemoradiation or chemotherapy. We aim to assess how certain disease parameters and chemoradiation may affect TILs, assess TILs clustering, and how these may impact outcomes. Our hypothesis is that spatial mapping of the lymphocyte distribution will provide robust and accurate predictions of response to neoadjuvant therapy and therefore guide treatment decisions in BC.

Methods: 240 hematoxylin and eosin stained slides were digitized using the Aperio ScanScope, with 120 pre-treatment and 120 post-treatment samples, where 30 patients underwent neoadjuvant chemoradiation and 90 neoadjuvant chemotherapy. Then image analysis was performed using QuPath, which included cell detections, training an object classifier with cell types, and a pixel classifier, which was used to separate intratumoural and stromal TILs. Both classifiers used an artificial neural network. Delaunay Triangulation was used to assess clustering between cell types. Immunohistochemistry was then performed for CD3, CD4, CD8, CD45, CD68, CD1a, PAX-5, and myeloperoxidase.

Results: Current results are underway, immunohistochemistry is completed, but image analysis is in progress still. Initial results show that chemoradiation does not diminish TIL population significantly differently from chemotherapy. Significance found between increased stromal and intratumoural TILs and pathological complete response in pre-treatment specimens for the chemotherapy group, with similar trends seen in chemoradiation but no significance. Chemoradiation saw a significant increase in stromal TILs post-treatment in patients that achieved pathological complete response.

Discussion: This is the first study to apply TIL assessment to a well curated study of concurrent neoadjuvant chemoradiation patients. Outcomes and correlations between TILs and treatment modality will further the possibility of using TILs for prognosis and guiding treatment decisions. The semi-automated approach utilized in this study can be relatively easily deployed and will serve as a basis to build completely automated workflows that can be rapidly deployed in clinical practice. Despite theories of radiotherapy in BC completely diminishing the body's immune efforts and immune cells found in tissues, this is not necessarily true, and a contrasting theory may be true where it induces immune response. Interestingly, the fractionation for radiotherapy was high for patients (25-30 fractions), which is not supported in the contrasting theory. Radiotherapy may indeed play an important role in the immune response for BC.

Outcomes after Definitive Radiation for Early-Stage Glottic Cancer in the Modern Era of Radiotherapy

Jane Lin¹, Terence Tang², Eric McArthur², Adam Mutsaers², Rohann Correa², Pencilla Lang², Nancy Read², David Palma², and Christopher Goodman²

¹Schulich School of Medicine & Dentistry

²Department of Radiation Oncology, London Regional Cancer Program

Introduction: Radiation treatment techniques for the definitive management of early-stage glottic cancer (ESGC) have evolved over the past decade with a transition from field-based planning to intensity modulated radiotherapy (IMRT). This study examined outcomes following definitive radiation for ESGC in the modern era of radiotherapy, with a focus on rates of laryngeal preservation.

Methods: All patients with T1-2N0 biopsy-proven cancers of the glottic larynx treated with definitive radiation between 2015 and 2021 at a single tertiary care centre were included in this study. All patients were assessed in a multidisciplinary clinic prior to treatment. Patients were excluded if they had previous laryngeal surgery or non-squamous cell carcinoma histology. Demographic, clinical, and treatment data were collected retrospectively. Outcomes of interest included recurrence-free survival, laryngectomy-free survival, and overall survival.

Results: A total of 83 patients were eligible for analysis. Most patients were male (n=73, 88%) and had a history of smoking (n=75, 90%) or alcohol use (n=61, 73%). Median age was 71 years (IQR 63–77). Eleven patients (13%) had T1a disease, 33 patients (40%) had T1b disease, and 39 patients (47%) had T2 disease. All patients were treated with IMRT with a high-dose volume covering the tumour plus a margin and a low-dose volume covering at least the entire larynx, with sparing of the contralateral arytenoid if possible. Median prescription dose was 61 Gy (range 50–70), with most patients (n=60, 72%) receiving a hypofractionated regimen of 61 Gy in 25 fractions. With a median follow-up of 3.6 years (IQR 2.0–5.1), 16 patients (19%) had recurrent disease, 11 of whom underwent salvage surgery for locoregional recurrence. The remaining 5 patients either recurred distantly, declined further treatment, died from other causes, or were lost to follow-up. The 3-year estimates for recurrence-free survival, laryngectomy-free survival, and overall survival were 77% (95% CI 67–88), 86% (95% CI 77–95), and 88% (95% CI 80–97), respectively. On univariate analysis, supraglottic extension (HR 5.21; p=0.0088) and a higher clinical T-stage (HR 3.37; p=0.036) were predictive of recurrence.

Discussion/Conclusion: In this modern cohort, definitive radiation for ESGC demonstrated high rates of local control and laryngeal preservation. Randomized trials comparing IMRT with modern surgical techniques like transoral laser microsurgery are necessary.

Antibody Drug Conjugates in Treatment of Genitourinary Cancers: An Updated Review of Data

Prathana Nathan ¹, Adnan Rajeh ², Meh Noor ¹, Gabriel Boldt ³, Ricardo Fernandes ^{2,4}

1 Department of Internal Medicine, Schulich School of Medicine & Dentistry, Western University, London, Ontario, Canada

2 Division of Medical Oncology, Department of Oncology, Schulich School of Medicine & Dentistry, Western University, London, Ontario, Canada

3 London Regional Cancer Program, Victoria Hospital, London Health Sciences Centre, London, Ontario, Canada

4 Cancer Research Laboratory Program, Lawson Health Research Institute, London, Ontario, Canada

Introduction: The treatment landscape of genitourinary (GU) cancers has significantly evolved over the past few years. Recent advancements have produced new targeted therapies, particularly antibody drug conjugates (ADCs). ADCs function as a ‘drug delivery into the tumor’ system. They are composed of an antigen-directed antibody linked to a cytotoxic drug that releases cytotoxic components after binding to tumor cell’s surface antigen. ADCs have been proven to be extremely promising in the treatment of several cancer types.

Methods: In this study, we thoroughly reviewed the current literature and summarized preclinical studies, clinical trials and retrospective studies that evaluated utility, activity, and toxicity of antibody drug conjugates in GU cancers, prospects of ADC development, and ongoing clinical trials.

Results: In particular, enfortumab vedotin (EV), sacituzumab govitecan, and trastuzumab deruxtecan have shown promise. For instance, Enfortumab Vedotin (EV) has shown high response rates in patients with metastatic urothelial cancer (mUC), even those who have undergone previous therapies. Several trials (EV-101, EV-201, and EV-301) have established its effectiveness, with manageable side effects. A phase III trial (EV-302/KEYNOTE-A39) combined EV with pembrolizumab and demonstrated significant improvements in progression-free survival (PFS) and overall survival (OS), suggesting its use as a first-line treatment for mUC. Trastuzumab deruxtecan’s (T-DXd) efficacy has been observed in advanced HER2-expressing urothelial carcinoma. Sacituzumab govitecan (SG) has shown notable efficacy in mUC after progression on other treatments, as demonstrated in the TROPHY-U-01 trial.

Discussion: As metastatic genitourinary cancers, in general, are associated with poor survival rates, along with the wide spectrum of toxicities that conventional treatments cause, ADCs, with their highly specific ability to target cancer cells, are an attractive option for clinicians and patients alike. This current narrative review illustrates that ADCs seem to be a rising star in cancer research and potentially the next big advancement in the cancer treatment paradigm.

Title: Evaluating Alternative Dosing Regimens of Consolidative Durvalumab in Patients with Stage III NSCLC Treated with Chemoradiotherapy: An Observational Cohort Study

Authors: Jonathan Moroniti¹, Sarah Ma^{1,2}, Gabrielle Pundaky¹, Eric McArthur^{2,3}, Nawar Tarafdar¹, Morgan Black^{2,3}, Kathie Baer^{2,3}, Robin Sachdeva⁴, Saritha Surapaneni^{2,3}, M. Sara Kuruvilla^{1,2,3}

Affiliations:

1. Schulich School of Medicine and Dentistry, Western University, London, ON, Canada.
2. Lawson Health Research Institute, 750 Base Line Rd E, London, ON N6C 2R5, Canada.
3. Department of Oncology, London Regional Cancer Program, London Health Sciences Center, 800 Commissioners Road East, London, ON, N6A5W9, Canada.
4. Precision for Medicine, 800 René-Lévesque Blvd. West, 26th Floor. Montréal, QC, H3B 1X9.

Introduction: Lung cancer is a leading cause of cancer-related mortality in Canada. Non-small cell lung cancer (NSCLC) accounts for approximately 85% of all new lung cancers, and more than two-thirds of patients are diagnosed with advanced disease (Stage III/IV). The standard of care for unresectable, Stage III NSCLC has been established by the PACIFIC trial, with patients receiving durvalumab immunotherapy at 10 mg/kg every two weeks for one year following chemoradiation. In response to the COVID-19 pandemic, Cancer Care Ontario approved an alternative durvalumab dosing scheme, 20 mg/kg every four weeks, to optimize patient care and minimize patient exposure to health facilities. Uncertainty remains regarding the impact of this modification, especially within the region of Southwestern Ontario, which serves a demographically distinct population. This study aimed to compare the effectiveness and tolerability of these two regimens.

Methods: We reviewed the medical records of consecutive adult patients diagnosed with Stage III NSCLC from January 1st, 2018, to May 4th, 2023, who were treated with chemoradiation at the London Health Sciences Centre, Ontario, Canada. Information collected included patient demographics, durvalumab dosing frequency, progression pattern, survival outcomes, and adverse events. Patients were categorized according to durvalumab dosing schedule. Descriptive statistics were applied to demographic, treatment-related, and clinico-pathologic characteristics. Overall survival and real-world progression free survival analyses were conducted using Kaplan-Meier curves and Cox proportional hazard models. The research protocol was reviewed and approved by the Institutional Research Ethics Board Review.

Results: A total of 196 patients were included. The median age was 70 years old, 53% were male, most were current or former smokers (>90%), and the majority had an ECOG-PS of 0-1 (89%). 45% of patients had adenocarcinoma, and 29% had squamous cell carcinoma. 66% of patients received carboplatin, while 36% received cisplatin. Following chemoradiotherapy, 27% of patients received the two-week durvalumab regimen (Durvalumab-Q2w) and 63% received the four-week regimen (Durvalumab-Q4w). 10% did not receive durvalumab. There was no significant difference in the risk of death (HR:0.70,95%CI:0.42-1.14;p=0.15) or progression (HR:0.77,95%CI:0.52-1.14;p=0.19) between the two dosing groups. Toxicity profiles were similar between the two groups.

Discussion: Overall, this study identified comparable effectiveness and tolerability of consolidative durvalumab administered every four weeks to every two weeks, supporting its use post-pandemic. An extended dosing regimen of durvalumab beyond the pandemic could provide a more convenient alternative for patients who may be challenged by the two-week schedule due to their clinical condition, or their distance from treatment centers. It could also reduce healthcare costs associated with treatment delivery. Limitations of this study include covariates (such as variation in patient characteristics and care provided), limited sample size, as well as errors in data collection and handling. Further studies are needed to validate our results.

Restaging old cancer reports: the role of language artificial intelligence models

Flaviu Trifoi, Deepshikha Deepshikha, Muskan Multani, Matthew J Cecchini¹

¹ Department of pathology and laboratory medicine, london health sciences centre

Introduction: Pathology reports play a crucial role in cancer diagnosis and treatment planning. However, maintaining cancer staging consistency with evolving guidelines can be challenging. This study proposes leveraging artificial intelligence (AI) language models, including ChatGPT 3.5 and Gemini 1.5 Pro, to re-stage old lung adenocarcinoma pathology reports with the most up to date guidelines.

Methods: 100 randomly selected pathology reports from the TCGA PanCancer Atlas were re-staged by three independent reviewers using the 8th edition American Joint Committee on Cancer (AJCC) guidelines. Then, AI language models ChatGPT 3.5 and Gemini 1.5 pro were prompted to create staging rulesets from the 8th edition AJCC guidelines. Reports were run through these language models to assess their accuracy in restaging cancers. T stages were either upstaged, downstaged, or subclassified (ex. From T2 to T2a).

Results: Of the 100 reports, 86 cancers received a new T stage—11 were downstaged, 56 were upstaged and 19 were further subclassified. Of these 100 reports, 4 cancers received a new N stage—3 were downstaged and 1 was upstaged. ChatGPT 3.5 was able to correctly re-stage 20/86 reports based on new guidelines while Gemini 1.5 pro was able to correctly re-stage 13/86.

Discussion: These results show that with constantly changing classification criteria, TNM staging varies significantly over time. This demonstrates the importance of tools to increase efficiency of re-staging old pathology reports if they ever need to be revisited for patient care. Our findings show that a language-model AI is currently only able to re-stage a proportion of reports correctly. Further research can investigate coupling language AI models with other computational tools better equipped to handle numeric data.

Elucidating the IBR class compound action on Rad51 using protein engineering

Stephen Ritter¹, Peter J. Ferguson², Mark D. Vincent², James Koropatnick², Yousef, Najajreh³, and Brian Shilton¹

¹Department of Biochemistry, Schulich School of Medicine and Dentistry, The University of Western Ontario, ²Lawson Health Research Institute-London Health Sciences Centre, ³Al-Quds University, Jerusalem, Palestine

Introduction: While DNA repair defects can cause genomic instability and drive tumour evolution, these defects also provide opportunities for targeted chemotherapies. The activity of Rad51, a recombinase that acts in homology-directed DNA repair by forming a nucleoprotein filament on damaged DNA, is increased in some cancers. Rad51 activity has been linked to treatment resistance, increased cell proliferation, and genomic instability. Inhibiting Rad51 in cancer cells appears to be a viable treatment strategy. Drug discovery efforts aimed at targeting Rad51 yielded the IBR class compounds IBR2, IBR120, and JKYN-1. These compounds slow growth, inhibit homologous recombination, induce apoptosis in cancer cell lines, and demonstrate synergy with existing therapies. However, how these compounds interact with Rad51 remains unclear. To better understand their mechanisms of action and to facilitate structure-guided drug optimization, this work aims to characterize the action of the IBR class compounds on Rad51 and determine high-resolution structures of the drug-bound complexes by X-ray crystallography.

Methods: The activity of Rad51 relies on protein multimerization, which complicates drug affinity determination and structure determination by X-ray crystallography. Our previous work has shown that an *E. coli* expression system can be used to express the core domain of Rad51 fused to the maltose binding protein (MBP). Though crystallization attempts failed, the MBP-Rad51 fusion protein retained a diminished capacity to form multimers. In an attempt to eliminate multimerization, a series of six circular permutations of Rad51 (circRad51) were developed. These constructs were then used in the fusion protein strategy to better situate the MBP fusion partner to disrupt multimerization. The multimerization of wtRad51 and its constructs were assessed using an array of biophysical techniques in the presence and absence of the IBR class compounds. Constructs that exhibit diminished multimerization are being used in ongoing crystal screens.

Results: All six of the MBP-circRad51 fusion proteins were efficiently expressed and purified from *E. coli*. Assessment of multimerization revealed that all the engineered constructs, like the standard MBP-Rad51 fusion protein, exhibited diminished multimerization when compared to wtRad51. This, in conjunction with circular dichroism spectroscopy and ATP/ADP binding assays, confirmed the correct folding of the core Rad51 domain. While drug-binding assays are ongoing, analytical ultracentrifugation and blots of native gel electrophoresis revealed that the IBR class compounds interfere with the multimerization of wtRad51.

Conclusions: The success of the circular permutation strategy with Rad51 is significant both in terms of addressing roadblocks for crystallization and for structural biology research. The array of Rad51 constructs with a limited capacity for multimerization may allow for protein crystallization, and, in the future, may also allow for novel drug screens based solely on disruptions to Rad51 multimerization. The effect of the IBR class compounds on Rad51 multimerization hints at a potential mechanism of action via disruptions to Rad51 activity. Achieving the objectives of this work will provide insight into the mechanisms of action for the IBR class compounds and provide information key for optimizing them for clinical use.

Enhancing the patient journey to clinical trial enrollment with navigation to optimize accrual: A pilot study for a pragmatic multicentre, stepped wedge, cluster randomized controlled trial (The Clinical Trial Navigator (CTN) Pilot Trial)

Deven Sharma¹, Caroline Hamm²

¹University of Windsor, ²Schulich School of Medicine and Dentistry

Introduction

Clinical trials are essential to the advancement of clinical therapies, yet accrual rates remain disappointing. Multiple challenges lead to less than 5% of cancer patients enrolled onto clinical trials. The Clinical Trials Navigator (CTN) program was established to assist patients and health care professionals identify appropriate clinical trials for patients.

Methods

Between March 2019 to January 2024, a novel navigator-assisted clinical trials search program was offered to Canadian patients. Three non-medical navigators were trained to receive referrals, review medical information, and search five different clinical trial search engines. Eligibility criteria was scrutinized. A second review of the clinical trial list was conducted by two physicians. The final curated list of clinical trials was provided to patients and their oncologist.

Results

A total of 373 patients were referred to the CTN program during the study period. A unique clinical trial search was performed for each patient yielding a median of only one potentially eligible trial per patient. Clinical trial enrolment occurred in 3.2% of patients in our database which translates to a 19% rate of successful enrolment of those referred to a trial by the CTN. Most patients (78%) were referred to clinical trial sites that conducted more than 100 clinical trials at any time.

Compared to the Canadian cancer statistics, lung, lymphoma, pancreatic and brain cancers were overrepresented in referrals to the CTN program while prostate cancer was underrepresented. Type of cancer played a significant role in the likelihood of a successful referral ($p < 0.01$). Lung cancer was the most frequently reported cancer that resulted in referrals and breast cancer showed a lower frequency of referrals. The cancer type, stage and number of lines of prior therapy were not significantly associated with the patient enrollment onto a clinical trial. An increase in survival of referred patients from last analysis from 3.0 months to 5.3 months.

Discussion

The CTN program is a successful tool to identify clinical trials for cancer patients and can improve clinical trial accrual, as almost one fifth of patients (19%) who were referred to a clinical trial were enrolled. Ongoing iterative changes to the program to improve these metrics are underway and efforts to improve implementation of the CTN program across Canada are ongoing.

SPoRTS: a novel, automated workflow for spatiotemporal analysis of ratiometric fluorescent biosensors in live ovarian cancer spheroids

Matthew J Borrelli^{1,2}, Bart Kolendowski¹, Yudith Ramos Valdés¹, Gabriel E DiMattia^{1,3,4}, Trevor G Shepherd^{1,2,3,5}

¹The Mary and John Knight Translational Ovarian Cancer Research Unit, Verspeeten Family Cancer Centre, London, Ontario, Canada; Departments of ²Anatomy & Cell Biology, ³Oncology, ⁴Biochemistry, ⁵Obstetrics & Gynaecology, Schulich School of Medicine & Dentistry, Western University, London, Ontario, Canada.

Introduction Formation of multicellular aggregates (spheroids) enhances the survival of epithelial ovarian cancer (EOC) cells during peritoneal metastasis, but knowledge of the underlying biology is limited. Furthermore, microenvironmental heterogeneity—innate to spheroids—complicates analyses of bulk materials (i.e., protein lysates, RNA, etc.), which lack spatial information. To address this deficit, we developed SPoRTS (spatial profiling of ratiometric trends in spheroids), a streamlined Python-based image analysis platform for spatiotemporal monitoring of fluorescent biosensor activity within live spheroids. To the best of our knowledge, SPoRTS is the only platform to implement a fully-automated algorithm for line profile acquisition, enabling the application of this approach to high-volume data sets for the first time.

Methods Time course image sets of EOC spheroids expressing a ratiometric biosensor for mitosis (ratiometric Fucci) were analyzed using SPoRTS and the results were validated via comparison to the current standard for spatial analyses—immunostaining of spheroid sections—which we stained for markers of proliferating cells. Following method validation, SPoRTS was used to analyze spheroids expressing ratiometric biosensors for autophagy and mitophagy. The results from these SPoRTS analyses prompted further investigations into mitochondria and mitochondrial dynamics proteins in spheroids with a spatial context.

Results Proliferating cells were found to occur in a depth-based gradient (greater frequency of proliferating cells closer to the spheroid's surface) using both SPoRTS and immunostaining, exhibiting a strong correlation between the two methods and confirming SPoRTS' capacity for automated spatial monitoring of biosensor activity in live spheroids. Autophagy and mitophagy were each found to exhibit a unique pattern of spatial regulation in EOC spheroids, ultimately leading us to discover region-dependent differences in the structural organization and regulation of mitochondrial networks within spheroids.

Conclusions Image analysis has the potential to be a powerful approach for interrogating the biology of EOC spheroids, but current automated methods are scarce and typically offer analyses of basic morphological features only. SPoRTS enables spatiotemporal monitoring of biosensor-reportable processes in live spheroids, and is equally applicable to any ratiometric signal(s) in any subject with approximately radial symmetry (e.g., organoids). Coupled with broader utilization of biosensor-expressing cancer cells, SPoRTS holds the potential to enable systematic characterization of intracellular processes impacting spheroid biology and metastatic potential, and provide new insights regarding the manner in which these processes may be influenced by spheroids' spatial heterogeneity.

Assessment of enantioselective metabolism of ondansetron in pediatric cancer patients

Nicholas Hamzea¹, Samantha Medwid¹, Alvira Khurram², Richard B. Kim^{1,3}, Alexandra Zorzi², and Ute I. Schwarz^{1,3}

¹ Department of Physiology and Pharmacology, Western University, London, Ontario

² Department of Paediatrics, Western University, London, Ontario

³ Department of Medicine, Western University, London, Ontario

Introduction: Chemotherapy-induced nausea and vomiting (CINV) is a common and distressing adverse effect in cancer therapy. Despite clinical guidelines, CINV control in pediatric oncology patients remains poor and up to 50% refuse or delay therapy. Ondansetron, a serotonin-receptor inhibitor prescribed to prevent CINV, is metabolized by cytochrome P450 (CYP)2D6 and CYP3A, and CYP2D6 genotype-guided dosing is recommended. Enantioselective metabolism has been reported in adults but has not been investigated in pediatric cancer patients. We aimed to determine the effect of CYP2D6 and CYP3A genotypes on ondansetron enantiomer concentration in pediatric cancer patients.

Methods: Demographic and clinical information was recorded, and blood collected ~2 and 4 hours after ondansetron administration (5 mg/m²) before chemotherapy. Enantiomers were quantified in plasma by mass spectrometry, and CYP2D6 (*3,*4,*6,*9,*10,*41,*5/*1xN) and CYP3A5 (*3) genotyping performed.

Results: Data of 42 patients (mean 7.2 years, 38% females) at 2 hours were analyzed. S+R-Ondansetron level was variable (mean±SD; 60.9±42.2ng/mL). R- (P=0.047, Kruskal-Wallis) and S-ondansetron (p=0.061) differed by CYP2D6 phenotype. Levels tended to be ~2.5-fold higher in poor metabolizers (PM, n=3) than normal metabolizers, and 0.6-fold lower in an ultrarapid metabolizer (n=1). CYP3A5 had no effect. Concentration was ~1.6-fold higher in females (p=0.005, Mann-Whitney). CYP2D6 PM-status (p<0.001) and sex (P<0.01) explained 41% of R- and S-ondansetron variability (adj.33%, linear regression).

Discussion: Our findings do not suggest enantioselective ondansetron metabolism. CYP2D6 genotype and sex predict ondansetron with potential relevance for antiemetic efficacy and toxicity in pediatric cancer patients.

Investigating the Role and Function of OATP Drug Transporters in relation to Tamoxifen Therapy

Michelle Wong¹, Samantha Medwid², and Richard B. Kim^{2,3,4}

¹Department of Physiology and Pharmacology, Western University, London, ON, Canada,

²Department of Medicine, Western University, London, ON, Canada, ³London Health Sciences Centre, London, ON, Canada, ⁴Lawson Health Research Institute, London, ON, Canada

Introduction: Breast cancer is one of the most frequently diagnosed cancers worldwide. Patients with estrogen receptor positive (ER+) breast cancer are commonly prescribed tamoxifen, an antiestrogen therapy. Therapeutic outcomes have mainly focused on characterizing the extent of tamoxifen metabolism into its principal active metabolite endoxifen. However, up to 40% of patients will develop *de novo* or acquired tamoxifen resistance during therapy. Furthermore, therapeutic failure in patients who attain normal endoxifen plasma levels suggests that there are contributing factors independent of tamoxifen metabolism. Based on previous studies, we propose that altered expression of drug uptake transporters may impact estrogen as well as tamoxifen and its metabolite disposition and thereby modulate the extent of ER activation in target breast cancer tissues. It has been previously shown that certain organic anion transporting polypeptides (OATPs; OATP2B1 and OATP1A2) have altered expression in malignant breast cancer tissue compared to healthy breast tissue. Therefore, the objective of our study is to characterize the impact of tamoxifen and endoxifen on OATP-mediated estrogen transport.

Methods: Cellular uptake assays were conducted by transiently transfecting HEK293T cells with vector-only control (pcDNA), OATP1A2, or OATP2B1 plasmids. To determine if endoxifen and tamoxifen inhibit transport of estrone 3-sulfate (E1S), cells were treated with 1 μ g/mL of E1S alone and in combination with 1 μ M endoxifen, tamoxifen, or rifampicin (OATP inhibitor) in a 10-minute co-incubation. Relative intracellular E1S concentration was measured using ultra-high performance liquid-chromatography tandem mass-spectrometry (UHPLC-MS/MS).

Results: HEK293T cells transfected with OATP1A2 and OATP2B1 showed a 224.6% ($p=0.0015$) and 521.7% ($p=0.0001$) increase in E1S uptake compared to control, respectively. As expected, rifampicin treatment markedly inhibited E1S transport by 52.6% ($p=0.02$) and 73.2% ($p=0.0001$) in both OATP1A2 and OATP2B1, respectively. Endoxifen treatment also significantly inhibited E1S transport in OATP1A2 and OATP2B1 transfected cells by 44.0% ($p=0.0395$) and 31.2% ($p=0.0017$), respectively compared to OATP transfection alone. Interestingly, tamoxifen treatment significantly decreased E1S transport by 58.9% in OATP2B1 ($p=0.0001$), but not in OATP1A2 ($p>0.05$) transfected cells.

Conclusions: Our study demonstrates that tamoxifen and endoxifen can directly modulate OATP-mediated transport of E1S. Accordingly, altered OATP transporter activity could play a significant role in modulating ER activation and possibly tamoxifen therapeutic response. Studying the functional implications of drug transporters in breast cancer could provide important insights to their clinical relevance.

Investigating sequential and combined treatments of carboplatin and PARP inhibitors using three-dimensional culture models of advanced high-grade serous ovarian cancer

J Davis^{1,2}, E Tomas^{2,3}, Y Ramos Valdes², G E DiMattia^{2,4,5} J McGee⁶ and TG Shepherd^{2,3,4,6}

¹Schulich School of Medicine and Dentistry, London, Ontario, Canada ²Mary & John Knight Translational Ovarian Cancer Research Unit, London Regional Cancer Program, London, ON Departments of ³Anatomy & Cell Biology, ⁴Oncology, ⁵Biochemistry, ⁶Obstetrics and Gynecology Western University, London ON

Introduction: Epithelial ovarian cancer is a deadly gynecological malignancy with an insidious disease onset and inadequate treatment options. PARP inhibitors (PARPi) are a targeted therapy that uses a synthetic lethal strategy to exploit homologous recombination repair deficiencies, which are present in over half of high-grade serous epithelial ovarian cancer (HGSOC) cases. Olaparib and niraparib are currently approved as maintenance therapy in platinum-sensitive HGSOC, and their utility in the neoadjuvant setting is recently under investigation. Thus, our objective is to determine the utility of PARPis as sequential or combination therapy with standard-of-care chemotherapy, carboplatin.

Methods: Ascites-derived malignant cells from eight patients with HGSOC who underwent cytoreductive surgery at London Health Sciences Centre have been established as new cell lines in adherent conditions. Tumour cells were grown as organoids in defined culture conditions, then drug treatments with PARPi (i.e., olaparib or niraparib) and carboplatin in combination or sequence were applied.

Results: The IC₅₀ values for treatment with olaparib and niraparib are heterogeneous across cell lines and variable between two inhibitors. A *BRCA1* mutant line showed sensitivity to both drugs, while other lines showed resistance. Organoid experiments with combination treatment of carboplatin and olaparib have shown increased tumour cell killing. However, sequential treatments revealed variable effectiveness dependent upon the order of agent used. Homologous recombination repair deficiency status of the cell lines will be pursued to identify potential biomarkers for optimal treatment sequencing of PARPi and carboplatin.

Conclusions: Ex vivo patient-derived tumour models could inform future clinical trials testing PARPi in the neoadjuvant setting for women diagnosed with advanced high-grade serous ovarian cancer.

Abstract Title: Detection and Delineation of Intraprostatic Lesions (IPLs) using multiparametric Magnetic Resonance Imaging (mpMRI) and Prostate Specific Membrane Antigen Positron Emission Tomography (PSMA PET) for Patients with Prostate Cancer – A Meta-Analysis.

Authors: Aneesh Dhar¹, Jose de Jesus Cendejas-Gomez¹, Lucas C. Mendez¹, Gabriel Boldt¹, Eric McArthur¹, Constantinos Zamboglou^{2,3}, and Glenn Stuart Bauman¹

Affiliations: ¹London Health Sciences Centre, London, Ontario, Canada, ²Department of Radiation Oncology, Medical Center – University of Freiburg, Freiburg, Germany, ³German Oncology Center, European University Cyprus, Limassol, Cyprus.

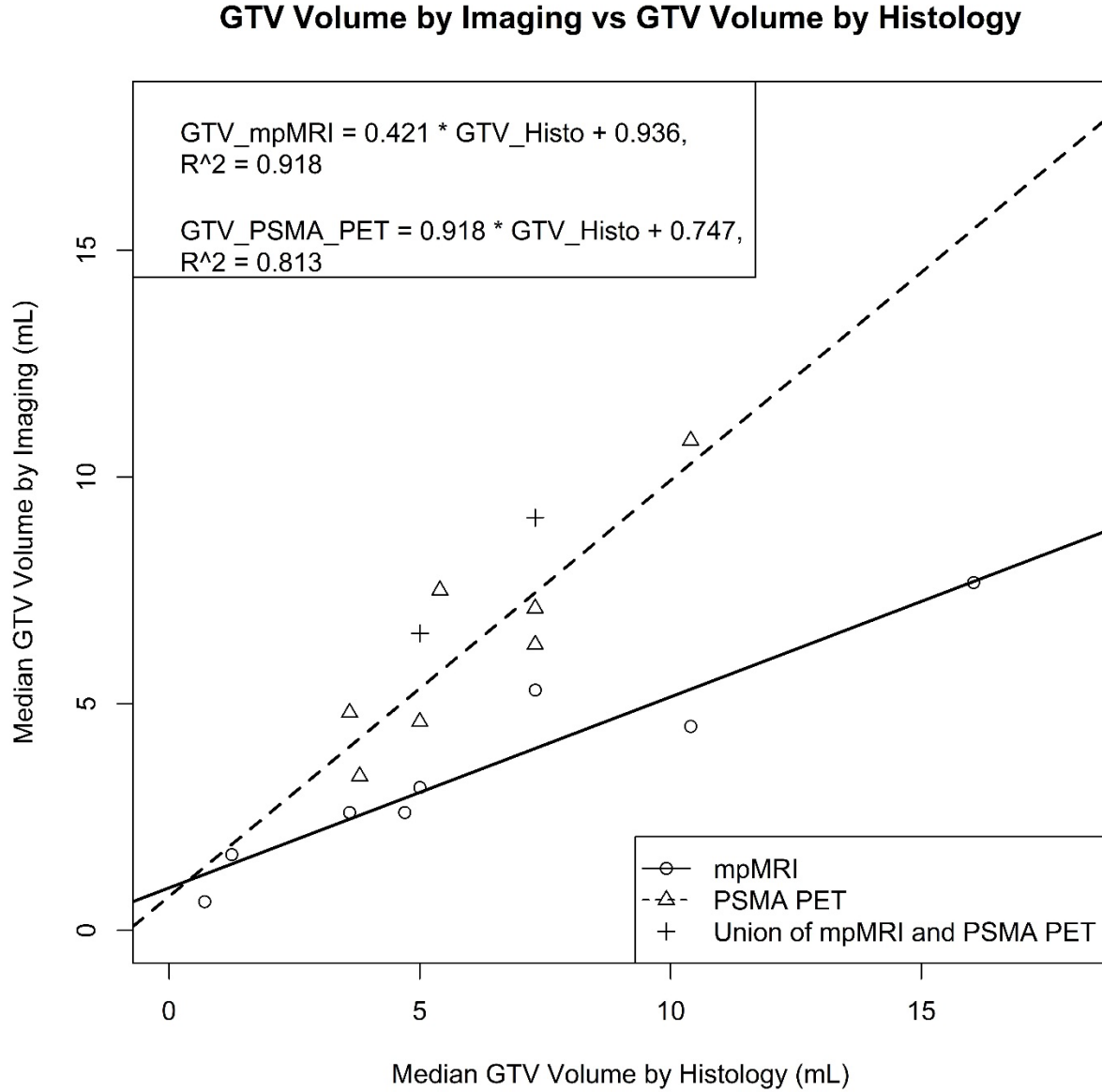
Introduction: Isolated local failures can occur in up to 13% of patients receiving EBRT for prostate cancer. Most ILFs occur at the location of the previously known intraprostatic lesions (IPLs). Treating patients using EBRT with a focal boost to the IPL improves cancer outcomes, without increasing toxicity. Both mpMRI and PSMA PET can be used to localize IPL for these patients.

Methods: A systematic review and meta-analysis was conducted for the use of mpMRI and PSMA PET for the detection and delineation of IPLs for patients with localized prostate cancer. Trials were included if patients received either mpMRI, PSMA PET, or both, prior to radical prostatectomy (RP). IPLs on RP specimens were used as the reference standard. The quality of the co-registration between imaging and histology was assessed as high or low for each study included in the systematic review. Outcomes that were recorded include sensitivity and specificity, the volume of the IPLs on imaging and histology, among others. A meta-analysis was conducted using a bivariate model to determine the sensitivity, specificity, and area under the receiver operating curve (AUROC) of mpMRI, PSMA PET, and their combination. This systematic review was registered through PROSPERO ([CRD42023389092](https://doi.org/10.1136/2023.01.12.2023389092)).

Results: After exclusions, 20 studies were incorporated into the bivariate meta-analysis. In total, there were 13 studies using mpMRI (n = 541 patients), 12 studies that used PSMA PET (n = 327), and 5 studies that used a combination (n = 180). The pooled sensitivity (95% CI), specificity (95% CI) and AUROC for mpMRI were 64.7% (50.2% – 76.9%), 86.4% (79.7% - 91.1%), and 0.852; the pooled outcomes for PSMA PET were 75.7% (64.0% - 84.5%), 87.1% (80.2% - 91.9%), and 0.889; for their combination, the pooled outcomes were 70.3% (64.1% - 75.9%), 81.9% (71.9% - 88.8%), and 0.796. When comparing the volumes of the IPLs, the volume on mpMRI tended to be smaller than the volume on histology, while the volume on PSMA PET correlated well with the volume on histology (Figure 1).

Conclusions: In this study, we conducted a meta-analysis of studies that used mpMRI, PSMA PET or their combination prior to RP for patients with localized prostate cancer. The pooled sensitivity and specificity for each modality had overlapping 95% confidence intervals, suggesting the modalities have similar accuracy in detecting IPLs on RP specimens. The volume of the IPL on mpMRI tended to be smaller than the volume on histology, while the volume on PSMA PET correlated well with histology.

Figure 1. Volume of the Gross Tumor Volume (GTV) based on imaging compared with the volume based on histology, for mpMRI, PSMA PET and their combination. The solid line represents the line of best fit for the mpMRI studies, and the dashed line represents the line of best fit for the PSMA PET studies.



Exploring the transferability of pathologists' visual search strategies to non-domain specific search tasks

Alana Lopes¹, Sean Rasmussen, MD², Ryan Au¹, Tricia Chinnery¹, Jaryd Christie¹, Bojana Djordjevic, MD², Jose A. Gomez, MD², Natalie Grindrod³, Robert Policelli¹, Anurag Sharma, MD², Christopher Tran, MD², Joanna Walsh, MD², Bret Wehrli, MD², Aaron D. Ward, PhD^{1,4}, and Matthew Cecchini, MD^{2,3}

¹Departments of Medical Biophysics, ³Pathology, and ⁴Oncology, Western University, London ON, Canada

²Department of Pathology and Laboratory Medicine, London Health Sciences Centre, London ON, Canada

Introduction: The role of a pathologist involves routinely completing numerous image search and classification tasks. The identification of tumour in lymph nodes is an example of a repetitive rare element search task that requires pathologists to identify and classify small foci of tumour, which can subsequently change the course of a patient's care by adding additional therapies to their treatment plan. In general, pathologists rely on their image search and classification skills to determine their final diagnostic assessment. For this reason, pathology is a field that requires years of training for visual search and classification of cellular features. This raises the question of whether this training gives pathologists an advantage in image search tasks outside of pathology. This study used eye tracking technology to determine if pathologists' training translates to a non-domain specific search task, and whether pathologists perform this search task differently from lay observers and differently than they perform a domain specific search task.

Methods: Six pathologists were recruited as observers and six graduate students were recruited as lay observers. The non-domain specific task had all observers search for Waldo in five "Where's Waldo?" puzzles. The domain specific task had pathologists search for a single mitotic figure in five digital breast pathology slide images (Fig. 1). Observers' eye gaze data were collected using the Tobii Pro Fusion eye tracker. False negative rate (FNR), when the observer misclassified the target of their fixation, was recorded. Linear discriminant analysis (LDA) was used to find the one-dimensional representation that best separated the observer groups based on their fixation and saccade rate, gaze transition entropy, and median fixation duration, saccade amplitude, peak saccade velocity, and image area covered by and overlapped with fixations. For reference, fixations are the maintenance of eye gaze on a single location, saccades are the rapid movement of eyes between fixations, and gaze transition entropy measures the complexity and predictability of eye movements. All significance thresholds were set to a p value of 0.004.



Fig. 1: Digital breast pathology image; mitotic figure circled in red.

Results: There was no significant difference between pathologists and laypeople for FNR. Pathologists' median fixation rate was 3.17/s vs. 2.61/s for laypeople ($p < 0.0001$). Saccade rate was 2.77/s for pathologists vs. 2.47/s for laypeople ($p < 0.0001$). Median gaze transition entropy was equivalent amongst both groups. Pathologists had shorter median fixation durations (244ms) than laypeople (300ms, $p < 0.0001$). Median saccade amplitude of pathologists was 1.47° vs. 1.40° for laypeople ($p = 0.60$). Pathologists' peak saccade velocity was $82.1^\circ/s$ vs. $77.8^\circ/s$ for laypeople ($p = 0.02$). No significant difference was found between the two cohorts for image area covered by and overlapped with fixations. Pathologists' scan paths differed from those of laypeople with an LDA misclassification rate of 10.2%. Further, pathologists' scan paths for Waldo vs. mitotic figures differed with a 0% LDA misclassification rate, indicating the scan paths were fully separable.

Conclusions: Pathologists' training does not improve accuracy in non-domain search tasks but does improve the speed of both their search and classification, without affecting FNR. This implies pathologists can rapidly classify the objects of their fixations without compromising accuracy.

A frame-averaging technique for low-dose volumetric 4D-CT image quality enhancement and motion assessment

Yau T^{1,2}, Mehrez H³, S Gaede^{1,2}

¹Department of Medical Biophysics, Western University, ²London Regional Cancer Program,

³Canon Medical Systems

Introduction: Currently, four-dimensional computed tomography (4D-CT) is standard-of-care imaging for thoracic cancers to visualize tumour motion. However, conventional CT scanners are only capable of imaging with a thin axial-field-of-view (aFOV) up to 40mm, making image reconstructions prone to motion artifacts while reproducing only a single respiratory cycle. Comparatively, volumetric 4D-CT (v4D-CT) is capable of imaging with up to a 160mm aFOV, allowing for true dynamic imaging of tumour motion over multiple respiratory cycles free from conventional motion artifacts. However, the extended scan duration and wider aFOV can significantly increase imaging dose to the patient. A low-dose v4D-CT scan may mitigate imaging dose to the patient while allowing for retrospective image quality enhancement via frame-averaging of the 4D dataset. This study investigates the utility of a novel, low-dose, v4D-CT imaging protocol that provides a more robust motion assessment compared to conventional 4D-CT without sacrificing image quality.

Methods: A Catphan 504 phantom and QUASAR motion phantom with Delrin spheres embedded within a cedar insert were imaged on an Aquilion ONE PRISM CT scanner for 1 minute using a 160mm axial-field-of-view and 0.275s rotation time. The Catphan was imaged using an x-ray tube current of 10mA and 300mA, while the QUASAR phantom was imaged at 10mA and 100mA. All Images were reconstructed using a Deep Learning Reconstruction Algorithm with 0.5mm slice thickness. Imaging dose was assessed using a CT dose index ($CTDI_{vol}$). Catphan modules for noise, line-pair resolution, and low-contrast resolution were analyzed. Line-pair resolution was assessed using a modulation transfer function (MTF) and low-contrast visibility was calculated according to the Rose model. The 10mA Catphan images were frame-averaged, and metrics reassessed as functions of number of frames. The QUASAR phantom was imaged during sinusoidal motion with a 2cm peak-to-peak amplitude and a period of 4s. QUASAR inserts were thresholded and the centroid tracked in the 10mA and 100mA scan to verify low-dose motion assessment.

Results: $CTDI_{vol}$ values for the 10mA scans were 28-32mGy, compared to 280mGy and 930mGy in the 100mA and 300mA scan respectively. The extracted motion profiles from the 10mA and 100mA QUASAR phantom datasets were found to be highly correlated ($r^2 > 0.88$, $p < 0.001$). MTFs did not change with frame averaging. CT noise as a function of frames averaged was found to decrease exponentially using a single-term power function ($r^2 > 0.99$, $p < 0.001$), with under 5 frames required to achieve CT noise in the 10mA equivalent to the 300mA scan. Low-contrast visibility scores improved with frame averaging, with no inserts visible initially in the 10mA scan increasing to 8 out of 9 inserts visible in the frame-averaged image.

Conclusion: Motion assessment is feasible using low-dose v4D-CT, with significant image quality improvements observed with retrospective frame-averaging at a fraction of the imaging dose.

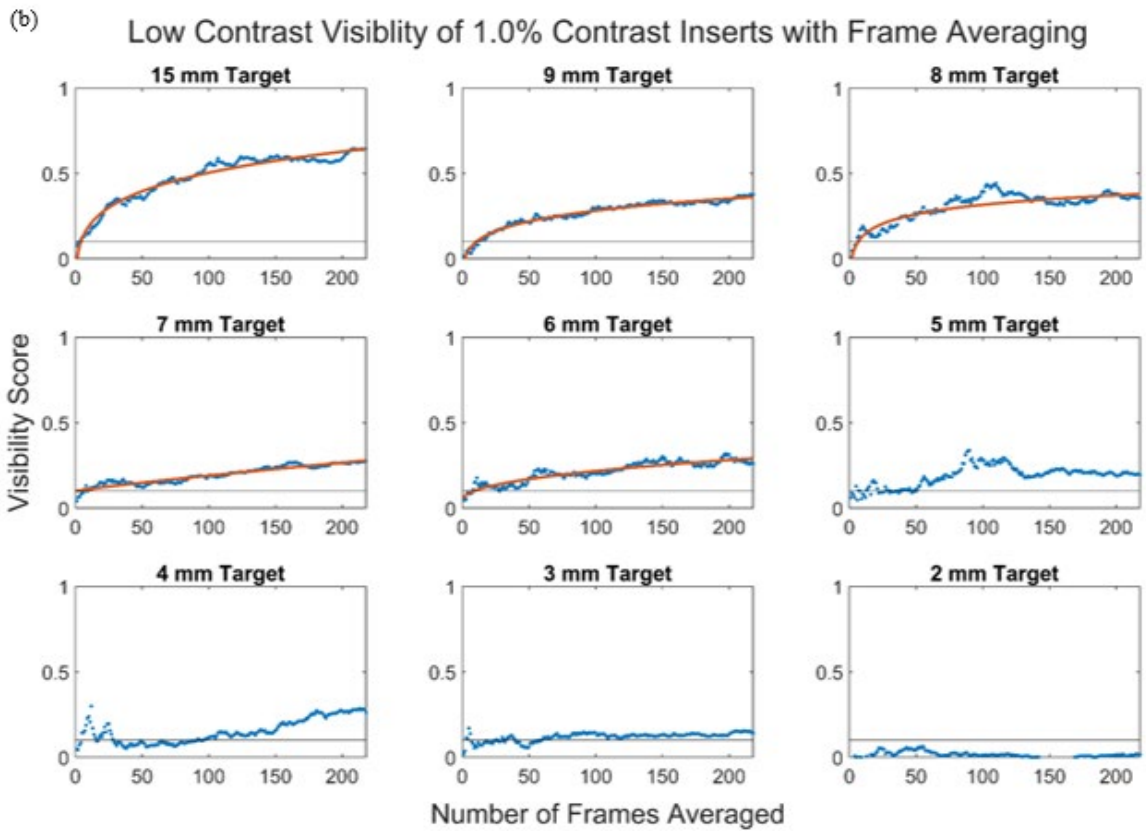
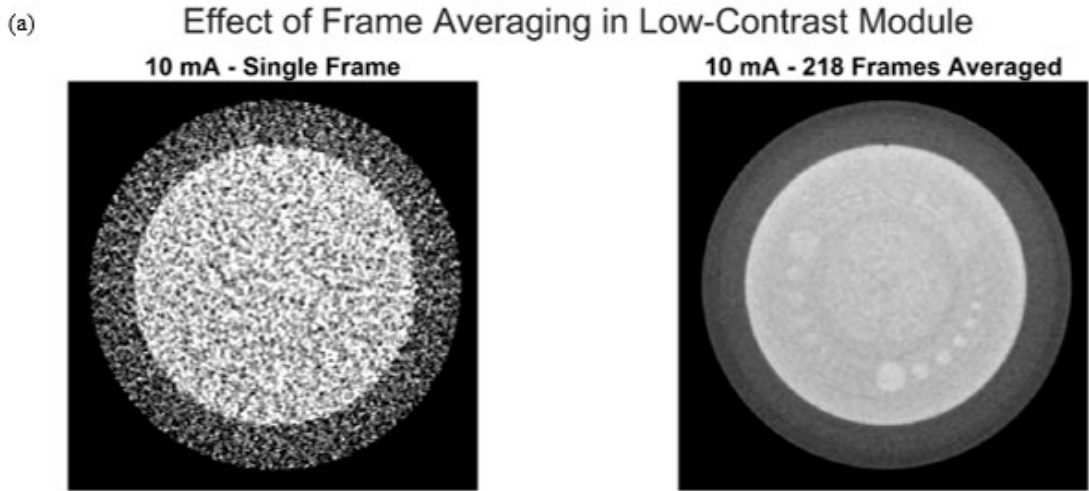


Figure 1: Scans of the low-contrast module before and after frame averaging displayed at a Window Level/Window Width of 20/120 (a). Visibility scores in the 10mA scan as a function of frames averaged is shown in (b), where the horizontal line in each graph identifies the visibility score from the 300mA scan.

#26 - Sawyer Badiuk - WITHDRAWN

Prediction of brain metastases progression after stereotactic radiosurgery: sensitivity to changing the definition of progression

Robert Policelli¹, David DeVries², Joanna Laba^{2,3}, Andrew Leung⁴, Terence Tang², Ghada Alqaidy⁵, Ali Albweady⁶, George Hajdok⁷, and Aaron D. Ward^{1,3}.

Department of ¹Medical Biophysics, Western University, London, Ontario; Department of ²Radiation Departments of Oncology, London Regional Cancer Program, London Health Sciences Centre, London, Ontario; Departments of ³Oncology, ⁴Medical Imaging, Western University, London, Ontario; ⁵Radiodiagnostic and Medical Imaging Department, King Fahad Armed Forces Hospital, Jeddah, Saudi Arabia; ⁶Department of Radiology, Unaizah College of Medicine and Medical Sciences, Qassim University, Unaizah, Saudi Arabia; ⁷Department of Medical Physics, Tom Baker Cancer Centre, University of Calgary, Calgary, Alberta

Introduction: Stereotactic radiosurgery (SRS) is a treatment option for patients with brain metastases (BMs), but BMs can progress post-treatment. Machine learning (ML) has been used to predict tumour progression post-SRS based on pre-treatment MRI, but there is variability in the definition of what constitutes progression, which could impede research comparisons and clinical translation. To better understand the impact of this variability in the definition of progression, we measured how the performance of a ML model changed in predicting post-SRS progression when the definition of progression was altered.

Methods: We collected pre- and post-SRS contrast-enhanced T1-weighted MRI scans from 62 BM patients (n=115 BMs). We extracted 107 radiomic features from the pre-treatment scans and then trained random decision forest models to predict progression vs. non-progression for each BM. We varied the definition of progression by changing (1) time post-SRS over which progression was measured (<9, <12, <15, <18, or <24 months), (2) whether tumour progression was measured by an increase in volume ($\geq 10\%$, $\geq 15\%$, $\geq 20\%$, or $\geq 25\%$), or by Response Assessment in Neuro-Oncology (RANO) BM diameter, and (3) whether patients with radiation oncologist-assessed treatment related size changes (pseudo-progression or radiation necrosis) were labeled as progression. We measured performance using the area under the receiver operating characteristic curve (AUC).

Results: When we varied the time, the measurement technique, and labeling of treatment related size changes, the AUCs had a range of 0.06 (0.69–0.75), 0.06 (0.69–0.75), and 0.08 (0.69–0.77), respectively (Table 1).

Conclusions: Variability in the definition of BM progression used in published studies has a measurable impact on the performance of an MRI radiomics ML model predicting progression. This variability caused AUCs to vary by as much as 0.08. A consistent, clinically-relevant definition of post-SRS progression across studies would enable robust comparison of proposed ML systems, thereby accelerating progress in this field. This could allow for more reproducible research that can help validate and create tools which will eventually assist physicians in determining the suitability of SRS for their patients.

Table 1: The experimental configurations we used and the corresponding model performance (area under the receiver operating characteristic curve [AUC]). Size change metric is the minimum size change to denote BM progression. CI = 95% confidence interval.

Experiment	AUC [CI]
Progression Follow Up Period	
< 24 Months	0.75 [0.74 – 0.76]
< 18 Months	0.73 [0.72 – 0.75]
< 15 Months	0.73 [0.72 – 0.75]
< 12 Months	0.73 [0.72 – 0.75]
< 9 Months	0.69 [0.68 – 0.71]
Size Change Metric	
> 25% Volume	0.75 [0.74 – 0.76]
> 20% Volume	0.75 [0.74 – 0.76]
> 15% Volume	0.71 [0.70 – 0.73]
> 10% Volume	0.70 [0.68 – 0.71]
> 20% RANO-BM Diameter	0.69 [0.67 – 0.70]
Treatment Related Size Change Inclusion	
Both Pseudo-Progression and Radiation Necrosis \neq Progression	0.75 [0.74 – 0.76]
Pseudo-Progression \neq Progression	0.69 [0.68 – 0.70]
Radiation Necrosis \neq Progression	0.77 [0.76 – 0.78]
Both Pseudo-Progression and Radiation Necrosis = Progression	0.73 [0.72 – 0.74]

Dual Molecular Imaging of Viable Breast Cancer Cells and Immune Cell Recruitment in Immunocompetent Mouse Models

Jasmine Lau¹, Sean McRae¹, Ying Xia¹, Rafael Sanchez Pupo¹, John A. Ronald¹

¹Robarts Research Institute, University of Western Ontario, London, ON, Canada

Introduction: Many imaging reporter genes can be used to dynamically track the fate of transplanted cells *in vivo*, including cancer cells or therapeutic cells. However, common optical reporters are foreign to mice and can alter normal immune responses or even provoke the rejection of cells one wants to track in immunocompetent animals. We previously developed human organic anion transporting polypeptide 1B3 (OATP1B3) as a translationally relevant magnetic resonance imaging (MRI) reporter, which takes up the clinically relevant contrast agent Gd-EOB-DTPA. OATP-mediated Gd uptake provides enhanced conspicuity of viable cancer cells within a tumour and therefore improves visualization of non-enhancing necrotic regions in the tumour.

In this work, we developed a novel mouse-derived MR reporter gene, mOatp1a1, for use in immunotolerant mice. We studied the relationship between viable cancer cells within a tumour, using mOatp1a1, and immune cell recruitment to the tumour microenvironment, using Fluorine-19 MRI, a complementary “hot-spot” imaging technique previously used to image tumour-associated macrophages (TAMs).

Methods: Cell Sorting: 4T1 murine breast cancer cells were transduced using 3rd-generation lentiviruses to stably express mOatp1a1. To sort for engineered cells, we tested various fluorescent dyes for mOatp1a1 transport via flow cytometry. **In vitro MRI:** Naïve and mOatp1a1-engineered cells were incubated with and without Gd-EOB-DTPA (1.6mmol/L) and MR images were collected on a 3T scanner using a fast spin echo inversion recovery (FSE-IR) pulse sequence to compare signal enhancement. **In vivo ¹H MRI:** Immunocompetent female Balb/c mice (n=2) were implanted bilaterally with naïve and mOatp1a1-expressing 4T1 cells. Mice were imaged weekly using a 3D-Spoiled gradient-recalled echo pulse sequence before and 5 hours after systemic injection of Gd-EOB-DTPA (1.5mmol/kg). **In vivo ¹⁹F MRI:** At the final imaging time point (day 26), mice were imaged with Balanced Steady-State Free Precession pulse sequence 24 hours after systemic injection of 200 µL of a perfluorocarbon agent (V-Sense, VS-1000H).

Results: Sulforhodamine-101 (SR-101) showed uptake into mOatp1a1-expressing cells, allowing sorting of engineered cells. mOatp1a1-engineered cells incubated with Gd-EOB-DTPA had significantly higher signal than naïve cells (p<0.0074). *In vivo*, mOatp1a1 tumours showed improved conspicuity, but not naïve tumours. Interestingly, heterogeneous intratumoral enhancement patterns were seen in mOatp1a1 tumours which increased at later time points, highlighting the value of this system for improved visualization of live cancer cells (Figure 1A-B). Furthermore, we observed TAMs at the periphery of both naïve and engineered tumours and the co-localization of TAMs within the non-enhancing regions of mOatp1a1-engineered tumours (Figure 1C).

Discussion: Overall, we have developed the first MRI reporter for positive-contrast detection of engineered cells in immunocompetent mice. Using this reporter gene, we demonstrated

improved ability to distinguish viable cancer cells from necrotic regions in a tumour within the context of the tumour microenvironment. Future experiments on a larger mouse cohort and histological analyses of tumor sections will be performed. Because very few immunotolerant reporter genes exist in the toolbox of cell tracking, these findings provide a system for tracking of gene and genome therapeutics or cellular therapies for cancer in immunocompetent murine models.

[490 words]

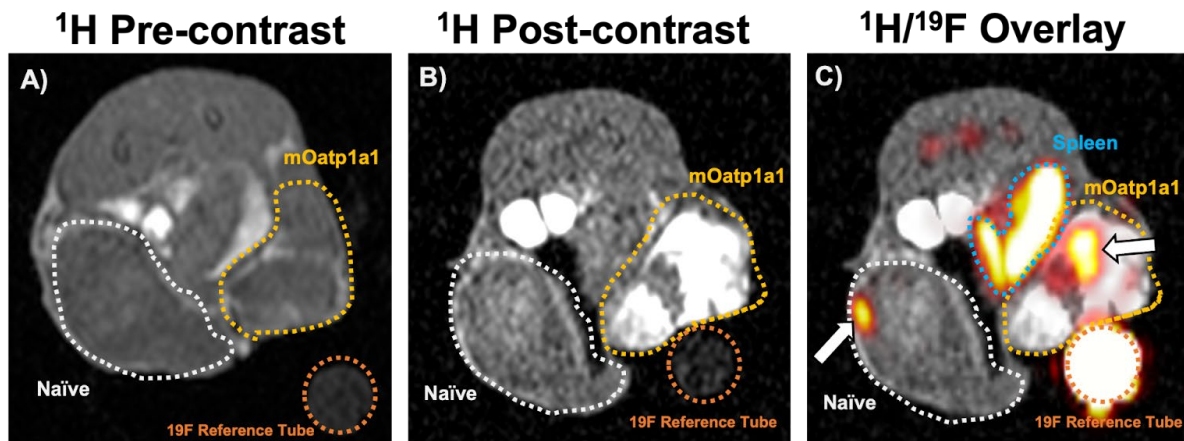


Figure 1. MR images showing mOatp1a1-mediated Gd uptake provides enhanced visualization of viable tumour cells, with corresponding TAM distribution at day 26 post-tumour implantation. The locations of the naive tumour are indicated by the white outline and the mOatp1a1-engineered tumour are indicated by the yellow outline. A) Pre-contrast ^1H MR image of a representative mouse (axial view). B) Post-contrast ^1H MR image (axial view) 5 hours after intravenous injection of Gd-EOB-DTPA (1.5mmol/kg). C) Overlay of ^1H and ^{19}F MR images (axial view) 24 hours after intravenous injection of a perfluorocarbon agent (V-Sense, VS-1000H). Image shows the relative co-localization of TAMs (indicated by the white arrows) at the periphery of viable cancer cells in the tumour.

Initial performance evaluation of helical and volumetric dual energy CT acquisitions using the Canon Aquilion Exceed LB

Samuel Blake¹, Timothy Yau^{1,2}, Hatem Mehrez³, Brandon Disher¹, and Stewart Gaede^{1,2}

¹London Health Sciences Centre, ²Western University, ³Canon Medical Systems Canada

Introduction: Single-energy (SE) x-ray computed tomography (CT) is the primary imaging modality used for radiotherapy simulation and treatment planning. Dual-energy (DE) scans using low and high tube voltages (e.g. 80/135 kVp) enable reconstruction of synthetic images that cannot be done using conventional SE scans (e.g. 120 kVp). Importantly, DE 80/135 kVp protocols can be used to generate synthetic 120 kV-equivalent images. While DE CT has been widely adopted in diagnostic imaging, literature characterizing DE for radiotherapy applications is scarce. The Canon Aquilion Exceed LB CT simulator at our centre is capable of DE data acquisition using helical and volumetric modes. This study's aim was to perform an initial evaluation of these DE scan modes relative to the SE helical scan mode used clinically for radiotherapy simulation and treatment planning.

Methods: Single-energy 120 kVp (SE-120), dual-energy 80/135 kVp helical (DEHEL) and volumetric (DEVOL) modes were used to acquire scan data of three phantoms. All images were reconstructed using Canon's Adaptive Iterative Dose Reduction 3D algorithm and synthetic 120 kV-equivalent images were reconstructed from the DEHEL (DEHEL-120) and DEVOL (DEVOL-120) data for comparison to the SE-120 reconstructions. The TomoTherapy "cheese" phantom was imaged to quantify CT number linearity across several tissue-mimicking inserts; the Catphan CTP604 image quality phantom was imaged to quantify noise, spatial resolution and low contrast visibility (LCV); and the Alderson RANDO anthropomorphic phantom was imaged to qualitatively assess images of humanoid anatomy. All images were analysed and compared using Matlab R2023b.

Results: SE-120, DEHEL-120 and DEVOL-120 images of the CTP604 (LCV module only) and RANDO anthropomorphic phantoms are shown in Figure 1. CT numbers from SE-120, DEHEL-120 and DEVOL-120 images agreed for all tissue-mimicking inserts (maximum differences from nominal values were 5.3, 7.8 and 21.3 HU, respectively), demonstrating consistent CT number linearity across the protocols examined. Noise (quantified as the standard deviation within a uniform region of interest) was 8.9, 13.2 and 8.0 HU for the SE-120, DEHEL-120 and DEVOL-120 images, respectively. Spatial resolution (quantified at 80% and 50% of the relative modulation transfer function) was 1.7 and 2.6; 1.8 and 2.7; 1.6 and 2.5 lp/cm for the SE-120, DEHEL-120 and DEVOL-120 images, respectively. LCV for the 15 and 9 mm inserts were 0.19 and 0.14; 0.16 and 0.10; 0.27 and 0.22 for the SE-120, DEHEL-120 and DEVOL-120 images, respectively.

Conclusions: DE synthetic helical and volumetric 120 kV-equivalent images acquired on the Canon Aquilion Exceed LB exhibited comparable CT number linearity and image quality relative to conventional SE helical 120 kVp images. Work is ongoing to explore how DE 80/135 kVp protocols may improve clinical radiotherapy simulation and treatment planning workflows.

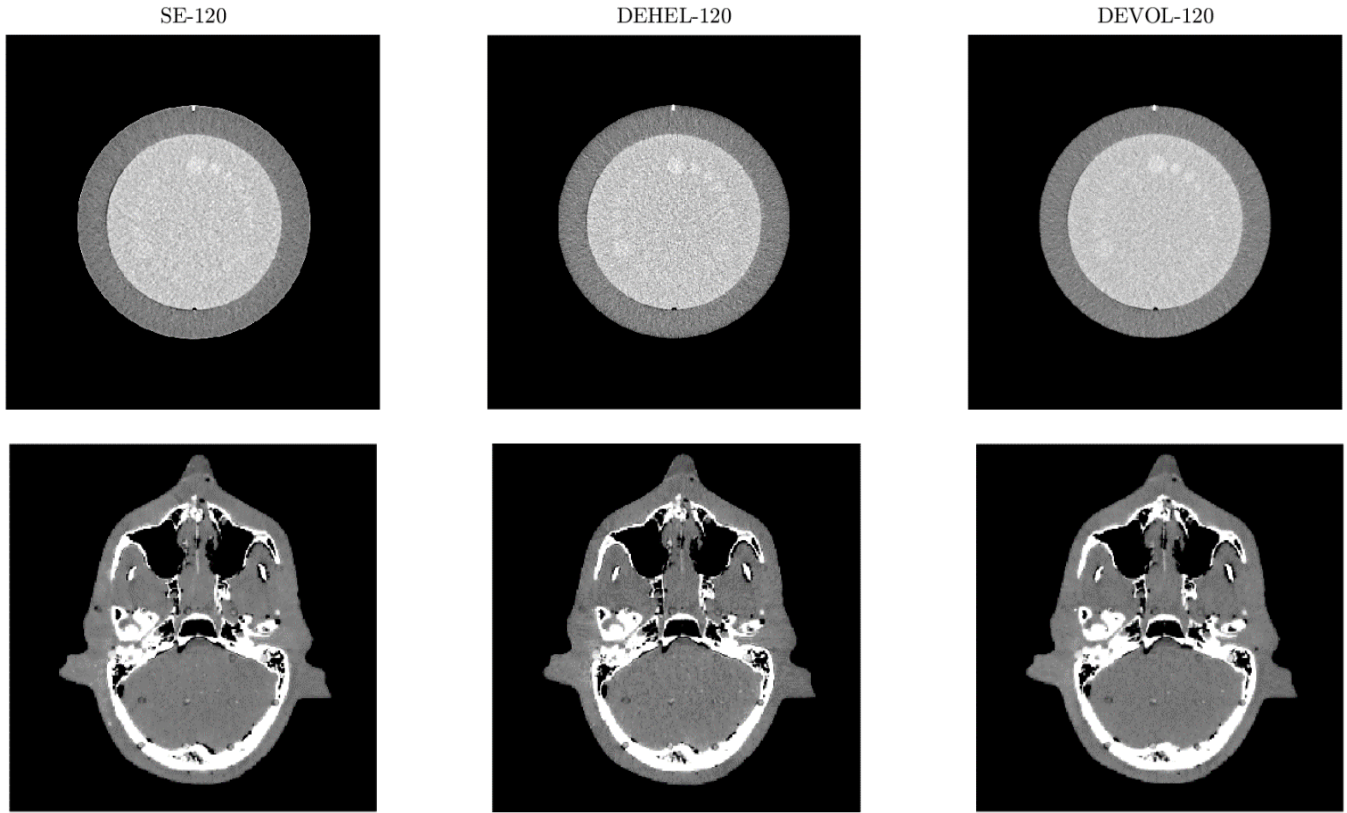


Figure 1. Single-slice SE-120, DEHEL-120 and DEVOL-120 images of the LCV module of the Catphan CTP604 image quality phantom (top row) and head region of the Alderson RANDO anthropomorphic phantom (bottom row).

Impacts of Automated Prostate Contouring on Brachytherapy Radiation Therapy Dose Delivery

David DeVries¹, Noah Blackburn-Hum^{1,2}, Lucas C. Mendez^{1,3}, David D'Souza^{1,3}, Vikram Velker^{1,3}, Rohann Correa^{1,3}, Joelle Helou^{1,3}, Aaron Fenster^{4,5,6}, and Doug Hoover^{1,3,4}

¹Department of Radiation Oncology, London Health Sciences Centre, ²Department of Physics, University of Waterloo, ³Department of Oncology, Western University, ⁴Department of Medical Biophysics, Western University, ⁵Robarts Research Institute, Western University, ⁶Department of Medical Imaging, Western University

Introduction: Brachytherapy radiation therapy treats prostate cancer by the insertion of a radioactive source through needles to various locations in the prostate to cover it with a radiation dose. Prostate brachytherapy is currently guided by manual contouring of the prostate on transrectal ultrasound (TRUS) by a radiation oncologist (RO) to ensure adequately radiation coverage. Automated prostate contouring on TRUS images would therefore potentially reduce procedure time and treatment variability. This study characterizes automated contouring's impact on brachytherapy radiation dose deliveries.

Methods: An artificial intelligence (AI) model was used to retrospectively re-contour the prostate on images from five patients treated with prostate brachytherapy. Five ROs also re-contoured each prostate four times generating two "manual" contours and two "AI-assisted" contours, where the AI contour was used a starting point. For each prostate contour, a new radiation plan/dose distribution was developed to cover the prostate using the same needle positions from the original treatment. Fully automated contouring was investigated by overlaying dose distributions from the treatment plans created using AI contours onto the ROs' manual contours to calculate the percentage of the prostate volume that received 90% and 100% of the prescribed radiation dose (V90 and V100), with V90>99% and V100>95% indicating clinically acceptable plans. Baseline metrics were calculated by overlaying the dose from an RO's manual contour plan onto the same RO's second manual contour (intra-RO) or other ROs' manual contours (inter-RO). AI-assisted contouring was investigated by overlaying the dose distributions developed using an RO's AI-assisted contour onto either the same RO's manual contours (intra-RO) or other ROs' manual contours (inter-RO).

Results: The plans created using the fully automated AI prostate contours met or exceeded V90>99% for 42% of the dose distributions on manual contour comparisons across all patients and ROs. This was lower than the intra-RO baseline (48%), but exceeded the inter-RO baseline (35%). For V100>95%, the AI contours achieved a 60% passing rate, which also was near the intra-RO baseline (62%) and exceeded the inter-RO baseline (47%). The plans created using AI-assisted contours resulted in higher V90 passing rates versus the baseline values when evaluated for both the intra-RO (53% vs. 48%) and inter-RO (50% vs. 35%) cases. The V100 showed similar trends, with the AI-assisted contours exceeding the intra-RO (63% vs. 60%) and inter-RO (59% vs. 47%) baselines. The attached figure shows the raw V90 and V100 values for plans made from the fully automated, AI-assisted (intra- and inter-RO), and manual/baseline (intra- and inter-RO) contours. Wilcoxon rank-sum tests across these groups show a statistically significant increase ($p<0.001$) of V90 and V100 for the AI-assisted method when compared inter-RO, with the fully automated method showing a more moderate increase in V90 and V100 ($p=0.06$ and $p=0.07$, respectively).

Conclusions: This study shows that using fully or semi-automated AI prostate TRUS contouring for prostate brachytherapy results in treatment plan radiation dose distributions that will acceptably cover the prostate. While fully automated contours were shown to not be inferior to manual contours, semi-automated contours demonstrated clear improvement, especially in reducing inter-clinician dosimetric variability.

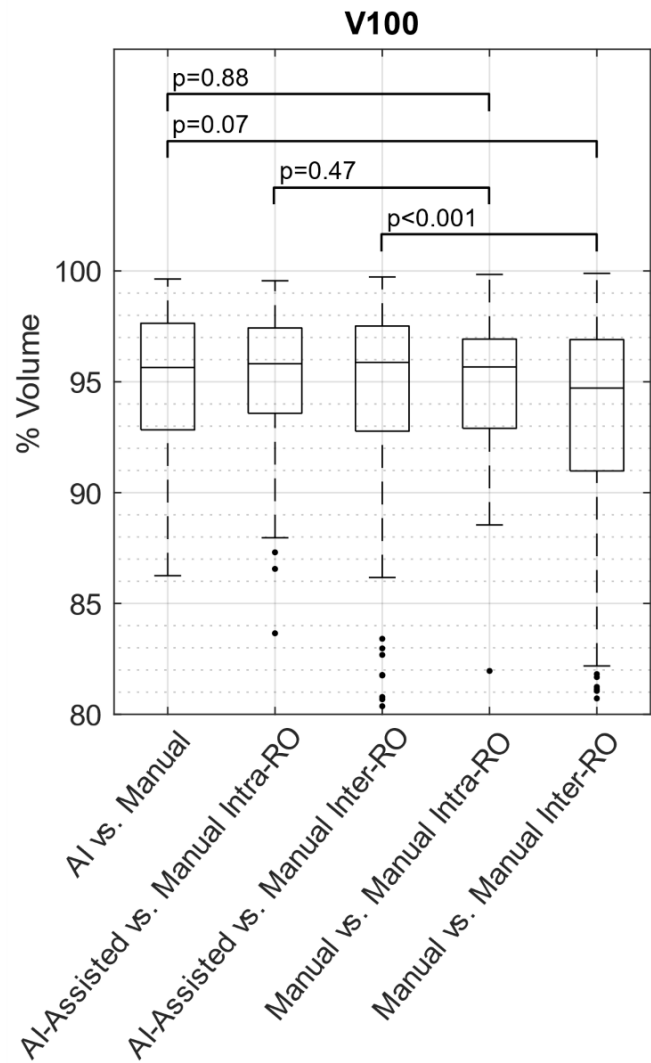
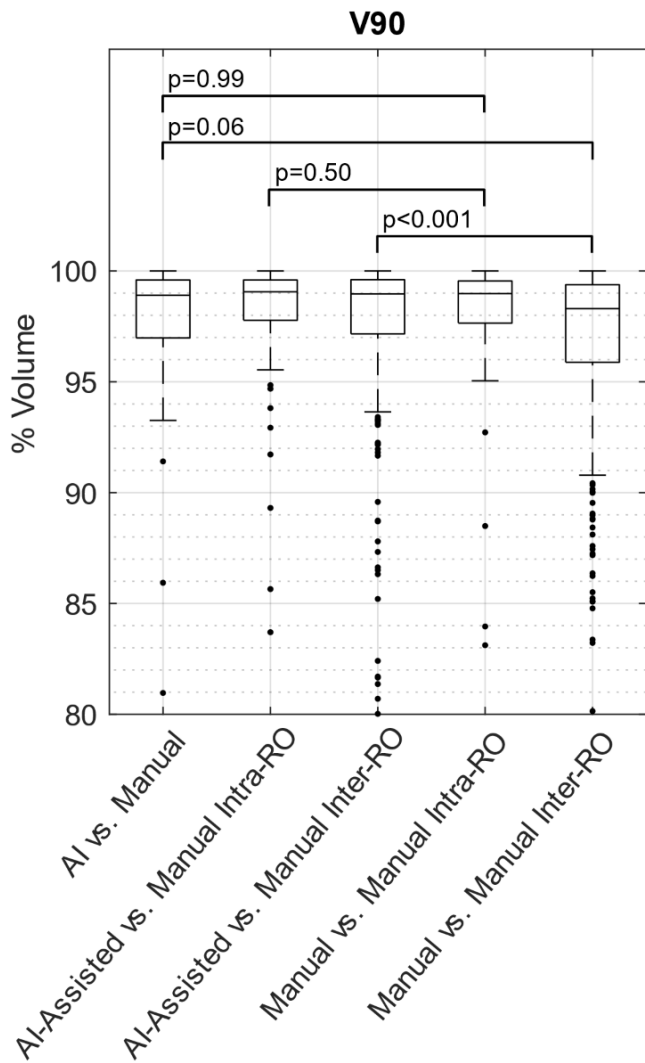


Figure Caption: Box-and-whisker plots of the raw V90 and V100 values for the five dose distribution vs. contour comparisons performed in the study. “AI vs. Manual” refers to a treatment plan generated using the fully-automated AI contours being evaluated on manual prostate contours from the ROs. “AI-Assisted vs. Manual” similarly assesses plans made using the AI-assisted contours being assessed on manual prostate contours from either the same RO that made the AI-assisted contours (“Intra-RO”) or the other ROs’ manual contours (“Inter-RO”). The baseline metrics are given by the “Manual vs. Manual” values, in which plans are made using manual contours from an RO and evaluated on either the same RO’s manual contours “Intra-RO” or the other ROs’ manual contours (“Inter-RO”). Wilcoxon rank-sum tests were performed across four pairings of dose distribution vs. contour comparisons to investigate differences from baseline.

Cyclic Peptide Assemblies as Nanoprobes for Prostate Cancer Imaging

Fátima Santillán¹, Leonard G. Luyt²

¹ Department of Chemistry, University of Western Ontario, London, Ontario N6A 3K7, Canada

² Departments of Chemistry and Departments of Medical Imaging and Oncology, University of Western Ontario, London, Ontario N6A 3K7, Canada; London Regional Cancer Program, Lawson Health Research Institute, London, Ontario N6A 4L6, Canada

Introduction: The use of peptide nanomaterials as imaging probes offers a promising alternative owing to its tailorable design, enhancing specificity towards molecular targets. In the realm of cancer diagnostics, optical imaging holds great potential, where precise targeting of biomarkers like the prostate-specific membrane antigen (PSMA) is relevant for prostate cancer detection. This study focuses on the design and co-assembly of cyclic peptide scaffolds that generates nanotubes. These nanotubes were fabricated through the aqueous pH-triggered self-assembly of D/L-alternating cyclic octapeptides. The main sequence is derived from cyclo-(D-Leu-Lys-D-Leu-Tyr)₂. Surface modification of the peptide was employed to improve its functionality, resulting in three additional peptides relevant for building the nanoprobes.

Methods: Purification of peptides was conducted using high-performance liquid chromatography. Characterization of the nanoprobes was performed using field emission scanning electron microscopy (FESEM), energy-dispersive X-ray (EDX) mapping, low-voltage transmission electron microscopy (LV-TEM), and circular dichroism (CD) spectroscopy. The binding specificity of the nanoprobes to prostate cancer cells was assessed using confocal fluorescence microscopy.

Results: FESEM imaging revealed the presence of arrays of nanotubes with an average diameter of 28 nm and lengths ranging from 100 – 400 nm. Complementary EDX mapping images confirm the presence of carbon, oxygen, and sodium distributed along the nanotubes surface. Low-voltage TEM also confirmed the formation of nanotubes with similar dimensions to FESEM. Moreover, CD spectroscopy demonstrated the presence of beta-sheet-like nanoassemblies that are stable at 22 °C and 37 °C.

Confocal fluorescence images demonstrated the targeting of the nanotubes to PSMA-expressing cancer cells. Z-stacking analysis of the images showed the partial internalization of our nanoprobes, indicating a possible mechanism involving endocytosis.

Discussion: The design of nanoprobes involved the co-assembly of four cyclic peptides. The parent octapeptide was cyclo-(D-Leu-Lys-D-Leu-Tyr)₂. The first modification entailed the integration of polymeric chains (methoxy-PEG) strategically designed to decrease the aggregation between nanotubes. Then, other modification included the attachment of a fluorescent dye (fluorescein) to serve as a signaling component, facilitating visualization, and tracking of the nanoprobes. Finally, the targeting peptide included a modified PSMA-targeting ligand, pivotal for prostate cancer imaging. This final modification ensures the selective binding to PSMA-expressing cancer cells, thereby maximizing the efficacy of the nanoprobes in diagnostic and therapeutic applications.

Conclusions: In conclusion, the development of these multifunctional nanoprobes underscores the potential for including other imaging modalities and opens the pathway to incorporate additional functionalities, such as drug delivery capabilities.

Acknowledgments: Natural Sciences Engineering Research Council of Canada (NSERC); Graduate Collaborative Program in Molecular Imaging (Western University).

The Synthesis of CXCR4-Targeted Alpha-Emitting Peptides as Theranostic Radiopharmaceuticals.

Nicholas Bainbridge¹, Len Luyt¹

¹University of Western Ontario, ²London Regional Cancer Program

Introduction: Alpha-emitting radionuclides offer exceptional killing efficiency and reduced collateral damage to healthy tissues owing to their short particle range and high linear energy transfer, distinguishing them from other beta emitting radionuclides. Actinium-225 therapeutics are of particular interest for its ten-day half-life, and five successive alpha decays making it a highly prominent option for cancer treatment, given a highly specific biological targeting agent. The extracellular chemokine receptor 4 (CXCR4) is overexpressed in numerous forms of cancers. To exploit the overexpression of CXCR4, we aim to develop a targeted actinium-225 radiopharmaceutical directed at the CXCR4 receptor. Previous work has found cyclic pentapeptides of high binding affinity to the CXCR4 binding site, however, few studies have investigated how the linker region between the targeting and chelator regions can interact with the receptor, affecting pharmacokinetic properties. The objective is to synthesize a diaza-18-crown-6 macrocyclic chelator analogue that conjugates to the peptide through solid phase peptide synthesis (SPPS) with high fidelity and design a linker region through molecular docking strategies to identify constituents for enhanced interactions with the surrounding binding pocket.

Methods: Peptide synthesis is accomplished using an orthogonal SPPS scheme. Chelator synthesis is conducted using standard synthetic chemistry practices and characterized using NMR spectroscopy and HPLC-MS. Molecular docking is performed using AutoDock 4, from a custom forcefield package calculated using Avogadro 4.2 from initial structures drawn in ChemDraw 22.4.

Results: A synthetic pathway has been successfully designed and carried out to yield the base diaza-18-crown-6 macrocyclic ring, and brominated, tert-butyl protected pendant arms for attachment to the ring. Initial molecular docking analysis of the binding pocket of CXCR4 reveals potential targets for binding enhancement interactions with the second extracellular loop such as hydrogen bonding with asparagine 181 and 182 and interactions with the N-terminus such as pi-pi stacking with phenylalanine 29.

Discussion: The biological targeting moiety was selected from previous studies optimizing the cyclic pentapeptide FC131. The chelator selected to contain the actinium-225 radionuclide is a macropa derivative with a free carboxylic acid handle on the base ring and the addition of tert-butyl ester protecting groups for the two carboxylic acid pendant arm moieties. Protected pendant arms enable the specific attachment of the chelator to the targeting components whilst on solid phase, creating a radiopharmaceutical scaffold that is readily adjustable in the peptide sequence for rapid linker optimization by installing variable amino acid sequences.

In future studies, the continuation along the synthetic path will yield actinium-225 radiopharmaceuticals targeting the CXCR4 receptor produced through SPPS with varying linker sequences to evaluate binding efficacy. Ultimately, this project emphasizes the importance of linker optimization when producing biological targeting therapeutics and develop a synthetic route to produce a modular actinium-225 chelator that can be attached to different peptides, producing alpha-decay radiopharmaceuticals in a high-throughput and efficient manner.

Acknowledgments: New Frontiers in Research Fund (NFRF); Collaborative Graduate Program in Molecular Imaging, Western University.

Fibroblast Activation Protein Targeted Theranostic Agents for Pancreatic Cancer

Priyanka Jagadeesa Prabhu^{1,2}, Len Luyt^{1,2,3}

¹Department of Chemistry, University of Western Ontario; ²London Regional Cancer Program; ³Departments of Oncology and Medical Imaging, University of Western Ontario

Introduction: Fibroblast activation protein (FAP) is a post-prolyl cleaving serine protease that is selective towards a Gly-Pro motif. Overexpression of FAP is seen in over 90% of epithelial carcinomas as well as in some non-epithelial cancer types.¹ In the tumour microenvironment, FAP is expressed in the Cancer-Associated Fibroblasts (CAF), where it is believed to promote angiogenesis and thus tumour growth.² UAMC-1110, a small molecule inhibitor of FAP, has been extensively used to develop FAP-targeting cancer imaging agents. These have been reported as promising alternatives to ¹⁸F-FDG PET scans for the diagnosis of pancreatic tumours due to the higher population of CAF.³ Yet, FAP-targeting agents for the more affordable and commonly accessible SPECT scans, have not been well studied. In this project, a recently reported inhibitor of FAP, BR102910 is used as a scaffold to develop ^{99m}Tc-based SPECT imaging agents. Structural similarity of ^{99m}Tc and Re complexes allows easier translation of a ^{99m}Tc-based SPECT agent into a ¹⁸⁶Re-based radiotherapeutic agent, leading to potential theranostic applications.

Method: The characteristic benzyl thiazole moiety of the BR102910 scaffold is introduced through the Hantzsch reaction, starting with benzyl thioamide. Additional synthetic steps include Buchwald-Hartwig cross-coupling, reductive amination, as well as peptide coupling reactions. [Re(CO)₃(H₂O)₃]OTf complex is used to synthesize the corresponding Re complexes.

Results: The synthesis of the radioligands involves the precursor, methyl 2-(4-bromobenzyl)thiazole-4-carboxylate, synthesized in three steps from 4-bromophenyl acetic acid with an overall yield of 70%. Linkers of different lengths will be introduced using tris(benzylideneacetone)dipalladium catalyzed reactions. Subsequently, the dipicolylamine chelator will be introduced via the reductive amination of 2-pyridinecarboxaldehyde. Hydrolysis of methyl ester followed by coupling of the glycyldifluoropyrrolidyl moiety will produce the required radioligands. In this context, tert-butyl (R)-(2-(2-cyano-4,4-difluoropyrrolidin-1-yl)-2-oxoethyl)carbamate has been successfully synthesized through the coupling of (S)-4,4-difluoropyrrolidine-2-carbonitrile and Boc-Gly-OH, yielding 61%. Radioligands complexed with the non-radioactive isotope, ¹⁸⁵Re will be used for the structural characterization in lieu of the radioactive ^{99m}Tc complex. A competitive binding assay will be used to evaluate their ability to target FAP. The most promising complex thus established, will also be evaluated for its affinity towards DPP4 and PREP to address its FAP selectivity. The radioligand will then be radiolabeled with ^{99m}Tc for *in vivo* evaluation of diagnostic potential in pancreatic cancer models. Further, the therapeutic potential will be evaluated using the ¹⁸⁶Re complexes. The outcomes of these evaluations will be compared to those of ⁶⁸Ga-FAPI-46, an established FAP-targeting theranostic agent.⁴

Conclusion: The highly aggressive nature of pancreatic cancers necessitates novel therapeutic approaches. In this project, ^{99m}Tc-SPECT imaging agents targeting FAP are being developed. ^{99m}Tc-SPECT agents often serve as models for the development of ¹⁸⁶Re-labelled therapeutic agents, suggesting the potential for theranostic applications. Additionally, the length of the spacer moiety between the BR102910 scaffold and the dipicolylamine chelator can be varied to study its effect and to modulate pharmacokinetics. Radiolabeling the lead compounds from the *in vitro* and *in vivo* evaluations with ^{99m}Tc and ¹⁸⁶Re will produce a theranostic agent with the potential to deliver targeted cancer imaging and radiotherapy for pancreatic cancer.

Acknowledgements: New Frontiers in Research Fund – Transformation; Natural Sciences and Engineering Research Council (NSERC) of Canada; Molecular Imaging Collaborative Program, University of Western Ontario; Nuclear Medicine, Victoria Hospital, London Health Sciences Centre

References:

- (1) Xin, L.; Gao, J.; Zheng, Z.; Chen, Y.; Lv, S.; Zhao, Z.; Yu, C.; Yang, X.; Zhang, R. Fibroblast Activation Protein- α as a Target in the Bench-to-Bedside Diagnosis and Treatment of Tumors: A Narrative Review. *Front. Oncol.* **2021**, *11*, 3187. <https://doi.org/10.3389/fonc.2021.648187>.
- (2) Santos, A. M.; Jung, J.; Aziz, N.; Kissil, J. L.; Puré, E. Targeting Fibroblast Activation Protein Inhibits Tumor Stromagenesis and Growth in Mice. *J. Clin. Invest.* **2009**, *119* (12), 3613–3625. <https://doi.org/10.1172/JCI38988>.
- (3) Lindner, T.; Giesel, F. L.; Kratochwil, C.; Serfling, S. E. Radioligands Targeting Fibroblast Activation Protein (FAP). *Cancers (Basel)*. **2021**, *13* (22), 1–12. <https://doi.org/10.3390/cancers13225744>.
- (4) Jung, H. J.; Nam, E. H.; Park, J. Y.; Ghosh, P.; Kim, I. S. Identification of BR102910 as a Selective Fibroblast Activation Protein (FAP) Inhibitor. *Bioorganic Med. Chem. Lett.* **2021**, *37* (January), 127846. <https://doi.org/10.1016/j.bmcl.2021.127846>.

Pharmacokinetic Investigations of Ghrelin(1-8) Analogues Towards Development of PET Imaging Probes for Prostate Cancer

Authors

Julia R. Mason¹, Lihai Yu², Marina Childs³, Leonard G. Luyt^{1, 2, 4}

¹University of Western Ontario, Canada, ²London Regional Cancer Program, Canada, ³Lawson Health Research Institute, ⁴Departments of Oncology and Medical Imaging, University of Western Ontario, Canada

Introduction

The growth hormone secretagogue receptor 1a (GHSR), known as the ghrelin receptor, is differentially expressed in various diseases compared to healthy tissue. Differential GHSR expression has been observed in many cancer types, including pancreatic, breast, prostate, and thyroid.¹ A ghrelin-based analogue was previously discovered with exceptional receptor affinity, however *in vivo* evaluation revealed an unfavourable pharmacokinetic profile with rapid clearance and accumulation in liver and intestinal tissue.² The metabolic stability was investigated, revealing a metabolic soft spot between amino acids Leu⁵ and Ser⁶.³ Subsequently, a library of analogues were synthesized and evaluated for their *in vitro* stability, revealing two analogues with improved metabolic stability with retained receptor affinity. In this investigation, the original lead peptide and two analogues are being radiolabelled with a fluorine-18 6-fluoro-2-naphthyl (6-FN) prosthetic group and evaluated *in vivo* to access pharmacokinetic profiles.

Methods

Peptides were synthesized using standard Fmoc solid-phase peptide synthesis, purified by preparative HPLC, and characterized by high-resolution mass spectrometry. An iodonium ylide precursor was synthesized and radiolabelled with fluorine-18 to yield the ¹⁸F-prosthetic group which was then conjugated to the peptides. Animal xenograft models were established where male nu/nu mice were subcutaneously inoculated with 2 x 10⁶ DU145 cells, a prostate cancer model. Radiolabelled probes will be administered to assess the ¹⁸F-PET probes *in vivo*.

Results

Ghrelin(1-8) peptide analogues were synthesized and conjugated to a fluorine-18 6-FN prosthetic group. The probes are being assessed in a prostate cancer mouse model for differences in pharmacokinetic profile, demonstrating the influence of small structural modifications on receptor affinity, metabolic stability, and biodistribution.

Conclusions

A previously discovered high affinity ghrelin-based PET probe demonstrated poor pharmacokinetics leading to investigations of analogues that retained nanomolar affinity with improved metabolic stability. Three lead compounds were synthesized and radiolabelled with a fluorine-18 6-FN prosthetic group. They are currently being evaluated *in vivo* in a prostate cancer xenograft model to access varying pharmacokinetic profiles. This study demonstrates the intricate radiopharmaceutical optimization pathway, accounting for affinity, stability and pharmacokinetics, towards the development of a peptide-based ghrelin-targeted PET probe for prostate cancer imaging.

Acknowledgements National Sciences and Engineering Research Council of Canada (NSERC).

References

- (1) Lin, T.-C.; Hsiao, M. *Biochim Biophys Acta* **2017**, *1868*, 51–57.
- (2) Childs, M. D.; Yu, L.; Kovacs, M. S.; Luyt, L. G. *Org. Biomol. Chem* **2021**, *19*, 8812.
- (3) Childs, M. D.; Chandrabalan, A.; Hodgson, D.; Ramachandran, R.; Luyt, L. G. *ACS Pharmacol Transl Sci* **2023**, *6*, 1075–1086.

Investigating the role of inflammatory signaling in a precursor model of ovarian high-grade serous carcinoma.

Jacob Haagsma^{1,2}, Bart Kolendowski¹, Yudith Ramos-Valdes¹, Gabriel E. DiMattia^{1,3,4}, James J. Petrik⁶, Trevor G. Shepherd^{1,2,3,5}

¹The Mary & John Knight Translational Ovarian Cancer Research Unit, London Regional Cancer Program, London, Ontario, Canada. Departments of ²Anatomy & Cell Biology, ³Oncology, ⁴Biochemistry, ⁵Obstetrics & Gynaecology, Schulich School of Medicine & Dentistry, Western University, London, Ontario, Canada.

⁶Department of Biomedical Sciences, Ontario Veterinary College, University of Guelph, Guelph, Ontario, Canada

Introduction: Ovarian high-grade serous carcinoma (HGSC) is a highly lethal malignancy that originates from distal fallopian tube epithelial cells with universal *TP53* mutations. Spread of these precursor lesions to the ovary and throughout the peritoneum may occur via multicellular clusters called spheroids. One emerging approach to improve HGSC outcomes is immunotherapy, which has yielded promising results in other cancer types. We sought to determine whether *TP53* mutations and spheroid formation of mouse-derived HGSC precursor cells affects inflammatory signaling to better understand mechanisms regulating the immune cell landscape of HGSC.

Methods: Two mouse oviductal epithelial (OVE) cells lines – OVE4 and OVE16 – were used to delete *Trp53* via CRISPR/Cas9-mediated genome editing or transduced to express mutant p53^{R175H} protein. Transcriptomic analysis on OVE cells cultured as spheroids was performed by RNA-sequencing followed by gene set enrichment analysis (GSEA). Inflammatory signaling pathways were explored by immunoblotting for transcription factor phosphorylation and RT-qPCR for target gene expression. STAT1-dependent *pd-l1* expression in response to interferon gamma was investigated by immunoblotting and RT-qPCR.

Results: GSEA identified STAT and NFκB signaling pathways that are dysregulated due to p53 mutation. Increased expression of STAT1, STAT3, STAT5 and NFκB target genes in parental spheroids compared to *Trp53* and p53^{R175H} spheroids was observed in the RNA-seq data and validated by RT-qPCR. Immunoblot analysis identified decreased STAT3, STAT5 and NFκB phosphorylation, but increased total protein expression in OVE spheroids compared to adherent cells. Phosphorylation of STAT1 was undetectable at basal conditions, but treatment with interferon gamma induced STAT1 phosphorylation in all cells lines with the highest induction occurring in OVE spheroids expressing p53^{R175H}.

Conclusions: *In vitro* characterization of this OVE model has demonstrated mutant p53- and spheroid-dependent changes in inflammatory signaling that may contribute to HGSC. To strengthen our *in vitro* findings, we will be applying these analyses to a syngeneic, orthotopic mouse model to assess how observed alterations in inflammatory signaling impact interactions with the microenvironment in the context of a functional immune system. These studies have the potential to increase our understanding of the HGSC microenvironment, and discover novel immunotherapies to improve patient outcomes.

Distinct cell signalling alterations during epithelial ovarian cancer metastasis elucidated by spheroid and organoid analysis

Emily Tomas^{1,2}, Yudith Ramos-Valdes¹, Jennifer Davis¹, Bartlomiej Kolendowski¹, Gabriel DiMattia^{1,4,5}, Trevor Shepherd^{1,2,3,4}.

¹The Mary and John Knight Translational Ovarian Cancer Research Unit, Verspeeten Family Cancer Centre, London, ON, Canada; ²Anatomy & Cell Biology, Western University, London, ON, Canada; ³Obstetrics & Gynaecology, Western University, London, ON, Canada; ⁴Oncology, Western University, London, ON, Canada; ⁵Biochemistry, Western University, London, ON, Canada

Introduction: Epithelial ovarian cancer (EOC) possesses a unique mode of metastasis with constant seeding of the peritoneal cavity with malignant disease. EOC metastasis is commonly mediated via spheroids; thus, our extensive research on EOC spheroid cell pathobiology has provided many new insights into cell signaling plasticity implicated during the metastatic process. We speculate that EOC cells change their biology significantly between tumour and spheroid states to withstand stress and promote cell survival, yet this switching behaviour is not fully understood. Herein, we describe new results obtained through direct comparisons between cultured EOC spheroids and the relatively new three-dimensional organoid culture model system.

Methods: High-grade serous carcinoma (HGSC) patient ascites-derived iOvCa cell lines (n=7) were used to generate spheroids in suspension on Ultra-Low Attachment[®] plates and organoids using modified patient-derived organoid (PDO) culture conditions. The Incucyte[®] S3 Organoid Module and immunohistochemistry were conducted for growth and morphology comparisons between spheroids and organoids. Immunoblotting was performed to evaluate altered cell signaling processes in spheroids and organoids from our previous studies, focusing on cell stress response. Bulk RNA-sequencing was completed on the 7 iOvCa cell lines and bioinformatics analyses identified new pathways implicated in EOC progression. Small molecule inhibitors targeting the G2M checkpoint were tested on spheroids and organoids to observe effects on cell viability.

Results: Organoids appeared heterogeneous in morphology with dense, cystic, or mixed phenotypes, whereas spheroids often existed as typical structures of compact, grape-like, or sparse clusters. Organoid growth dynamics were similarly variable amongst lines. As expected, spheroids had high AMP-activated protein kinase (AMPK) T172 phosphorylation and low Akt S473 phosphorylation as compared with organoids. Transcriptomic analyses yielded elevated signaling pathways for G2M checkpoint and E2F targets in organoids as compared with spheroids, which could provide a new avenue for targeted therapeutics on EOC cells. Preliminary results suggest that indirectly targeting CDK1 with clinically relevant inhibitors (i.e. adavosertib, alisertib, and volasertib) showed resistance to treatment in spheroids, yet organoids showed sensitivity based on the IC₅₀ values under each model system.

Conclusions: The cellular adaptations of EOC throughout disease progression have become increasingly evident, particularly with the unveiling of phenotypic and molecular disparities between spheroids and organoids. Our findings emphasize the significance of targeting both proliferative and dormant cells in the development of novel treatment modalities. Hence, parallel assays using these translational models of advanced EOC will be essential experimental approaches for uncovering new therapeutic targets.

Characterizing the Role of AXL and MET in Triple-Negative Breast Cancer through Secretome-Mediated Immune Regulation

Alyssa Wu¹, Shanshan (Jenny) Zhong¹, Owen Hovey¹, Tomonori Kaneko¹, Shawn S.C. Li^{1,2}

¹ Department of Biochemistry; ² Department of Oncology, Western University, London, ON, Canada

Introduction: Triple-negative breast cancer (TNBC) has the worst outcome among the various subtypes of breast cancer due to the lack of targeted therapies and the inefficiency of existing immunotherapies. However, recent studies from our lab and others have underscored the crucial role of receptor tyrosine kinases (RTKs), particularly AXL and MET, in modulating the proliferation of cancer cells in the tumour microenvironment (TME). Our lab has also shown that AXL and MET tyrosine kinase inhibitors (TKIs) curb tumour growth in Balb/c mice. Therefore, it is hypothesized that AXL and MET play a pivotal role in TNBC through intrinsic oncogenic properties and extrinsic effects on the TME. Furthermore, AXL and MET may promote tumour immune evasion through secreted proteins enriched in these RTKs. This implies that targeting AXL and/or MET with specific inhibitors may have dual anti-tumour effects, inhibiting tumour growth and promoting anti-tumour immune responses.

Methods: Previously generated shRNA-mediated knockdown cell lines targeting AXL and MET in TNBC cell lines were used in these experiments. Whole cell lysates (WCL) and conditioned media (CM) samples were analyzed using mass spectrometry-based proteomics. Secretome profiling was conducted on CM samples collected from cancer cells incubated with serum-free media for 48 hours. Differential centrifugation was used to remove apoptotic bodies and cell debris.

Results: Proteomics analysis revealed functional differences in the AXL and MET knockdowns. In the WCL samples, clustering analysis revealed that AXL is associated with peptide antigen binding and immune escape, while MET is associated with growth factor binding and mediates cancer invasion and cytoskeleton remodelling. The CM data was matched to the Secreted Proteins Database (SEPDDB) and Vesiclepedia to identify components of the secretome. Interestingly, AXL and MET are secreted proteins observed in the cancer CM.

Conclusion: There is great potential to elucidate the roles of AXL and MET in the TNBC secretome to further understand their functions in modulating the TME through immune and stromal cells. If significant enrichments in immune cell markers (e.g., M1/M2 macrophage polarization) and stromal functional markers (e.g., CAFs, ECM) are observed, this will suggest that knocking down AXL and MET play roles in diminishing tumour growth through modulating the secretome in the TME. By profiling macrophage polarization markers in the TME, we can identify substrates that are responsible for the classically activated M1 (anti-tumour, pro-inflammatory) macrophages. Subsequently, alternatively activated M2 (pro-tumour, anti-inflammatory) macrophages will be identified as being linked to the activity of tumour-associated macrophages (TAMs), which are responsible for inflammation, ECM remodelling, intravasation, and angiogenesis. Novel insights into the mechanisms of AXL and MET function in tumorigenesis and cancer progression will strengthen the framework for therapeutic targeting of these RTKs in TNBC and other cancers.

Keywords: Receptor tyrosine kinases (RTKs), breast cancer, tumour microenvironment (TME), secretome, extracellular vesicles (EVs), exosomes, proteomics, phosphoproteomics

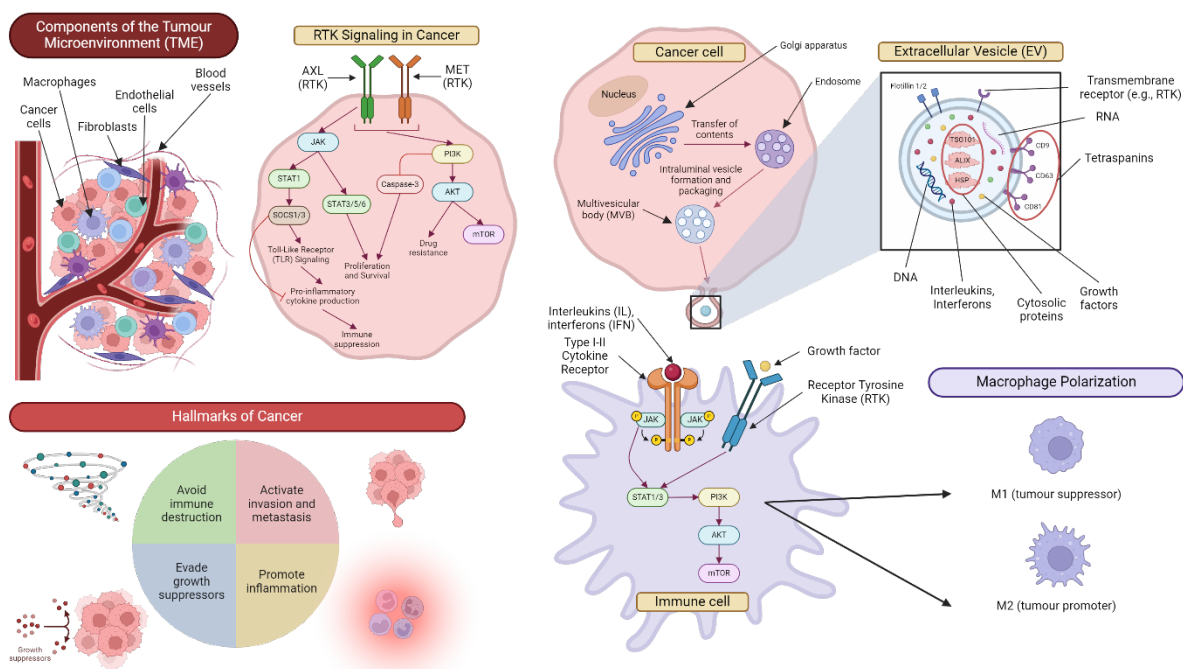


Figure 1. The TME is a complex ecosystem of cancer cells, blood vessels, immune cells, and fibroblasts that surround the tumour. The cancer cell secretome drives a pro-tumorigenic environment, enhancing tumour growth. The secretome facilitates tumour-stromal communication, which is composed of growth factors, cytokines, and chemokines. Growth factors activate receptor tyrosine kinases, including AXL and MET. These RTKs phosphorylate substrate proteins that are induced by ligand binding. Interleukins and interferons bind to cytokine receptors expressed on the surface of immune cells which activate the JAK pathway. Combined, these phosphorylation events activate transcription factors such as STAT3, which leads to downstream activation of PI3K, AKT, and mTOR pathways. The interactions that occur within the TME serve to avoid immune destruction, evade growth suppressors, promote inflammation, and activate invasion and metastatic pathways.

LKB1 and STRAD α promote epithelial ovarian cancer spheroid cell invasion

Charles B. Trelford^{1,2}, Adrian Buensuceso^{1,2}, Emily Tomas^{1,2}, Yudith Ramos Valdes¹, and Trevor G. Shepherd^{1,2,3,4}

1 The Mary & John Knight Translational Ovarian Cancer Research Unit, London Regional Cancer Program, London, Ontario, Canada.

2 Department of Anatomy & Cell Biology, Schulich School of Medicine and Dentistry, Western University, London, Ontario, Canada.

3 Department of Oncology, Schulich School of Medicine & Dentistry, The University of Western Ontario, London, Ontario, Canada.

4 Department of Obstetrics & Gynaecology, Schulich School of Medicine and Dentistry, Western University, London, Ontario, Canada.

ABSTRACT

Introduction: Late-stage EOC involves widespread dissemination of malignant disease throughout the peritoneal cavity, oftentimes accompanied by ascites fluid. EOC metastasis relies on the formation of multicellular aggregates called spheroids. Given our findings that Liver kinase B1 (LKB1) is required for EOC spheroid viability and LKB1 loss in EOC cells decreases tumour burden in mice, herein we investigated whether the LKB1 complex controls invasive properties of human EOC spheroids.

Methods: LKB1 signalling was antagonized through CRISPR/Cas9 genetic knockout of LKB1 and RNAi-dependent targeting of STE20-related kinase adaptor protein (STRAD; an LKB1 activator). Migration and invasion were assessed in spheroid culture via Transwell chambers, spheroid reattachment assays, and mesothelial clearance assays. EOC spheroids expressing nuclear GFP or mKate2 constructs were generated using Ultra-Low Attachment culture plates and embedded in Matrigel where an IncuCyte S3 real-time live-cell imager monitored invasion.

Results: The loss of LKB1 and STRAD signalling decreased mesothelial clearance as well as cell invasion through Matrigel and across Transwell membranes. A three-dimensional EOC organoid model demonstrated that organoid area was reduced by LKB1 knockout. In the absence of LKB1, zymographic assays identified a loss of matrix metalloproteinase (MMP) activity whereas spheroid reattachment assays found that coating plates with fibronectin restored their invasive potential.

Conclusions: LKB1 and STRAD facilitate EOC metastasis through MMP activity and fibronectin expression. Given that LKB1 and STRAD are crucial to EOC metastasis, targeting LKB1 could disrupt the dissemination of EOC making LKB1-specific inhibitors an alternative therapeutic strategy for EOC patients.

altered, showing a decrease in the relative abundance of bacterial species commonly present in hosts with intact gut microbiota (permanova, $p < 0.005$). A depleted gut microbiota further promoted idMMR neuroblastoma tumour progression, evidenced by larger tumour volumes (figure 1). ABX treatment significantly reduced the presence of CD3⁺CD45⁺TILs, including both CD4⁺ and CD8⁺ subtypes. These TILs exhibited an increase in dysfunctional and exhausted CD8⁺TIL phenotypes, as indicated by elevated expressions of PD1⁺CD38⁺ as well as PD1⁺CD39⁺, PD1⁺LAG3⁺, PD1⁺TIM3⁺, TIM3⁺CD39⁺, and TIM3⁺LAG3⁺ cells, respectively. Interestingly, treatment with anti-CTLA-4 therapy not only counteracted the detrimental effects of microbiota depletion on tumour size, but also fostered immune memory in responsive hosts, irrespective of previous PBS or ABX treatment (figure 1).

Conclusions: This study underscores the critical influence of gut microbiota on the progression and immune response of idMMR N2a tumours, highlighting the interaction between microbiota depletion and enhanced tumour growth alongside diminished efficacy of tumour-specific T-cell populations. These alterations contribute to increased T-cell exhaustion and dysfunctionality and suggest a significant modulation of the tumour immune microenvironment by the gut microbiota, potentially affecting the sensitivity to immunotherapy. Our findings advance the understanding of gut microbiota's complex role in shaping the tumour immune microenvironment and potential effects on cancer immunotherapy.

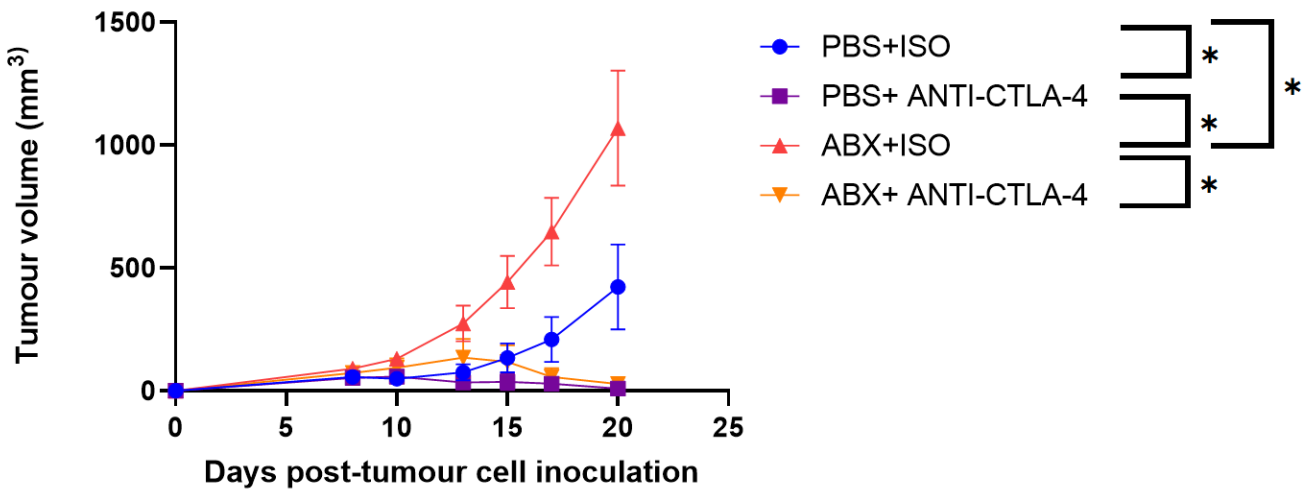


Figure 1. A depleted gut microbiota promotes idMMR neuroblastoma (N2a) tumour progression, but anti-CTLA-4 overcomes this effect. A/J mice were administered an antibiotic cocktail consisting of 1 mg/mL ampicillin, 1 mg/mL neomycin, 0.5 mg/mL vancomycin, and 1 mg/mL metronidazole to modulate their gut microbiota (n=12) or phosphate-buffered saline (PBS) (n=12). A four-day ABX withdrawal period was given, after which idMMR N2a cells (5×10^5) were inoculated. Once tumours were palpable, PBS- and ABX-treated mice received three intraperitoneal doses of 200 µg of Syrian Hamster isotype IgG (ISO) or Anti-cytotoxic-lymphocyte-associated protein-4 (CTLA-4) every three days (n=6 for each paired treatment). Tumour volumes in idMMR N2a-mice across PBS+ISO-, PBS+Anti-CTLA-4-, ABX+ISO-, and ABX+Anti-CTLA-4-treated groups were monitored every 2-3 days upon palpable tumour detection.

ULK1 is required for spheroid cell viability during metastatic transit in epithelial ovarian cancer

Jack D. Webb^{1,2}, Adrian Buensuceso¹, Emily Tomas^{1,2}, Matthew J. Borrelli^{1,2}, Lauren Viola¹, Owen Hovey³, Yudith Ramos Valdes¹, Bipradeb Singha^{1,2}, Shawn S-C Li³, and Trevor G. Shepherd^{1,2,4,5}

¹The Mary & John Knight Translational Ovarian Cancer Research Unit, London Regional Cancer Program, London, Ontario, Canada. Departments of ²Anatomy & Cell Biology, ³Biochemistry, ⁴Oncology, and ⁵Obstetrics & Gynaecology, Schulich School of Medicine & Dentistry, The University of Western Ontario, London, Ontario

Introduction: Epithelial ovarian cancer (EOC) is the most lethal gynecological cancer, attributed to its late-stage detection and development of chemotherapy resistance. EOC metastasis involves the spread of cancer cells into the peritoneal cavity forming multicellular clusters, or spheroids. Our research has identified autophagy, mediated by ULK1 (unc-51-like kinase-1), as a crucial survival mechanism in these spheroids. Herein, we have generated new *ULK1* knockout cells to further study its requirement during tumour growth and metastasis.

Methods: CRISPR/Cas9 technology facilitated *ULK1* gene ablation in EOC cell lines OVCAR8, HEYA8, and the FT190 control line, while autophagy markers were verified by western blot. Cell viability was assessed by Trypan Blue and Caspase-Glo assays, bioluminescent imaging monitored tumour progression in xenografts, and *ex vivo* assessments of tumour and ascites specimens. Ascites-derived spheroid invasion was determined using the mesothelial clearance assay. Phospho-proteomic mass spectrometry and bioinformatics analyses were performed on OVCAR8 spheroids and validated by western blot.

Results: ULK1 knockout disrupted autophagy in EOC spheroids, as shown by altered LC3 processing, p62 accumulation, and reduced Beclin-1 phosphorylation. ULK1 loss decreased spheroid viability and increased apoptosis *in vitro*, and significantly decreased tumour burden and metastatic potential *in vivo*. ULK1 deletion hindered organoid growth and significantly decreased spheroid invasiveness. Further analysis revealed that ULK1 loss leads to significant changes in the MAPK and PI3K-AKT-mTOR pathways within spheroids, and also underscores the tumour microenvironment's role in modulating ULK1's impact on these essential signaling networks.

Conclusion: Our findings reveal that ULK1 is pivotal for autophagy induction, spheroid viability, and ultimate metastatic progression *in vivo*. However, additional autophagy-independent ULK1 mechanisms may be implicated in EOC progression, too. We hope to discover new ULK1 signaling effects through future interrogation of the phospho-proteomic data.

Mechanisms of Anticancer Effects of Radiotherapy and CFI-400945 in Triple-Negative Breast Cancer

Harjot Athwal¹, Sierra Pellizzari¹, Vasudeva Bhat^{1,2}, Alison L. Allan^{1,2,3}, Armen Parsyan^{1,2,3,4}

¹Department of Anatomy and Cell Biology, Schulich School of Medicine and Dentistry, Western University, London, ON, N6A 3K7, Canada, ²London Regional Cancer Program, London Health Sciences Centre, London, ON, N6A 5W9, Canada, ³Department of Oncology, Schulich School of Medicine and Dentistry, Western University, London, ON, N6A 3K7, Canada, ⁴Department of Surgery, Schulich School of Medicine and Dentistry, Western University, London, ON, N6A 4V2, Canada, ⁵St Joseph's Health Care London, London Health Sciences Centre, London, ON, N6A 4V2, Canada

Introduction: Triple-negative breast cancer (TNBC) is the most aggressive subtype of breast cancer with the overall worst prognosis and oncological outcomes. Radiation therapy is an integral part of TNBC treatment. However, radiotherapy responses are sometimes not optimal due to inherited or acquired resistance. Enhancing radiotherapy responses by radiosensitizing drugs to improve response to treatment is a promising strategy for TNBC patients. We have demonstrated that CFI-400945, a novel Polo-like Kinase 4 (PLK4) inhibitor, when combined with radiotherapy leads to synergistic anticancer effects in TNBC *in vitro* and *in vivo*. However, the mechanisms responsible for the synergistic effects are not well understood. The mechanisms of CFI-400945 and radiation are likely related to mitotic abnormalities and/or the DNA-damage response (DDR) aberrations. Hence, we hypothesize that the synergy is achieved through aberrant cell cycle progression and/or perturbations in DDR.

Methods: This study aims to understand the underlying anticancer mechanisms of the combination treatment using TNBC cell lines (MDA-MB-231, MDA-MB-468 and SUM159) and patient-derived organoid (PDO) models. Cells were treated with CFI-400945 (Selleck Chemicals, Houston, TX) and ionizing radiation (Colbat-60 radiation unit, London Regional Cancer Program) only or in combination. Cell cycle analysis was performed using flow cytometry with propidium iodide. Protein expression was assessed by immunoblotting and cellular localization was examined with immunohistochemistry using standard protocols. Gene expression analysis was also performed using genome-wide transcriptomics to compare genes/pathways that are differentially expressed between treatment groups and control.

Results: We confirmed the expression of PLK4 in all studied TNBC cell lines. Immunocytochemistry for Centrin showed a significant increase in centriole amplification in MDA-MB-468 cells treated with 8 Gy radiation and 50 nM CFI-400945 compared to single-agents and control. Cell cycle analysis revealed that MDA-MB-468 cells treated with 8 Gy radiation and 50 nM CFI-400945 have arrested in G2/M and that SUM159 cells had an increase of polyploid cells following combination treatment, compared to single-agents and control. These differences in the cell cycle are likely related to the genetic background of the studied cell models. Preliminary analysis of RNA-sequencing data implicated enrichment in DNA-damage and cell cycle pathways, such as G2/M checkpoint, as well as multiple differentially regulated genes in combination treatment, compared to single-agents and control.

Conclusion: Overall, our preliminary data indicate that cell cycle and DNA-damage pathways might contribute to the antiproliferative effects of CFI-400945 and radiation, which supports our hypothesis. Specifically, the mechanisms could be related to increased centriole amplification and polyploid cells, which can cause abnormal cell cycle progression, eventually leading to cancer cell death or arrest. G2/M arrest could also be the potential mechanism involved in the combination's anticancer effects. G2/M arrest indicates a delay in DNA-damage repair and the inhibition of cancer cell proliferation. Overall, the results from this study will help us better understand the mechanisms of radiosensitivity and how drugs targeting mitotic checkpoints can mediate radiation responses. It will also help identify novel targets that could serve as biomarkers for treatment and drug development. Thus, the results of this study have significant translational potential.

Acinar cell-specific deletion of ATRX restricts KRAS^{G12D}-mediated formation of precancerous pancreatic neoplasia in male mice

Aswin Sureshkumar,^{1,5} Simone Benitz,⁶ Jiaqi Shi,⁸ Liena Zhao,² Howard Crawford,^{6-7,9} and Christopher L. Pin^{1,3-5}

¹Departments of Physiology and Pharmacology, ²Pathology and Laboratory Medicine, ³Oncology, and ⁴Paediatrics Schulich School of Medicine & Dentistry, University of Western Ontario, Canada; ⁵Verspeeten Family Cancer Centre, London, ON, Canada; ⁶Department of Surgery, Henry Ford Health System, Detroit, Michigan, USA, ⁷Department of Pharmacology and Toxicology, and ⁸Department of Pathology, Michigan State University, Lansing, Michigan, USA, ⁹Department of Oncology, Wayne State University, Detroit, Michigan, USA

Introduction: Pancreatic ductal adenocarcinoma (PDAC) ranks as the third leading cause of cancer-related deaths in Canada. While somatic mutations in *KRAS* that lead to constitutively active isoforms (e.g. *KRAS*^{G12D}) are found in >90% of PDAC patients, other genetic, environmental, or epigenetic events are needed to promote PDAC progression. This study examines the contribution of α -thalassemia, mental retardation, X-linked (*ATRX*), a SWI/SNF chromatin remodeling protein, to early stages of PDAC development. Previous work from our laboratory suggested acinar cells of the pancreas of female mice were more susceptible to *KRAS*^{G12D}-mediated transformation upon *ATRX* deletion, displayed by increased spontaneous acinar-to-ductal metaplasia (ADM), fibrosis, inflammation, and pancreatic intraepithelial neoplasias (PanINs). However, the implications of ADM in a more susceptible pre-clinical model of PDAC were not previously explored. This study evaluates the effects of acinar cell-targeted loss of *ATRX* towards cancer development combining *KRAS*^{G12D} activation with acute pancreatic injury. I hypothesize that loss of *ATRX* enhances acinar cell sensitivity to *Kras*^{G12D} in PDAC development in a sex-specific fashion.

Methods: Mice with an inducible, acinar-specific *Atrx* deletion and *KRAS*^{G12D} expression were generated (*Ptf1 α* ^{creERT}*KRAS*^{LSL-G12D}*Atrx*^{fl Δ 18}; termed *PKX*). Acute pancreatic injury was induced using cerulein in mice 10 days post-tamoxifen treatment. Mice are sacrificed 2- and 5- weeks following cerulein treatment, and pancreatic tissue harvested for analyses. Additionally, pancreatic organoids were established from *KRAS*^{G12D} mice with and without *ATRX* expression (*Ptf1 α* ^{creERT}*KRAS*^{LSL-G12D} and *PKX*, respectively) and characterized to assess the role of *ATRX* in acinar-cell oncogenesis.

Results: Consistent with past results, increased sensitivity to pancreatic injury was observed in *PKX* female mice, as evidenced by further advanced precancerous lesions and elevated functional dysregulation, compared to *Ptf1 α* ^{creERT}*KRAS*^{LSL-G12D} mice. In contrast, male *PKX* mice showed a protective response characterized by reduced ADM/PanIN lesions and acinar tissue regeneration following pancreatic damage. This acinar-dependent protection was reflected in the restricted growth of derived neoplastic organoid cultures and an increased rate of organoid death after passage.

Discussion: These findings may identify new therapeutic targets aimed at alleviating or inhibiting PDAC initiation and progression. The increased maintenance and regeneration of acini in *PKX* male mice suggests reduces susceptibility to activated *KRAS*^{G12D}, and *ATRX*-dependent protective mechanisms against oncogenic *KRAS* exist only in female mice. The sex-specific disparity in *KRAS*^{G12D}-mediated oncogenesis in *PKX* mice implies a differential role of *ATRX*, potentially influenced by differences in hormone expression or impaired X chromosome inactivation mechanisms that may regulate *Atrx*. Future studies will aim to further explore organoid lines derived from both murine and human pancreatic neoplasia to uncover signaling pathways affected by *ATRX* to preserve acinar tissue in male *PKX* mice. In particular, we will examine the resolution of double-stranded DNA breaks through non-homologous end joining, a function previously identified for *ATRX* in glioblastomas.

A multi-biomarker approach to defining the oligometastatic state using liquid biopsies: A correlative study of a randomized phase III trial

Vasudeva Bhat^{1,2}, Linda Beeloo⁸, Nora Purcell⁸, Emily Shen⁹, Rohann J. M. Correa^{2,3}, Aisling Barry⁴, Houda Bahig⁵, Darin Gopaul⁶, Andrew Pearce⁷, Tanja de Gruijl⁸, Famke L. Schneiders⁸, Max Diehn⁹, David A. Palma^{2,3} and Alison L. Allan^{1,2,3}

¹Department of Anatomy and Cell Biology, Schulich School of Medicine and Dentistry, Western University, London, Ontario, Canada, ²Verspeeten Family Cancer Centre, London, ON, Canada, ³Department of Oncology, Schulich School of Medicine and Dentistry, Western University, London, Ontario, Canada, ⁴Department of Radiation Oncology, Princess Margaret Cancer Centre, University of Toronto, Toronto, ON, Canada, ⁵Department of Radiology, Radiation Oncology and Nuclear Medicine, University of Montreal, Montreal, QU, Canada, ⁶Department of Oncology, Grand River Hospital, Kitchener, ON, Canada, ⁷Northern Ontario School of Medicine, Sudbury, ON, Canada, ⁸Department of Radiation Oncology, Amsterdam University Medical Centre, Amsterdam, Netherlands, ⁹Department of Radiation Oncology, Stanford University, Stanford, California, USA.

Introduction: Metastasis is the cause of >90% of cancer-related deaths. Current treatments are ineffective in the metastatic setting and instead are given with the goal of palliation rather than with curative intent. The “oligometastatic” theory proposes that in some patients, metastasis is not widespread but instead develops only in a limited number of sites and may be curable using targeted local therapies, such as surgery or stereotactic ablative radiotherapy (SABR). Recent randomized trials, including the SABR-COMET phase II trial in patients with 1-5 metastases, have demonstrated that addition of SABR to the standard of care (SOC) treatment significantly improves outcomes. However, a biological definition of the oligometastatic state remains to be established. This could aid in patient selection, identifying those most or least likely to benefit from SABR. We have launched a phase III randomized trial for patients with 4-10 oligometastases (SABR-COMET10) that includes a multi-biomarker translational component assessing circulating tumor cells (CTCs), circulating tumor DNA (ctDNA) and host immune cells.

Methods: Patients (n=204) are randomized to pre-specified SOC±SABR. Blood samples are collected at 3 timepoints in both arms (randomization, 3-months post-randomization, progression), and at 2 extra timepoints in the SABR arm (1-3 days after first fraction and 1-4 weeks after completing SABR). Analysis of CTCs is being carried out using FDA and Health Canada-approved CellSearch (Menarini Silicon Biosystems). Peripheral blood mononuclear cells (PBMC) are subjected to high-dimensional flow cytometry to determine differences in immune activation, exhaustion, and/or suppression. Finally, the analysis of ctDNA will include assessment of differences in concentration as well as methylation changes.

Results: To date, the accrual of 204 patients has been completed. Of these, CTCs were detected in ~28% of patients at baseline/randomization with a range of 1-24 CTCs (mean 4 ± 4.8) and ~9% having ≥ 5 CTCs. At follow-up, CTCs were detected in ~35% of patients at 3 months post-randomization with a CTC range of 1-48 CTCs (mean 8 ± 13.1) and ~11% having ≥ 5 CTCs. At progression, CTCs were detected in ~28% of patients with a CTC range of 1-22 CTCs (mean 6 ± 6.9) and ~10% having ≥ 5 CTCs. Preliminary analysis (n=80) of PBMCs revealed changes in immune cell phenotype across different timepoints. Ongoing analysis is aimed at methylation profiling of ctDNA. Further, we aim to define the relationship between CTCs and metastatic volume/sites of metastasis, analysis of ctDNA and immune response, and correlation with oncologic outcomes.

Conclusion: Our ultimate goal is to identify novel blood-based biomarkers that can stratify truly oligometastatic patients versus those with progressive metastatic disease, with the potential to shift the current clinical paradigm by defining the oligometastatic state as a highly treatable or even curable subset of metastatic disease.

Untargeted metabolic profiling of Pin1 inhibition in pancreatic cancer

Fatema Abdullatif¹, Xiao Zhen Zhou^{1,2}, Kun Ping Lu^{1,2}, Teklab Gebregiworgis^{1,2}

¹Department of Biochemistry, Schulich School of Medicine & Dentistry, Western University, London, ON

²Department of Oncology, Schulich School of Medicine & Dentistry, Western University, London, ON

Introduction: Pancreatic ductal adenocarcinoma (PDAC) is one of the most aggressive solid malignancies, with a mortality rate almost equal to its incidence, being projected to be the second leading cause of cancer deaths by 2030. Commonly, diagnosis occurs once distant metastasis has taken place, rendering surgical resection of the primary lesion not useful. However, chemotherapy poses major challenges for this disease, leaving limited treatment options for patients with the disease. One first-line chemotherapy used for PDAC is Gemcitabine (GEM), either alone or in combination with other drugs, however, issues of toxicity or resistance often arise. Some mechanisms of resistance include the rewiring of metabolism in the surrounding GEM-resistant cells and limiting access of the drug to the tumour due to the dense desmoplastic microenvironment. Pin1 is a peptidyl-propyl isomerase that is overexpressed in many cancers, including PDAC, and has also been found to be overexpressed in cancer-associated fibroblasts (CAFs), which comprise a large proportion of the desmoplastic microenvironment of PDAC tumours. Pin1 impacts many hallmarks of cancer, controlling many oncogenes and tumour suppressors, and is therefore a promising target for therapeutics. A recent study by Koikawa et al., has shown that, in combination with GEM, Pin1 inhibitors resulted in tumour regression and sensitization to chemotherapy in preclinical models. Here, my aim is to elucidate the metabolic reprogramming of Pin1 inhibition in PDAC cell lines, as well as determine the metabolic hot spot for treatment to aid in determination of the optimal time to induce co-treatment methods.

Methods: Initially, dose response assays using the Pin1 inhibitors are used to determine the concentration of drugs to use for the Nuclear Magnetic Resonance (NMR) experiment. Untargeted NMR metabolomics are then conducted to determine alterations in metabolic profile following treatment with Pin1 inhibitors (n=5) at different time points (e.g. 6, 12, and 24 hours) for cell lysates and media. Different analytical tools, (e.g. MetaboAnalyst) are then used to identify metabolite pathways of interest by analysing the data.

Results: Dose response curves for Pin1 inhibitors (e.g. Compound 1, Sulfopin, and ATRA) in pancreatic cancer cell lines are conducted after treatment for 72 hours, and inhibitory concentrations at which around 50% of cells were impacted are identified. The values determined here will be used for treatment of cells used for the NMR metabolomics experiment.

Conclusions: My goal here is to determine what metabolic pathways are impacted by Pin1 in PDAC cell lines. Potential metabolic enzyme targets have been identified based on the binding specifications of Pin1. This, in combination with the results of the experiments that are being conducted help determine metabolic pathways Pin1 influences and identifies vulnerabilities that can be exploited for therapeutic advancements, especially in the context of combination with GEM, a drug that is often faced with resistance resulting from metabolic rewiring. Finally, due to the time experiment course that is conducted, a hot spot of increased metabolic activity occurring within PDAC cells may be identified, further aiding in co-treatment methods with GEM and Pin1 inhibitors.

Understanding and overcoming innate and acquired MAPK-inhibition resistance in lethal thyroid cancer

Peter YF. Zeng^{1,2}, Jalna Meens^{3,4}, John W. Barrett¹, Harrison Pan¹, Matthew J. Cecchini^{2,5}, Laura Jarycki¹, Sarah B. Ryan¹, Alice E. Dawson¹, Amir Karimi¹, Mushfiq Shaikh¹, David A. Palma⁴, Eric Winquist⁴, Joseph S. Mymryk^{1,5}, Paul C. Boutros⁷⁻¹¹, Laurie Ailles^{3,4*}, Anthony C. Nichols^{4,5*}

1. Department of Otolaryngology – Head & Neck Surgery, Western University, London, Ontario, Canada; 2. Department of Pathology and Laboratory Medicine, Western University, London, Ontario, Canada; 3. Department of Medical Biophysics, University of Toronto, Toronto, Ontario, Canada; 4. Princess Margaret Cancer Centre, University Health Network, Toronto, ON M5G 1L7, Canada; 5. Department of Oncology, Western University, London, Ontario, Canada; 6. Department of Microbiology & Immunology, Western University, London, Ontario, Canada; 7. Department of Human Genetics, University of California, Los Angeles, California, USA; 8. Department of Urology, University of California, Los Angeles, California, USA; 9. Eli and Edythe Broad Center of Regenerative Medicine and Stem Cell Research, University of California, Los Angeles, California, USA; 10. Institute for Precision Health, University of California, Los Angeles, California, USA; 11. Jonsson Comprehensive Cancer Centre, University of California, Los Angeles, California, USA.

Introduction: Anaplastic thyroid cancer (ATC) is one of the most lethal human cancers, with some patients succumbing to disease within weeks of diagnosis. Despite a subset of BRAF^{V600E} mutant ATC patients responding to monomeric type I RAF inhibitor (RAFi) dabrafenib in combination with MEK inhibitor (MEKi) trametinib, almost all patients rapidly develop adaptive or acquired resistance. These patients, along with those who do not harbor the BRAF^{V600E} alteration, have limited treatment options.

Methods: To understand the mechanism of resistance to dabrafenib and trametinib, we utilized multi-region whole genome, high-coverage whole exome and single nuclei RNA-sequencing of ATC patient tumours to unravel genomic, transcriptomic, and microenvironmental evolution during type I RAFi and MEKi therapy. We then utilized *in vitro* cell line and *in vivo* patient-derived xenograft models to identify and test novel RAF therapeutics in ATC.

Results: Single-nuclei RNA sequencing of matched primary and resistant ATC patient tumours identified transcriptomic reactivation of MAPK-pathway, along with immunosuppressive macrophage proliferation, underlying the development of acquired resistance. Our translational genomics led us to hypothesize that deeper inhibition of the MAPK-pathway can be efficacious in overcoming treatment resistance. Screening of a panel of type II RAFi revealed that ATC cell lines are exquisitely sensitive to the type II RAFi naporafenib by inhibiting EphA2-mediated MAPK-signaling. We further demonstrate that naporafenib in combination with MEKi trametinib can durably and robustly overcome both innate and acquired treatment resistance to dabrafenib and trametinib using ATC cell lines and patient-derived xenograft models, including in multiple PDX models from ATC patients who developed acquired resistance to dabrafenib and trametinib. Finally, we describe a novel mechanism of acquired resistance to type II RAF inhibitor and MEK inhibitor through compensatory mutations in *MAST1*.

Conclusions: Taken together, our work using translational and functional genomics have unraveled the differential mechanisms of treatment resistance to type I and type II RAFi in combination with trametinib and rationalizes the clinical investigation of type II RAFi in the setting of thyroid cancer.

Coping with Costs: Analyzing GoFundMe Financial Aid Requests from Brain Tumor Patients in Ontario, Canada

Kaviya Devaraja^{1,2}, Jonathan Avery^{1,3}, Yajur Iyengar⁴, Yunyi Zhang⁵, Seth A. Climans⁶

Affiliations

1. Adolescent and Young Adult Program, Department of Supportive Care, Princess Margaret Cancer Centre, University of Toronto, Toronto, ON M5G 2C4, Canada
2. Department of Medical Science, University of Toronto, Toronto, ON M5S 1A5, Canada
3. School of Nursing, University of British Columbia, Vancouver, BC V6T 1Z4, Canada
4. Temerty Faculty of Medicine, University of Toronto, Toronto, ON M5S 1A8, Canada.
5. Independent Researcher, Toronto, Canada
6. Department of Oncology, Western University, London, ON N6A 5W9, Canada.

Background

Primary CNS tumors significantly affect individuals globally, with patients in Ontario, Canada, often bearing financial burdens for treatments such as oral chemotherapy due to insufficient coverage, resulting in complex insurance processes or out-of-pocket payments. However, limited understanding exists regarding other direct and indirect financial implications of their diagnosis. This study examines the financial strains, unmet needs, and overarching challenges encountered by Ontario's brain tumor patients, utilizing GoFundMe posts as a unique data source to explore additional financial costs linked to CNS tumor diagnoses in the region.

Methods

A qualitative descriptive design employing thematic analysis analyzed GoFundMe posts supporting CNS tumor patients in Ontario from 2014 to 2021. A search strategy targeted posts featuring primary CNS tumor keywords, with NVivo 10 software facilitating post organization and coding.

Results

Focused on Ontario, the study yielded a final dataset of 154 posts from an initial pool of 9025, revealing further financial strain due to income loss among patients and caregivers. Posts highlighted various concerns: 1) lack of awareness about available financial, psychosocial, and medical support; 2) uncertainty regarding accessing support services; 3) worries about family's long-term financial and overall well-being; 4) insufficient public awareness about the financial and emotional burden on those affected; and 5) seeking emotional support, hope, and encouragement from the community.

Conclusions

These GoFundMe posts highlight a connection between financial burden, emotional distress, and the need for improved access to financial and emotional support services. The results emphasize distinct financial challenges faced by CNS tumor patients within Ontario's healthcare system.

HYALURONAN IS A CRITICAL TUMOR RESISTANCE FACTOR THAT BLOCKS UVB-INDUCED KERATINOCYTE TUMOR INITIATION.

C. Tolg¹, V. Liu², H. Pavanel³, C. Taylor³, D. Chen³, K. Cousteils², K.A. Hill³ E.A. Turley^{1,4}

¹ LRCP, LHSC, Victoria Hospital, London ON, CA; ² Dept. Biochemistry, Schulich School of Medicine and Dentistry, Western University, London, ON, CA; ³ Dept. Biology, Faculty of Science, Western University, London ON, CA; ⁴ Depts Oncology, Biochemistry and Surgery, Schulich School of Medicine and Dentistry, Western University, London ON, CA.

INTRODUCTION

Mutant clones accumulate in normal tissues over time in a process known as field cancerization, but few of these result in cancer. With age, chronic inflammation and UV exposure, somatic mutations can be as high as 10,000/cell in skin, most of which display a UV mutagenesis signature. The majority of these pre-neoplastic mutant clones remain relatively small in size. The host factors that limit or permit their expansion are currently poorly understood. Identification of these host factors has clinical implications for the prevention and treatment of cancers that recur in cancerized fields.

Studies of the cancer-resistant naked mole rat have identified the polysaccharide hyaluronan (HA) as one host cancer-resistance factor, which is associated with the attenuation of organism-wide inflammation and TP53 signaling. This together with evidence that skin HA diminishes with age and UV exposure inspired us to assess if replenishing HA in UVB-exposed skin modifies mutations acquisition and clonal expansion to limit tumor initiation.

METHODS

HAPE or vehicle control was applied to UVB-exposed skin of keratinocyte tumor-susceptible (squamous and basal cell carcinoma) *Hr^{-/-}:Ptch1^{+/-}* mice. RNAseq and whole exome sequencing was performed on bulk RNA and DNA isolated from dorsal UVB-exposed skin. Histology sections were processed for immunofluorescence and spatial transcriptomics (10X genomics).

We developed a patented topical HA co-polymer (HAPE) that penetrates skin to replenish UVB-induced HA loss.

RESULTS

HAPE prevents UVB-induced keratinocyte tumors and blocks oncogenic signaling but not the development of a cancerized field. Both the UVB-induced DNA damage and total mutation load are similar in HAPE vs. control-treated skin. Unexpectedly, somatic mutations in driver oncogenes for squamous and basal cell carcinoma are also present in both HAPE and control skin. One notable exception is mutant *Trp53*, which contributes to keratinocyte tumor initiation, is not detected in HAPE-treated skin samples as monitored by whole exome sequencing.

Spatial transcriptomic and immunofluorescence data indicate that HAPE selectively culls keratin-15⁺ keratinocyte progenitor cells, which are tumor-initiating cells in *Hr^{-/-}:Ptch1^{+/-}* mice. HAPE both reduces the number of KRT15⁺ progenitors and their TRP53 mRNA and protein expression. We hypothesize that HAPE promotes the death of KRT15⁺ keratinocytes that acquire gain- or loss-of-function mutations in TRP53, and this effect suppresses keratinocyte tumor initiation. We are currently assessing this possibility using human HaCaT keratinocytes that were isolated from UVB-exposed skin and that consequently express *TP53* mutations.

CONCLUSIONS

We conclude that HA is a critical tumor-resistance factor for UVB-exposed keratinocytes, which acts downstream of oncogenic driver mutations to block tumors by culling tumor initiating cells bearing *Trp53* mutations.

Title: The spatial transcriptomic and proteomic landscape of breast cancer brain metastasis

Authors: Rober Abdo¹, Qi Zhang¹, Shawn S. Li²

¹Department of Pathology and Laboratory Medicine, Western University, London, ON, Canada

²Department of Biochemistry, Western University, London, Canada

Background: Brain metastases (BrM) represent a leading cause of cancer mortality, exhibiting notorious resistance to treatment despite advances in systemic therapies. Breast cancer is one of the most common primary tumors for brain metastasis. The unique brain tumor microenvironment (BTME) further complicates the challenges associated with treating brain metastases.

Methods We identified 34 cases of patient-paired surgically resected brain metastases with a breast origin. Additionally, six cases of non-tumoral brain controls were included. Two tissue microarray (TMA) blocks were constructed. NanoString GeoMX Digital Spatial Profiling (DSP) using the whole-transcriptome atlas (WTA) was employed. For each patient, three ROIs were analyzed: primary breast cancer (BC), metastatic tumor cells (MTC), immediate tumor brain microenvironment (TBME). Furthermore, proteomics and phosphotyrosine profiling were conducted on the primary triple-negative breast cancer (TNBC) cell line (4T1) and its metastatic-brain tendency derivatives (4T1-BrM5) using tandem mass tag (TMT) labeling and SH2 superbinder agarose beads methods. Subsequently, an immune-competent mouse model of triple-negative breast cancer brain metastasis was established and monitored by MRI.

Results: 1) Analysis of the PAM50 gene signature revealed almost half of primary breast cancer cases change molecular subtypes at their matched brain metastatic sites. Interestingly, nearly all luminal A shifted to luminal B and HER-2 enriched subtypes. The majority of the triple negative BC, however, remained the same genotype at the metastatic site. 2) The shifting BC was coupled with enrichment in interferon pathways whereas non-shifting BC featuring with immune evasion and worse survival 3) TBME exhibited cellular and molecular plasticity characterized by three distinct subtypes (TBME 1-3) identified through unsupervised clustering. The “neural-like” TBME-1 shared signaling pathways with non-tumoral brain controls defined by cytokine and interferon enrichment. The “fibro genic” TBME-3 is distinguished by an abundance of tumor-facilitating endothelial and myeloid cells modulated by PTK7, while TBME-2 exhibits glutamatergic signaling prominence, immune depletion, and shortest survival with 4) Integrated proteomics and phosphotyrosine analysis on the cell lines identified an enrichment of the PI3K-AKT-mTORC1 axis in 4T1-BrM5. 5) Knocking out PTK7 in an immune-competent mouse model of triple-negative breast cancer brain metastasis halted the metastasis.

Discussion: This study provides transcriptomic evidence of breast cancer plasticity during brain metastasis, highlighting significant cellular and molecular remodeling of the brain microenvironment to accommodate metastatic breast cancer cells.

Identification and functional characterization of the cancer-initiating cell population in human ovarian clear cell carcinoma (OCCC) lines

Blane Gebreyes⁵, Bart Kolendowski^{1,3}, Vasu Bhat^{2,3}, Yudith Valdes^{1,3}, Trevor Shepherd^{1,3,4,6,7}, Gabriel DiMattia^{1,3,5,7}.

¹The Mary & John Knight Translational Ovarian Cancer Research Unit, Verspeeten Family Cancer Centre, London, ON, Canada; ²Translational Breast Cancer Research Unit, Verspeeten Family Cancer Centre, London, ON, Canada; ³LHSC Research Institute, London Health Sciences Center, London, ON, Canada; ⁴Anatomy and Cell Biology, Western University, London, ON, Canada; ⁵Biochemistry, Western University, London, ON, Canada; ⁶Obstetrics & Gynaecology, Western University, London, ON, Canada; ⁷Oncology, Western University, London, ON, Canada

Introduction: OCCC is a rare histotype of epithelial ovarian cancer with poor late-stage prognosis. One determinant of OCCC mortality is the extent of regional and distant metastases within the peritoneal cavity. Metastasis is responsible for 90% of cancer deaths and can be attributed to a small subpopulation of highly tumorigenic cells with a capacity for self-renewal, known as cancer stem cells (CSCs). Despite making up only 0.01-2% of the average tumour mass, these cells play a crucial role in treatment resistance, disease spread, and recurrence, emphasizing the urgent need for novel therapeutics specifically targeting the drivers of metastasis.

Methods: RT-qPCR, Western blotting, spheroid formation, and FLOW cytometry will be employed to establish a baseline expression profile for well-characterized CSC markers in bulk cells. Select lines will undergo CSC enrichment through the development of drug-resistant (carboplatin, paclitaxel, AZD-8055) lines or through specialized culture conditions meant to sustain only CSCs. Changes in the expression of well-characterized CSC markers in enriched cell lines will be investigated relative to the parental cell line and will be functionally characterized using RNAseq and different cell-based and *in vivo* xenotransplantation assays.

Results: The expression of different stem cell markers (NANOG, SOX2, c-MYC, KLF4) did not correlate with the expression of aldehyde dehydrogenase (ALDH) 1A1, nor the activity of ALDH family members, in human OCCC cell lines. The ability to proliferate in suspension culture in standard media did not predict cell line viability in suspension culture using CSC-enriching media. KOC-7c, JHOC-5, ES2, and RMG-I lines were viable in both conditions, however, OVTOKO and TOV-21G were only able to grow in standard media.

Conclusions: This is the first time human OCCC cell lines have been enriched with CSCs for identification and functional characterization. These results may provide a platform for future studies aimed at understanding how various epigenetic features define OCCC CSCs to potentially identify existing epigenome-targeted therapies which may selectively kill CSCs.

Title: Primary cancer-associated fibroblasts alter tumor organoid chemosensitivity through epigenetic regulation

Author list: Emilie Jaune-Pons^{1,2}, Zachary Klassen^{1,2}, Joana Ribeiro Pinto^{1,2}, Maria Nica^{1,2}, Nadeem Hussain³, Michael Sey³, Ken Leslie⁴, Ephraim Tang⁴, Anton Skaro⁴, Matthew Cecchini⁵, Crystal Engelage⁴, Danielle Porplycia⁷, Stephen Welch⁷, Brian Yan³, and Christopher Pin^{1,2,6,7}

Affiliations: Departments of ¹Physiology and Pharmacology, ³Medicine (Division of Gastroenterology), ⁴Surgery, ⁵Pathology and Laboratory Medicine, ⁶Paediatrics, and ⁷Oncology, Schulich School of Medicine and Dentistry, Western University, London, Ontario, Canada
²Verspeeten Family Cancer Centre, London, Ontario, Canada.

Abstract (500 words):

Introduction: Pancreatic adenocarcinoma (PDAC) is the 3rd leading cause of cancer-related deaths in Canada with a 5-year survival rate at ~12%. Two factors contribute to this poor survival rate. First, current treatments are insufficient. Only 20% of patients are eligible for surgical resection while the other 80% of patients are treated with chemotherapies (nab-paclitaxel, Gemcitabine, FOLFIRINOX) that show limited efficiency. Second, the PDAC tumour microenvironment (TME), and specifically cancer-associated fibroblasts (CAFs), contribute to chemoresistance.

While there is evidence that CAFs and the TME effect tumour growth, chemoresistance and metastasis, the mechanisms underlying these effects are unknown. Given the involvement of environmental cues from the TME, we suggest epigenetic reprogramming occurs in pancreatic cancer cells in response to secreted factors from CAFs. Our laboratory developed a translational research program in which we isolate cancer and non-cancer cells from tumour biopsies obtained through endoscopic ultrasound. Using patient-derived cells allows us to examine the cross talk that occurs between these cell populations in a patient-specific manner. We hypothesize that CAFs promote cancer cell chemoresistance through epigenetic reprogramming.

Methods: Supported by the Baker Centre for Pancreatic Cancer, we established a living biobank of patient-derived organoids (PDO) grown in 3D cultures and CAFs grown in 2D cultures. These samples are linked to the DERIVE (Determination of Response to Therapy in Individual Patients) clinical database. To examine the effects of patient CAF populations on PDO growth, we grew CAFs for 48 hours in culture, then supplemented organoid cultures with this CAF-conditioned media (CM). Organoid growth and response to gemcitabine treatment was examined over 14 days using an Incucyte system. To identify the effects on the epigenome, we performed RNA-seq, global DNA methylation analysis and ATAC-Seq 14 days after CAFs-CM treatment.

Results: We showed CAF-CM altered the phenotype and molecular profiles of PDOs, and increased resistance to both chemotherapy (Gemcitabine) and radiotherapy in multiple PDOs. Exposure to CAFs-CM induce changes in DNA methylation and accessibility of chromosomal regions which favour chemoresistance. Metabolomic and cytokine analysis on CAFs-CM identified differential expression of specific metabolites linked to epigenetic mediators and TGF β , respectively. We are currently determining if these factors secreted by the CAFs promote chemo and radio-resistance.

Conclusions: This study shows the importance in integrating TME components in cancer research to offer new therapeutic opportunities for patients. In addition, we show (1) CAFs secrete factors that enhance chemo and radio resistance in PDOs and (2) these changes may be due to altered epigenetic reprogramming. Future experiments will identify the epigenetic factors that can be targeted to counteract chemoresistance.

Fc3TSR Remodels the Tumour Microenvironment to Enhance Efficacy of Immunotherapies and Immune Cell Migration in a Murine Model of Pancreatic Ductal Adenocarcinoma.

Garlisi, B¹., Aitken, C¹. Lauks, S¹., Lawler, J²., Petrik, J¹.

¹Department of Biomedical Sciences, University of Guelph, Canada, ²Beth Israel Deaconess Medical Center and Harvard Medical School.

Introduction: Pancreatic Ductal Adenocarcinoma (PDAC) has a poor survival rate due to late diagnosis where metastasis has often occurred. Angiogenesis, the process by which new vessels form from pre-existing vasculature, is crucial for tumor growth and metastasis. Tumors aggressively upregulate expression of pro-angiogenic factors, stimulating rapid vessel formation. These vessels often lack pericyte coverage and have dysfunctional morphology, leading to high interstitial fluid pressure (IFP). Impaired perfusion and high IFP impede not only therapy uptake, but also immune cell migration to the tumour and then to the tumour draining lymph nodes. Fc3TSR is a novel fusion protein derived from the potent angiogenic inhibitor thrombospondin 1, which we have shown to induce ovarian tumor regression and normalize vasculature which enhances uptake of many therapies. In this study, we evaluated Fc3TSR's ability to remodel the tumor microenvironment, induce tumor regression and enhance efficacy of immune checkpoint inhibitors.

Methods: We developed an orthotopic syngeneic murine model of PDAC, whereby we surgically injected 2.5×10^4 murine PDAC cells (KPC) into the tail of the pancreas of C57BL/6 mice. Tumors were allowed to progress for 14 days before intraperitoneal (IP) administration of Fc3TSR (0.158mg/kg) or PBS (control) on day 14 and 21 which allowed for optimal tumour microenvironment (TME) remodelling. Immune checkpoint inhibitor (CTLA-4 and PD-L1 (25ug) IP injections were administered on day 23 and 26. Mice were euthanized on day 30, metastatic lesions were counted, and tumours were weighed and collected. Tumors were cryo-preserved, sectioned, and stained using immunofluorescence for apoptosis (cleaved caspase-3), proliferation (ki-67), hypoxia (Hypoxyprobe), blood and lymphatic vasculature (CD31, alpha-smooth muscle actin (a-SMA), LYVE-1), and immune cells (CD4, CD11c, CD68, CD138).

Results: Fc3TSR significantly reduced tumour weights and secondary lesions compared to PBS. Fc3TSR + CTLA-4, but not PD-L1, significantly reduced tumour weights compared to Fc3TSR. Fc3TSR + CTLA-4 or PD-L1 significantly reduced secondary lesions compared to both Fc3TSR and CTLA-4 or PD-L1 alone. Fc3TSR significantly reduced area of hypoxia, and increased normalized blood vessels (as shown by a-SMA coated vessels) compared to PBS. Fc3TSR alone significantly increased CD4 and CD11c in tumours, but the combination of Fc3TSR + CTLA-4 or PD-L1 significantly increased this further compared to both Fc3TSR and CTLA-4 or PD-L1 alone. Tissues stained for cleaved caspase-3, LYVE-1, CD68 and CD138 are currently being analyzed, and CD8, FoxP3, and NK cells are currently being optimized. Lymph nodes were collected and are also being optimized for staining of these immune cells and TME markers.

Discussion: Our data suggests that normalizing the TME can enhance the uptake and efficacy of immune checkpoint inhibitors and potentially other secondary therapies which have shown limited efficiency *in vivo* for PDAC patients. Enhanced perfusion through normalization of blood and lymphatic vasculature could facilitate the migration of activated immune cells and may enhance immune responses in PDAC patients. Here we demonstrate a novel approach to optimize therapeutic efficacy and immune cell migration in advanced stage PDAC.

Rachel Barboza -WITHDRAWN

EvoDiffuse: Diffusion Models Fine-tuned with Reinforcement Learning for De Novo Molecule Design

Lianghong Chen¹, Mike Domaratzki¹, Pingzhao Hu^{1,2,3,4,5}

¹Department of Computer Science, Western University, Canada

²Department of Biochemistry, Schulich School of Medicine & Dentistry, Western University, Canada

³Department of Epidemiology and Biostatistics, Schulich School of Medicine & Dentistry, Western University, Canada

⁴Department of Oncology, Schulich School of Medicine & Dentistry, Western University, Canada

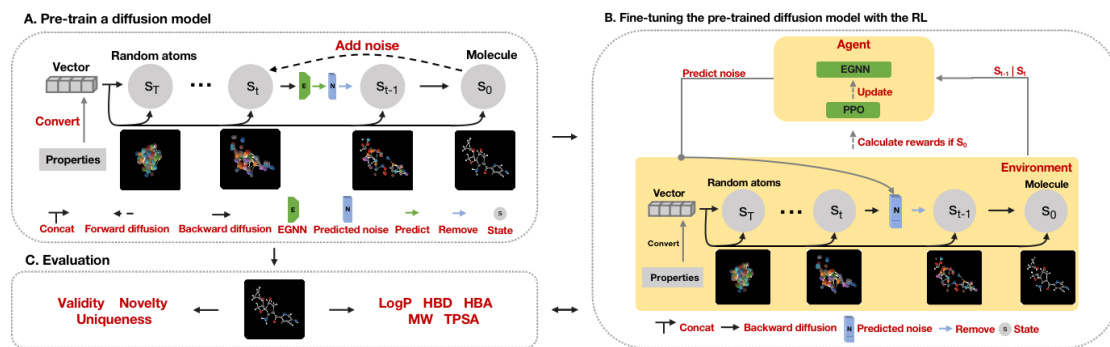
⁵The Children's Health Research Institute, Lawson Health Research Institute, London, Ontario, Canada

Introduction: Designing molecules with oral bioavailability (OB) is a cornerstone of drug development tasks. It ensures the drug can be effectively absorbed from the gastrointestinal tract into the bloodstream, crucial for achieving the desired therapeutic effect. Generative Artificial Intelligence (AI) has been widely used to design these functional molecules in recent years. However, most molecules generated by current state-of-the-art (SOTA) generative models lack stable functional properties. We hypothesize a diffusion model fine-tuned with reinforcement learning (EvoDiffuse) can address this problem.

Methods: I pre-trained an Equivariant Diffusion Model (EDM) to generate 3D molecules with baseline OB. Sequentially, we utilized a SOTA reinforcement learning technique Proximal Policy Optimization (PPO) to fine-tune the pre-trained EDM to optimize the OB of generated molecules, according to the logarithmic probability of the model generating new molecules. The models were evaluated on the validity, uniqueness, and novelty of the generated molecules. We tested the robustness of our framework by training the model on the four different datasets and compared the model performance with other SOTA AI-based generative techniques. The overall workflow is shown in **Figure 1**.

Results: We have verified the performance of our pre-trained EDM for functional (OB) molecular generation. We got a validity of 81.70%, a uniqueness of 99.88%, and a novelty of 88.85% within 1000 generated molecules. By analyzing the distribution of the OB-related properties of molecules, we found most of the generated molecules possess our desired properties.

Conclusion: We proposed a novel reinforcement learning fine-tuned diffusion framework EvoDiffuse for 3D molecular generation. This provides a new perspective for designing de novo molecules with OB. The EvoDiffuse will be able to be used in wide functional molecular generation tasks in the future.



Role of Kindlin-1 in Cutaneous Squamous Cell Carcinoma Cytoskeletal Organization

A. Varela^{1,2,3}, I.A. Ivanova^{1,2,3}, L. Dagnino^{1,2,3,4}

¹ Department of Physiology and Pharmacology, University of Western Ontario, London, ON N6A 5C1, Canada

² Children's Health Research Institute, University of Western Ontario, London, ON N6C 2V5, Canada

³ Lawson Health Research Institute, University of Western Ontario, London, ON N6C 2R5, Canada

⁴ Department of Oncology, Western University, London, ON N6A 5C1

Introduction: Kindlin-1 is a scaffold protein whose expression is restricted to epithelial tissues and contributes to integrin activation, cell-matrix attachment, and proper cytoskeletal organization. Loss-of-function mutations in *FERMT1*, which encodes Kindlin-1, lead to Kindler Syndrome, an inherited disease that affects skin integrity and function. Humans with Kindler Syndrome are also at a higher risk of developing cutaneous squamous cell carcinomas (cSCC). These tumours constitute the fifth most prevalent malignancy globally and arise from malignant transformation of epidermal keratinocytes.

Methods: To investigate the role of Kindlin-1 in cytoskeletal organization and mechanotransduction in cSCC cells, we generated two monoclonal Kindlin-1-deficient populations derived from SCC-13 cSCC cells, hereafter termed Kin1-KO cells. Cytoskeletal filaments were imaged by immunofluorescence microscopy using an anti- β -tubulin monoclonal antibody and Phalloidin staining.

Results: We have found that Kin1-KO cells display altered microtubule networks relative to parental cells. Specifically, microtubule filaments in Kindlin-1-expressing parental cells emanate from the perinuclear area and reach regions juxtaposed to the plasma membrane. In contrast, the microtubule network in Kin1-KO cells is disorganized and abundant branched filaments are apparent. Further, whereas thick cortical actin bundles and stress fibers are present in Kindlin-1-expressing cells, F-actin filaments in Kin1-KO cells tend to be thinner. Morphologically, Kin1-KO cells also exhibit a substantially higher abundance of actin-reach filopodial extensions than parental cells.

Discussion: These observations are consistent with the notion that Kindlin-1 is necessary for normal F-actin and microtubule organization in cSCC cells. Cytoskeletal filaments are essential for tumour cell migration, invasion, and metastasis. Disrupted cytoskeletal organization by Kindlin-1 deficiency suggests Kindlin-1 may be a potential target for novel therapeutic strategies.

Supported with funds from CIHR, NSERC and the London Regional Cancer Program (LRCP).

Role of Kindlin 2 in Epidermal Cell Proliferation, Migration, Adhesion, and Spreading

A. Dutta*, M. Calder*, and L. Dagnino*[†].

*Department of Physiology and Pharmacology, Children's Health Research Institute, Lawson Health Research Institute, and [†]Department of Oncology, The University of Western Ontario, London, Ontario, N6A 5C1.

Introduction: The Kindlin family of scaffold proteins plays critical roles in epidermal function and homeostasis. Hereditary mutations in the *FERMT1* gene, which encodes Kindlin 1, give rise to Kindler syndrome. The latter is a blistering disease characterized by epidermal fragility and increased susceptibility to cutaneous squamous cell carcinoma (cSCC) formation. Epidermal cells express Kindlins 1 and 2, and Kindlin 1 is known to modulate keratinocyte proliferation, migration, adhesion, and spreading. However, little is known about the roles of Kindlin 2 in epidermal cells.

Methods: We used siRNA pools to silence *FERMT2* in three lines of transformed keratinocytes (PM1, MET1, and MET4). Next, we assessed directional migration using scrape-wound assays, evaluated cell adhesion using a colorimetric assay substrate 4-Nitrophenyl N-acetyl- β -D-glucosaminide (NPAG), measured the incorporation of bromodeoxyuridine (BrdU) into DNA, and analyzed cell spreading by visualizing the plasma membrane using wheat germ agglutinin (WGA). We analyzed alterations in the actin cytoskeleton, microtubule organization, and focal adhesions, visualizing by immunofluorescence microscopy using F-actin, β -tubulin, and phospho-paxillin, respectively.

Results: Kindlin 2 protein levels decrease by $\geq 80\%$ 66 h after siRNA transfection. Reduced Kindlin 2 levels resulted in decreased directional migration in PM1, MET1, and MET4 cells by 33%, 27%, and 25%, respectively. *FERMT2* silencing also hindered the ability of PM1 cells to adhere to culture surfaces, but was without effect on MET1 and MET4 adhesion. Decreased Kindlin 2 levels in MET4 cells resulted in a 5-fold reduction in the proportion of cells capable of incorporating BrdU into DNA. We also observed impaired spreading in Kindlin 2-deficient MET4 cells, relative to Kindlin 2-expressing controls. Moreover, MET4 cells lacking Kindlin 2 displayed a disorganized F-actin cytoskeleton, characterized by reduced cortical actin bundles and prominent stress fibers. These cells also had shorter and fewer focal adhesions, suggesting that Kindlin 2 plays a role in focal adhesion formation and maturation through direct or indirect mechanisms. Microtubules in Kindlin 2-expressing MET4 cells were observed as long filaments extending radially from perinuclear regions toward the cell periphery. In contrast, only shorter, densely packed microtubule filaments that failed to reach the plasma membrane were present in Kindlin 2-deficient cells.

Discussion: Collectively, these data indicate that Kindlin 2 is essential for normal forward migration in epidermal cells and that it may play cell-type or context-dependent roles in their adhesion. Kindlin 2 is essential for normal proliferation and efficient spreading of cSCC cells. Reduced Kindlin 2 levels also lead to disruptions in the actin cytoskeleton, microtubule organization, and focal adhesion assembly in cSCC cells.

Supported with funds from the Canadian Institutes of Health Research, the Children's Health Research Institute, and the Natural Sciences and Engineering Research Council.

Title: Epigenetic modifications in OCCC cell lines in response to hypoxia

Authors: Meruthulaa Kayilaasan⁴, Bart Kolendowski^{1,2}, Yudith R Valdes^{1,2}, Trevor G Shepherd^{1,2,3,5,6}, Gabriel E DiMattia^{1,2,3,4}

Affiliations: ¹Mary & John Knight Translational Ovarian Cancer Unit, London Regional Cancer Program, London, ON, Canada; ²Lawson Health Research Institute, London, ON, Canada; ³Oncology, Western University, London, ON, Canada; ⁴Biochemistry, Western University; ⁵Anatomy & Cell Biology, Western University; ⁶Obstetrics & Gynaecology, Western University

Introduction: Ovarian clear cell carcinoma (OCCC) is a histotype of epithelial ovarian cancer which is characterized as a hypoxic tumour type. Metastases in EOC occurs primarily by dissociation of cells from the tumour into the peritoneal cavity as clusters of cells, termed spheroids. Hypoxia remains an important feature during this process. To maintain viability under these conditions, cells undergo rapid changes in gene expression, mediated in part by hypoxia inducible factors (HIFs), of which HIF1a is a key regulator. Changes in gene expression are accomplished in part by altering the epigenetic landscape and controlling chromatin accessibility. We seek to investigate the epigenetic dynamics in response to hypoxia in OCCC cell lines relative to non-physiologic room air conditions.

Methods: OCCC cell lines were cultured for 3 days under 1% O₂ conditions in a hypoxia incubator chamber in adherent and spheroid (ULA) conditions. Western blot analysis measured induction of HIF1a as a biomarker of hypoxia in whole cell lysates and measured global levels of H3 marks (H3K27ac, H3K4me3, H3K27me3) isolated by acid extraction. These were paired with a screen of viability in 17 human OCCC cell lines under hypoxic conditions.

Results In response to hypoxia, changes in the global abundance of activating marks, H3K27ac and H3K4me3 are observed under monolayer and spheroid conditions. Increases in global abundance of H3K4me3 and decreases in global abundance of H3K27ac are recorded. No changes are observed in levels of the repressive mark H3K27me3. These are accompanied by induction of HIF1a. Differences in viability exist between OCCC cell lines under hypoxic conditions. In spheroids, an average 2-fold increase in viability was recorded for 105C cells while a 6-fold decrease is observed in KOC-7C.

Discussions: Hypoxia is an important factor of the tumor microenvironment of OCCC. The changes identified in two histone H3 marks under hypoxia present an epigenetic state which may be more representative of the tumor biology of OCCC. Further investigation into the epigenetic landscape in the context of these specific marks may allow us to identify potential therapeutic targets.

The impact of *Akkermansia muciniphila* administration on immune system modulation and response to immunotherapy in pancreatic cancer

Amanda Liddy¹, Megan M Y Hong¹, Kelly J. Baines¹, Rene Figueredo⁷, Kait Al^{2,4}, Aswin Sureshkumar³, Christopher L. Pin^{3,6,7,8}, Jeremy P. Burton^{2,4,5}, and Saman Maleki Vareki^{1,7,8,9}

¹Department of Pathology and Laboratory Medicine, University of Western Ontario, London, ON, Canada; ²Department of Microbiology and Immunology, University of Western Ontario, London, ON, Canada; ³Department of Physiology and Pharmacology, Western University, London, ON, Canada; ⁴Canadian Research and Development Centre for Probiotics, Lawson Research Health Research Institute, London, ON, Canada; ⁵Division of Urology, Department of Surgery, Western University, London, ON, Canada; ⁶Department of Paediatrics, University of Western Ontario, London, ON, Canada; ⁷Verspeeten Family Cancer Centre, Lawson Health Research Institute, London, ON, Canada; ⁸Department of Oncology, Western University, London, ON, Canada; ⁹Department of Medical Biophysics, Western University, London, ON, Canada

Introduction: Immunotherapy remains ineffective against advanced and metastatic pancreatic adenocarcinoma (PDAC), therefore, novel treatment strategies to increase the immunogenicity of PDAC as adjuvants for immunotherapy are necessary to improve treatment outcomes. Supplementation with *Akkermansia muciniphila* (AM), a bacterium routinely found enriched in immunotherapy responders, has the potential to modulate the immune system and increase the efficacy of immunotherapy. This study investigated the effects of oral AM supplementation in combination with anti-PD1 immunotherapy, in modifying the gut microbiome and T-cell activation in PDAC.

Methods: Subcutaneous KPC tumour-bearing mice (n=24) were orally administered AM or PBS and intraperitoneally administered anti-PD1 or isotype control over the course of three weeks. At endpoint, tumour and spleen tissues were harvested for immune profiling by flow cytometry. To further investigate the effects of AM treatment on immunotherapy response, a tamoxifen-inducible PDAC mouse model, Ptf1a^{creERT/+}KRAS^{G12D}, (n=21) was used, and pancreas tissues were harvested for immune profiling after treatment with AM+anti-PD1. Stool was collected at various timepoints throughout both experiments to be characterized by 16S rRNA gene sequencing. To elucidate the anti-tumour effects of AM in-vitro, KPC cells were treated with 15% AM cell free supernatant (CFS) and proliferation, apoptosis, and cell migration were assessed.

Results: KPC mice treated with AM+anti-PD1 exhibited decreased levels of CD4+ T-cells, coupled with increased expression of T-cell activation markers, ICOS and PD1, on CD8+ T-cells within the tumours. Systemically, there was decreased levels of CD8+ T-cells, indicating that these cells may be migrating from the spleen to the tumour. In Ptf1a^{creERT/+}KRAS^{G12D} mice, there were significant increases in T-cell activation in the pancreas and spleen of mice treated with AM+anti-PD1, coupled with decreased T-cell exhaustion in the pancreas. When comparing PBS and AM-treated mice in both mouse models, there were no significant changes in microbial composition or diversity within the gut. More specifically, there was no detection of AM in PBS or AM-treated groups, indicating that AM treatment exerted immunogenic effects as it transiently passed through the digestive tract. In-vitro, KPC cells treated with 15% AM CFS exhibited significantly decreased proliferation and increased early and late apoptosis. Wound healing assays indicated that KPC cells had significantly reduced cell migration, a hallmark of tumour invasion and metastasis, when exposed to 15% AM CFS.

Discussion: As the proportion of PDAC mortality continues to increase, new therapeutic interventions are imperative for improving patient survival and quality of life. This study demonstrates anti-tumour and immunogenic effects of AM supplementation alone and in combination with immunotherapy in a model of PDAC such as increased T-cell activation and decreased T-cell exhaustion in-vivo and decreased tumour cell proliferation and migration in-vitro. Together, this work offers a novel combination therapy for PDAC and provides further insight into the relationship between the gut microbiome and cancer therapeutics.

Dissecting the roles of the tumour suppressor, Tuberin, in cell cycle dynamics tumorigenesis

Ali Nadi¹, Elizabeth Fidalgo da Silva¹, Lisa Porter^{1,2}

¹Department of Biomedical Sciences, University of Windsor, Windsor, Ontario, Canada

²St. Joseph's Health Care London, London, Ontario, Canada

Introduction

The growth and proliferation of a cell, whether it be prokaryotic or eukaryotic in nature, is heavily rooted in its ability to sense both internal and external conditions and mount appropriate physiological responses. The cell cycle describes biological mechanisms whereby environmental conditions, metabolic cues, and stressors are integrated during periods of cellular growth and division. The tumour suppressor, Tuberin (gene *TSC2*) is a key regulator in the cell cycle that helps the cell gauge such cues. While Tuberin and its roles in metabolic modulation have been well studied, **how Tuberin regulates cell proliferation and the core cell cycle machinery remain largely unexplored** and is the overall focus of this proposed research. Our lab has previously shown that nutrient signalling cascades converge on Tuberin to directly control the G2/M transition by binding to the mitotic cyclin, Cyclin B1 (gene *CCNB1*).

Methods

To better understand the constitution of the Tuberin-Cyclin B1 complex and the post-translation modification (PTM) profile of Tuberin through the cell cycle, we will use proteomic techniques such as protein-protein interaction analysis through co-immunoprecipitation and immunoblotting. In addition, co-localization assays were conducted using immunocytochemistry techniques and confocal microscopy. Mitotic index implications of ectopic expression of Tuberin SNV were investigated using flow cytometry following staining with mitotic and DNA markers. Proliferation rates of cells were determined with alamarBlue proliferation assays over the course of 72-hours. To further understand the physiological implications of the mutants, prime editing CRISPR mediated genomic editing has been used to insert the single point mutations into endogenous Tuberin of human cell lines.

Results

Ectopic expression of Tuberin single-nucleotide variants, Tuberin A614D and Tuberin C696Y, in HEK293 *TSC2*^{-/-} background, demonstrate significantly abrogated Tuberin-Cyclin B1 interaction. The implicated reduced Tuberin-Cyclin B1 complex is phenotypically corroborated with reduced Tuberin and Cyclin B1 co-localization within the HEK293 cells (Figure 1). These Tuberin SNV also demonstrate increased populations of mitotic cell populations.

Conclusions

The Tuberin-Cyclin B1 complex is a key modulator of the G2/M checkpoint of the cell cycle, acting as an integration point for nutrient and stressor signalling. When this complex is dysregulated by LOF Tuberin mutations, cells prematurely enter mitosis, resulting in increased proliferation. By studying Tuberin, a non-canonical regulator of the G2/M checkpoint of the cell cycle, this work aims to add to the growing efforts to understand the intricate biological workings behind cellular proliferation and disease.

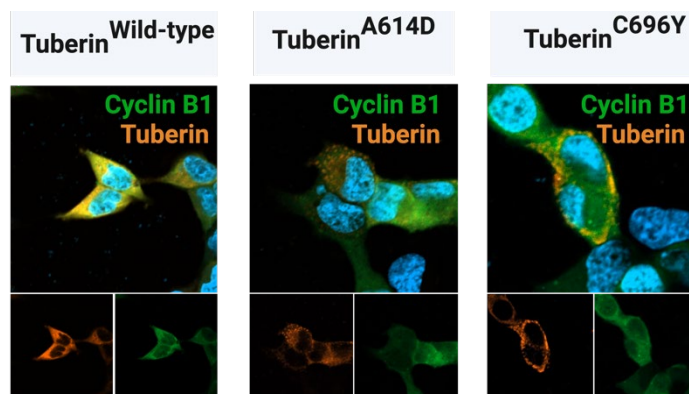


Figure 1. Tuberin missense mutations within the cyclin B1 binding domain result in reduced co-localization between the two proteins and abrogated G2M regulation of the cell cycle.

ATF3 functions within fibroblasts and immune cells to promote pancreatic cancer initiation

Mickenzie Martin^{1,3,4}, Christopher Pin^{1,2,3,4}

Departments of ¹Physiology & Pharmacology, ²Paediatrics, and ³Oncology, Schulich School of Medicine and Dentistry, University of Western Ontario; ⁴Verspeeten Family Cancer Centre, London, Ontario

Background: Pancreatic ductal adenocarcinoma (PDAC) is the 3rd leading cause of cancer-related deaths in North America with ~12% survival 5 years after initial diagnosis. A majority of The PDAC tumour consists mainly of tumour microenvironment (TME) containing ECM, fibroblasts, and immune cell populations. The TME contributes to tumour resistance but also promotes stressful conditions in the tumour such as hypoxia and nutrient scarcity, which will trigger the unfolded protein response (UPR). We examine Activating Transcription Factor 3 (ATF3), a mediator of the UPR. Global loss of ATF3 restricts preneoplastic lesion progression in mice expressing oncogenic KRAS (KRAS^{G12D}). However, ATF3 is expressed in multiple cell compartments during PDAC progression, and recent work with epithelial cell-specific deletion of ATF3 indicates ATF3 has distinct roles in these different compartments. The goal of this study was to determine the role for ATF3 in non-tumour cells, such as the fibroblasts and immune cells of the TME. We hypothesized that ATF3 functions within fibroblasts and immune cells to promote tumour growth.

Methods: To examine the role of ATF3 in the various components of the pre-malignant pancreatic environment, we compared fibroblasts and immune cell populations after injury induction in mice expressing KRAS^{G12D} with (*Ptf1a*^{creERT/+}KRAS^{G12D/+}) or without ATF3 (*Atf3*^{-/-}*Ptf1a*^{creERT/+}KRAS^{G12D/+}; referred to as *APK*). We also assessed a mouse line that allows for acinar cell-specific *Atf3* deletion and KRAS^{G12D} expression (*A*^{acinar}*PK* mice) following tamoxifen treatment. To assess the relative amounts of different fibroblast populations, we performed IHC for α -smooth muscle actin (α SMA), which marks myofibroblasts, or vimentin, which marks all fibroblasts. To assess immune cell populations we performed flow cytometry using markers for macrophages and T-cells. We also queried single cell analysis of PDAC tumours to determine genes associated with ATF3 within fibroblasts and macrophages of the microenvironment.

Results: Histological analysis comparing *Ptf1a*^{creERT/+}KRAS^{G12D/+}, *APK*, and *A*^{acinar}*PK* mice following injury induction showed no change in overall fibroblast accumulation based on analysis of vimentin, a pan-fibroblast marker. However, analysis of a fibroblast activation marker, α -SMA, showed significantly higher accumulation of activated fibroblasts in *Ptf1a*^{creERT/+}KRAS^{G12D/+} and *A*^{acinar}*PK* mice compared to *APK* mice. Flow cytometry analysis of immune cells showed no differences in total immune cell infiltration but did show a reduction in CD4⁺ T-cells when ATF3 is lost. Single cell analysis showed genes positively associated with ATF3 expression in fibroblasts were genes involved in IL-17 and TNF signaling while genes positively associated with ATF3 expression in macrophages were genes involved in regulation of macrophage migration and IL-17 signaling.

Discussion: These results suggest ATF3 functions within fibroblasts and immune cells of the microenvironment during initiation and growth of pancreatic cancer. Within fibroblasts ATF3 regulates fibroblast activation and subtype identity. Results also suggest ATF3 regulates immune infiltration and signaling within the microenvironment. Future directions will assess the *in vivo* effects of ATF3 deletion in fibroblasts and immune cells of the PDAC microenvironment.

Characterization of a Novel 25 kDa Pannexin 1 Isoform

Dan Stefan¹, Brooke O'Donnell¹, Stephanie Leighton¹, Danielle Johnston¹, and Silvia Penuela^{1,2}

¹Department of Anatomy and Cell Biology, Schulich School of Medicine and Dentistry, University of Western Ontario, London, Ontario, Canada, N6A 5C1.

²Department of Oncology, Division of Experimental Oncology, Schulich School of Medicine and Dentistry, University of Western Ontario, London, Ontario, Canada, N6A 5C1.

Introduction: Pannexin 1 (PANX1 WT) is a channel-forming membrane protein that facilitates the passage of ATP and ions and is upregulated in a diverse set of cancers. We recently identified a low molecular weight PANX1 WT isoform by mass spectrometry which is abundant in various human cancer cell lines. The isoform has a molecular weight of 25 kDa (PANX1-25K) and preliminary data suggests that it is not a product of PANX1 transcript alternative splicing. The novel protein retains the PANX1 C-terminal tail, which houses many of the known PANX1 WT post-translational modification and protein-protein interaction sites, thus we aimed to classify the biochemical properties and cellular localization of the PANX1-25K isoform.

Methods: A breast cancer cell line (Hs578T) devoid of full length PANX1 WT was used throughout this study to overexpress PANX1 WT and PANX1-25k constructs. To characterize the cellular localization of PANX1-25k, fixed Hs578T PANX1-KO cells were co-immunofluorescent labelled for PANX1 WT and PANX1-25k as well as for a variety of cell markers. The post-translational modifications of PANX1-25k were assessed by deglycosylation and dephosphorylation Western blot assays. Co-immunoprecipitation assays were also performed to assess the interaction between the PANX1 WT and PANX1-25k constructs in our overexpression model.

Results: Co-immunofluorescence revealed that the overexpressed PANX1-25k protein was largely retained at the Golgi network, and the isoform co-localized with the full length PANX1 WT here. PANX1-25k localization at the lysosomes, nucleus and the cell surface were also apparent, though accumulation of the putative isoform was not evident at the endoplasmic reticula. PANX1-25k appeared to be mostly high-mannose but not complex glycosylated, consistent with the Golgi localization observed. In our model PANX1-25k was not serine, threonine or tyrosine phosphorylated. Immunoprecipitation of PANX1-25k and PANX1 WT each revealed a direct interaction between the two proteins.

Discussion: Along with our prior results that indicate an increase in PANX1-25k expression in cancer (cutaneous squamous cell carcinoma), the Golgi localization of the novel isoform could be suggestive of its role in regulating the canonical isoform. Our work indicates that PANX1-25k has a distinct localization pattern at the nucleus, lysosome, endoplasmic reticulum, and the cell surface relative to PANX1 WT indicative of a distinct but unknown function of PANX1-25k. This work is part of the first report of a novel PANX1 isoform and its oncological implications.

Investigating the role of netrin signaling in high-grade serous ovarian cancer

Authors: Sumaiyah Wasif^{1,2}, James MacDonald², Pirunthan Perampalam^{1,2}, Frederick A. Dick^{1,2}

Affiliations:

1. Department of Pathology and Laboratory Medicine, Schulich School of Medicine & Dentistry, Western University, Canada
2. Department of Pathology and Laboratory Medicine, London Health Sciences Centre, Canada

Introduction: Ovarian cancer (OC) is the most lethal gynecological cancer, and high-grade serous ovarian cancer (HGSOC) is its most common subtype. OC spreads through the development of spheroids within the peritoneal cavity, allowing them to persist in the abdomen and making them resistant to surgery and mainline therapeutics. A genome wide CRISPR screen from our lab identified Netrins and MAPK pathway as essential for spheroid survival. Therefore, I hypothesize that Netrins enhance the survival of HGSOC cells and contribute to chemotherapy resistance.

Methods: To investigate MEK inhibition in various HGSOC cell lines in suspension and adherent conditions, crystal violet (CV) and trypan blue assays were used to determine viability and proliferation. To elucidate whether survival signal is solely netrin-dependent, we will test downstream interactions with netrin-receptor knockouts and MEK inhibitors in cells using epistasis tests. We will investigate the cell death mechanisms responsible for cytotoxicity of HGSOC spheroids upon MEK inhibition, as well as the role of EMT in HGSOC spheroids. Future work will include *in vivo* experiments to assess the therapeutic window of MEK inhibition and its correlation between netrin expression and immune regulation in both immunocompromised and immunocompetent mice. Additionally, we plan to investigate associations between netrin expression and surgical outcome, therapy resistance and other comorbidities, in clinical samples.

Results: Based on CV and trypan blue assays we determined that a dose of under 10nM was enough to inhibit 50% survival in HGSOC spheroids. Our findings also show that adherent, proliferating HGSOC cells show a cytostatic response, whereas dormant spheroids show a cytotoxic response to MEK inhibition.

Conclusion: Investigating the role of netrin signaling in ovarian cancer is essential to provide molecular insights into mechanisms underlying therapy resistance, cancer dormancy, and disease progression to potentially develop cancer therapeutics to improve patient outcome.

Custom prospective viable tissue procurement from the Ontario Tumour Bank (OTB) London Health Sciences Centre (LHSC) site: supporting the next generation of precision medicine initiatives

Carolyn Shire¹, Jennifer Petzke¹, Riley Cox², Gino Celebre³, Anbreen Zaidi³, Waad Matar⁴, Larry Phouthavongsy², Katarina Maksimovic², Ilinca Lungu², Dianne Chadwick^{2,5}, Lincoln Stein^{2,5}, Jeremy Parfitt^{1,6}

¹London Health Sciences Centre (London, Ontario), ²Ontario Tumour Bank, Ontario Institute for Cancer Research (Toronto, Ontario), ³St. Joseph's Healthcare Hamilton (Hamilton, Ontario), ⁴The Ottawa Hospital (Ottawa, Ontario), and ⁵University of Toronto (Toronto, Ontario), ⁶Western University (London, Ontario)

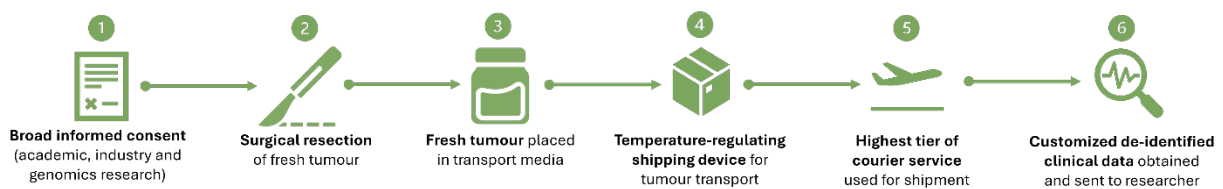
Introduction: OTB has historically provided tissue samples for research that have been stored frozen or fixed. Recently, there has been an increased demand for viable fresh tumour to support advanced precision medicine. Fresh tumour has many applications, including interrogating the tumour microenvironment, creation of patient-derived (PD) models (PDOrganoids/PDXenografts), and AI-fueled drug development.

Methods: Biobanking fresh tumour poses several challenges, including amending Research Ethics Board (REB) documents to include PD models; ensuring fresh tumour collection prioritizes patient care/pathological diagnosis; keeping sample temperature between 2-8 °C during distribution; and delivering tumour to the client within 24 hours. Some industry clients are also unfamiliar with requirements for ethics review of their study or privacy standards. The OTB LHSC team mitigated these challenges by amending our REB protocol and informed consent form; targeting cases where clinical chart review (diagnostic imaging and prior biopsy) indicated a large malignancy; using temperature-regulating shipping devices; preparing customs and shipping documentation in advance; and scheduling shipments using the courier's highest service tier available.

Results: This led to the successful provision of multiple lung tumour cases from the OTB LHSC site to an American industry biotechnology startup. Due to this achievement, numerous new inquiries to acquire fresh tumour from the OTB LHSC site have been received and contracting with academic and industry researchers is in progress. OTB has also been included as collaborators on living biobank grants involving rare tumours.

Conclusions: OTB is one of the few comprehensive solid tumour banks in North America and its LHSC site is an ideal source of fresh tumour for research. Viable fresh tumour is essential for many types of research by OTB clients, including rapid drug screening, PDOrganoid/PDXenograft model generation and tumour infiltrating lymphocyte analysis. By creating a custom workflow, the OTB LHSC site now broadly offers custom prospective procurement of fresh tumour (as well as matched fresh blood) to the academic and industry research community across North America. Next steps will involve the addition of clinical molecular biomarkers, whole genome sequencing and whole transcriptome sequencing data to OTB's data annotations to continue to meet the evolving needs of research.

Figure 1 – Custom fresh tumour collection workflow



Title: Switch of SPCA2C to Larger Isoform Remodels Store-Operated and Store-Independent Calcium Entry During Pancreatic Cancer Progression

Petra Samardzija¹, Oneeb Hassan¹, Stephanie Chen¹, Aswin Sureshkumar¹, Fatemeh Mousavi, Mickenzie B. Martin¹, Joana R. Pinto¹, Emilie Jaune-Pons^{1,4}, Peter B. Stathopoulos¹, Christopher L. Pin¹⁻⁴.

Departments of ¹Physiology and Pharmacology, ²Oncology, and ³Paediatrics, Schulich School of Medicine and Dentistry, University of Western Ontario, ⁴Verspeeten Family Cancer Centre and Baker Centre for Pancreatic Cancer, Lawson Health Research Institute, London, Ontario, Canada.

Introduction: Pancreatic ductal adenocarcinoma (PDAC) is the 3rd leading cause of cancer-related death in Canada with a five-year survival rate of ~12%. Identification of novel biomarkers and therapeutic targets are necessary to improve earlier prognosis and treatment of PDAC. Calcium (Ca²⁺) is an essential second messenger required for the integration of signals from the extracellular environment and regulation of numerous signaling proteins, transcription factors and enzymes. Increased Ca²⁺ influx through ORAI1 channels on the plasma membrane via the store-operated and store-independent Ca²⁺ entry pathways (SOCE and SICE, respectively) results in increased cancer cell migration, proliferation and chemoresistance. SOCE and SICE are therefore attractive therapeutic targets for cancer, however, little is known about their role in PDAC. Our laboratory studies a truncated pancreas specific isoform of secretory pathway Ca²⁺ ATPase 2 (SPCA2C), which modulates both SOCE and SICE. Proximity-dependent biotin identification revealed a network of candidate SPCA2C interactors involved in Ca²⁺ regulation including stromal interaction molecule 1 (STIM1), coiled-coil domain containing protein 47 (CCDC47) and ORAI1. The goal of this study is to examine the role of SPCA2C and its Ca²⁺-regulating interactors in PDAC.

Methods: Co-immunoprecipitation (Co-IP) was performed to examine SPCA2C interactions with CCDC47 and STIM1. SPCA2C-CCDC47 and -STIM1 co-localization was examined via immunofluorescence (IF). To assess SPCA2C, CCDC47, STIM1 and ORAI1 expression during PDAC progression, RNA sequencing was performed on wild type mouse pancreatic acinar cells, pancreatic organoids derived from mice expressing oncogenic KRAS (*Ptf1a^{creERT/+}Kras^{G12D/+}*; *PK*) and patient-derived organoids from pancreatic cancer biopsies. Expression of SPCA2C at the protein level was also examined via western blot in mouse pancreatic acinar cells, *PK* organoids and cells from the KPC (*Kras^{G12D/+}*; *Trp53^{R172H/+}*; *Pdx-1-Cre*) PDAC mouse model. The influence of CCDC47 on STIM1 and ORAI1 protein expression was assessed via western blot in cells from patient-derived xenografts treated with CCDC47 siRNA.

Results: We revealed interactions and co-localization of SPCA2C with CCDC47 and STIM1. RNA sequencing and western blot showed a loss of SPCA2C expression in the *PK* organoids and KPC cells, however, expression of a larger SPCA2 isoform was observed instead. mRNA expression of STIM1, ORAI1 and CCDC47 remained consistent between the acinar cells and *PK* organoids. A decrease in STIM1 protein expression was observed in PDAC cells from patient-derived xenografts with CCDC47 knockdown.

Discussion: We identified SPCA2C interactions with STIM1 and CCDC47. During PDAC progression SPCA2C expression switches to a larger isoform and CCDC47 stabilizes STIM1 in PDAC cells. Overall our results suggest that the SOCE and SICE pathways are remodelled during early PDAC progression, highlighting a potential diagnostic and therapeutic target of PDAC.

Quinone Reductase 2 (NQO2) regulates cell proliferation and the activity of several clinical chemotherapeutic kinase inhibitors

Faiza Islam¹, Matthew D. Walker, Matthew Maitland, Brian H. Shilton¹

¹Western University, London, Ontario

Introduction

Quinone Reductase 2 (NQO2) is a pseudoenzyme from a family of flavin-dependent detoxification enzymes, with physiological roles in memory and learning behaviours. NQO2 is a notorious off-target interactor of clinical chemotherapeutic kinase inhibitors – it binds to at least 30 drugs and has a nanomolar affinity for 10 of them. Because of the frequency and potency of these interactions, we hypothesized that NQO2 inhibition could contribute to the pharmacological effects of these drugs in cancer patients. Given NQO2's role in memory, its inhibition may also lead to unintended cognitive side effects in patients. We wanted to understand the cellular function of NQO2 and investigate the effect of NQO2 inhibition by kinase inhibitors.

Methods

We investigated the mechanism of NQO2 inhibition by kinase inhibitors with kinetic and structural analysis. To understand NQO2 cellular function, we derived NQO2 knock-out cell lines, HeLa and HCT116, by CRISPR-Cas9 targeting and used mass spectrometry to identify changes in the proteome due to NQO2 loss. The NQO2-dependent effect of different kinase inhibitors was assessed by measuring cell viability after drug treatment.

Results

As a pseudoenzyme, NQO2 is unable to efficiently catalyze the required oxidation of reducing co-substrates. Because of its minimal enzymatic activity in cells, it was challenging to understand the effect of NQO2 inhibition by kinase inhibitors. Kinetic and structural analysis showed that NQO2 can function as a flavin redox switch, and its binding to different inhibitors stabilizes distinct redox forms of the sensor protein. To understand NQO2 cellular function, we characterized changes in the proteome due to NQO2 knock-out in colon cancer-derived HCT-116 cell line. NQO2 knock-out slowed the proliferation of the cancer cells. The NQO2 knock-out cell line also had a significantly different proteome than the parental cell; we identified novel roles for NQO2 in regulating lysosome and exosome proteins. Finally, consistent with our hypothesis we found that several NQO2 interacting clinical drugs had NQO2-dependent cytotoxic effects.

Conclusion

The cellular function of NQO2 was unknown, but it was shown to be a frequent off-target interactor of several clinical kinase inhibitor drugs. We showed that NQO2 may affect the activity of these drugs and be involved in cancer-related processes, proliferation, and apoptosis.

Oncogenic KRAS-mediated epigenetic reprogramming is altered by loss of Activating Transcription Factor 3

Fatemeh Mousavi^{1,5}, Parisa Shooshtari^{1,3}, Christopher Pin^{1,2,4,5}

Departments of ¹Physiology & Pharmacology, ²Paediatrics, ³Pathology and Lab Medicine and ⁴Oncology, Schulich School of Medicine and Dentistry, University of Western Ontario;

⁵Verspeeten Family Cancer Centre, London, Ontario

Introduction: With a five-year survival rate ~12%, Pancreatic Ductal Adenocarcinoma (PDAC) is the 3rd leading cause of cancer-related deaths in North America. Over 90% of PDAC patients harbour a *KRAS* mutation, the most common form being *KRAS*^{G12D}. However, without additional genetic mutations or environmental events, such as chronic pancreatitis, *KRAS* mutation alone does not lead to PDAC. Our laboratory showed Activating Transcription Factor 3 (ATF3) was required for histone deacetylation at genes that stabilize the mature acinar cell phenotype and the progression from low to high grade pancreatic intraepithelial neoplasia (PanIN) in the presence of *KRAS*^{G12D}. However, ATF3 contributes to both gene activation and repression and how it affects PDAC progression remains unknown. Examination of potential ATF3 co-regulators has identified epigenetic regulators, such as histone deacetylase 5 (HDAC5). Therefore, we hypothesize that *KRAS*^{G12D} requires ATF3 for epigenetic reprogramming in precursor PanINs lesions. The focus will be primarily on histone acetylation events.

Methods: Mice were generated that allowed cre recombinase-mediated pancreatic acinar-specific *KRAS*^{G12D} activation combined with (*Ptf1a*^{creERT}*KRAS*^{LSL-G12D}) and without ATF3 (*Ptf1a*^{creERT}*LSL-KRAS*^{G12D}*Atf3*^{-/-}; **APK**). Mice were treated with tamoxifen to induce cre-mediated *KRAS*^{G12D} induction and then subjected to cerulein-induced pancreatitis 10 days later to induce PanIN progression. Cerulein-treated mice were sacrificed 2 weeks after CIP and used for establishing 3D tumour organoid lines. RNA-seq and chromatin immunoprecipitation for H3K27 acetylation (H3K27ac) followed by sequencing (ChIP-seq) was performed. Sequenced datasets were aligned to the mm10 genome using STAR (RNA-seq) or Bowtie2 (ChIP-seq). Differential expression and differential binding analyses were performed using DESeq2 (RNA-seq) or DiffBind (ChIP-seq). The levels of acetyl-CoA, the substrate for acetylation, were also assessed and compared. In addition to H3K27ac, H3K04me1, H3K04me3, and H3K09me3 were examined through western blots.

Results: Assessment of different epigenetic marks showed *KRAS*^{G12D} expression promoted epigenetic reprogramming in PanINs, including significant dysregulation of H3K27ac enrichment. ChIP-seq results for H3K27ac showed the absence of ATF3 reduces H3K27 acetylation, preferentially at gene promoter regions. Functionally, many of the affected genes are involved in *KRAS* signaling, corroborating the RNA-seq results showing a differential activation of *KRAS* signaling pathways. This suggests a role for ATF3 in regulating oncogenic *KRAS* activity in preclinical models. Comparing the genes with an ATF3-dependent acetylation pattern to a curated list of *KRAS*-targeted genes indicated presence of genes, such as *SMARCC2* (*BAF170*), a SWI/SNF complex subunit, and *KDM1B*, a histone demethylase affecting H3K4. This suggests a potential role for ATF3 in widespread epigenetic regulation. This is in line with public sequencing data from PDAC patients, which shows ATF3 expression positively correlated with expression of several SWI/SNF complex subunits and demethylases.

Discussion: There are currently no clinically approved therapeutic options targeting oncogenic *KRAS* in pancreatic cancer. This study proposes a potential avenue for targeting

oncogenic KRAS's activity while preventing epigenetic dysregulations aiding KRAS's promotion of PDAC. Future studies will elucidate binding partners and mechanism of action of ATF3 and the effect of inhibiting them on PDAC progression in patient-derived samples.

The Role of Spy1 in Mammary Involution and Oncogenic Susceptibility

Hinch, I¹, Fifield, B. ¹, Porter L.A. ¹

¹University of Windsor, Windsor, Ontario. N9B 3P4. Porter Lab, Department of Biomedical Sciences

Introduction: From puberty to menopause, factors attributed with breast cancer fluctuate with the natural mammary development. A period of increased breast cancer risk with increased metastasis and mortality occurs following childbirth – potentially linked to mammary involution: gland remodeling post lactation, which balances high rates of apoptosis and cell regeneration. Two processes controlled by the cell cycle and its regulators. The cyclin-like protein Spy1 can enable cell proliferation and override apoptosis. Spy1 levels have been found to be elevated breast cancer. Interestingly, levels of Spy1 are also elevated during involution. We hypothesized that Spy1 protects the cell population necessary for normal mammary gland reconstitution post involution.

Methods: To address this, an *in vitro* mock involution model was deployed with the murine epithelial cell line (HC11) over a delivery and withdrawal of hormonal time course. This was paired with *in vivo* tissue collection of the mouse model overexpressing Spy1 in the mammary gland (MMTV-Spy1) over an involution time course as well as DMBA (7,12-Dimethylbenz[a]anthracene) for cancer susceptibility.

Results: *In vitro* results suggest the ability of Spy1 of maintaining stemness post-differentiation, and *in vivo* data indicates failure of healthy epithelial clearing during involution and increase oncogenic susceptibility.

Discussion: This research begins to articulate the role of Spy1 during normal mammary involution in and how overexpression prevents healthy mammary healing potentially play a role in the predisposition of the breast to oncogenesis.

Investigating synergistic combinations of MRT68921 and afatinib as a therapeutic strategy in epithelial ovarian cancer

T Johnston^{1,2}, Y Ramos Valdes¹, M Borrelli^{1,2}, E Tomas^{1,2}, B Kolendowski¹, G E DiMattia^{1,4,5}, and T G Shepherd^{1,2,3,4}

¹The Mary & John Knight Translational Ovarian Cancer Research Unit, Verspeeten Family Cancer Center, London, Ontario, Canada; Departments of ²Anatomy and Cell Biology, ³Obstetrics & Gynaecology, ⁴Oncology, ⁵Biochemistry, Schulich School of Medicine and Dentistry, The University of Western Ontario, London, Ontario, Canada

Introduction: Epithelial ovarian cancer (EOC) bears the highest mortality rate among gynaecological cancers in the developed world due to late-stage detection and a lack of effective strategies against chemoresistant disease. Due to the absence of distinguishing symptoms, women are often diagnosed at advanced stages with metastatic disease. The unique metastatic pattern of EOC involves cells detaching from the primary tumor and forming multicellular aggregates termed spheroids, which disseminate and aggregate within the intraperitoneal cavity, leading to malignant ascites. Spheroids possess enhanced adhesive capacities and are inherently difficult to treat due to adaptive metabolic reprogramming. Our group has shown that autophagy, an evolutionarily conserved intracellular recycling process, is required to maintain spheroid integrity and viability. Autophagy activation has been implicated as a protective mechanism that helps cancer cells evade chemotherapeutic insults. Here, we investigated the inhibition of unc51-like-kinase 1 (ULK1), a crucial regulator of autophagy, using MRT68921 and explored its combination with the tyrosine kinase inhibitor afatinib to investigate drug synergism.

Methods: Cell lines representing high-grade serous (HGSC) and clear cell carcinoma (OCCC) were cultured in both adherent and spheroid conditions. To compare cell line sensitivity to MRT68921 under adherent and spheroid conditions, 12-point dose-response curves were generated using alamarBlue cell viability assays. Immunoblotting was performed to verify the on-target effects of MRT68921 and afatinib, along with markers of autophagy and apoptosis. Autophagic flux was monitored using mCherry-eGFP-LC3 cell lines. Drug combination matrices evaluated spheroid cell viability, followed by Synergy Finder analysis to identify drug synergy. Synergistic combinations of MRT68921 and afatinib were further analyzed using spheroid reattachment assays, trypan blue exclusion cell counting, and alamarBlue viability assays across a broader range of cell line spheroids. These synergistic combinations were also assessed in ascites- and patient-derived organoids.

Results: Across a panel of HGSC and OCCC cell lines, cell lines in adherent culture exhibited greater sensitivity to MRT68921 compared to when cultured as spheroids. MRT68921 rapidly inhibited ULK1 activity, leading to effective autophagy inhibition at low micromolar concentrations. Afatinib treatment induced autophagy likely via AKT blockade. Notably, MRT68921 blocked autophagic flux while afatinib increased autophagic flux in mCherry-eGFP-LC3 cell line spheroids. Additionally, the combination of MRT68921 and afatinib impaired autophagic flux. Spheroid reattachment and cell viability assays demonstrated robust effects of combination treatment primarily driven by MRT68921. Early results in ascites- and patient-derived organoids support these findings.

Conclusions: We are the first to assess the potential drug synergism of MRT68921 and afatinib in EOC. These results lay the groundwork for further exploration of combined autophagy and tyrosine kinase inhibition and its potential as a novel therapeutic strategy against chemoresistant disease.

Structure-guided rational drug design of novel Pin1 inhibitors

Shaunik Sharma¹, Brian Shilton¹, and Kun Ping Lu^{1,2,3}

1. Department of Biochemistry, Western University
2. Department of Oncology, Western University
3. Robarts Research Institute, London, Ontario

Introduction: Targeted cancer therapies exploiting specific pathways have revolutionized the treatment of some cancers, but many do not respond to treatments due to alternative pathways or immune tumor environments. There is a dire need for drugs that block multiple cancer-driving pathways and turn immune tumors “hot” to render drug-resistant cancers treatable. Pin1 is a unique enzyme that is widely overexpressed in most cancers, drives tumorigenesis by activating over 70 oncoproteins and turning off over 30 tumor suppressors, promotes cancer resistance and the epithelial-to-mesenchymal transition (EMT), and immunosuppression. Pin1 inhibitors identified in the past three decades are not good candidates for drug development as they lack either potency, selectivity, or cell permeability. A novel high-affinity Pin1 inhibitor (Cpd1) was previously identified by the Lu lab with a high-throughput fluorescence-polarization-based screen. Cpd1 not only inhibits catalytic activity but also triggers robust Pin1 degradation through the ubiquitin-proteasome pathway, exhibits a dose-dependent effect on cell viability in multiple cancer cell lines, and suppresses tumor growth in mouse models. The inhibitory mechanism of Cpd1 was unknown and it exhibited a very low half-life of 2.7 minutes in plasma and only 1 hour in PBS buffer.

Methods: To rationalize this discrepancy between the *in vitro* stability, and the anti-cancer effects in cell lines and mouse models, the inhibition mechanism of Cpd1 was investigated through scanning absorption spectroscopy, degradation kinetics, RP-HPLC, and a PEG-maleimide assay. The Cpd1 degradation mechanism was validated using in-solution digestion ESI mass spectroscopy, and Pin1 was crystallized for structure determination. Cpd1 derivatives synthesized by collaborators from McMaster were characterized, and a competition-based fluorescence-polarization assay was used to determine the K_i of a novel set of hybrid cyclic molecules identified by a collaborator from Johns Hopkins.

Results: Cpd1 degrades in buffer at physiological pH, with a peak shift in absorption spectra that research equilibrium within 1 hour but is stable under acidic conditions. RP-HPLC indicated that Cpd1 was forming a new less hydrophobic species after degradation, and the rate of degradation was linearly proportional to hydroxide ion concentration, suggesting that Cpd1 was getting hydrolyzed. The PEG-switch assay strongly indicated that hydrolyzed Cpd1 was binding covalently or with picomolar affinity, while the intact drug did not bind Pin1. Covalent Cpd1 binding was confirmed with mass spectroscopy, and Pin1 crystals were diffracted to 2.0 Å but no bound drug was observed. Cpd1 derivatives protect the molecule against hydrolysis, which introduces the potential of using certain chemical groups to modulate the rate of Cpd1 hydrolysis. From nine potential hybrid cyclic inhibitors, four inhibited Pin1 with low micromolar affinity (K_i).

Conclusion: Cpd1 is a pro-drug that gets hydrolyzed in physiological conditions with the secondary molecule binding covalently to a key catalytic cysteine in the Pin1 activity site. The non-essentiality of Pin1 offers further potential for combination therapies as it can reduce the effective dose and limit the broad cytotoxic effects observed with chemotherapy. Identification of the bio-active pro-drug and characterizing Cpd1 derivatives allows for iterative structure-guided rational drug design, working towards clinical development as a novel cancer therapeutic.

The role of Spy1 in Cell Cycle Checkpoint Evasion in Glioblastoma

Mahendran, H.¹, Lubanska, D.¹, and Porter, A.¹

¹ Department of Biomedical Sciences, University of Windsor, Ontario. N9B 3P4.

Introduction:

Glioblastoma (GBM) is a lethal type of brain tumour evading all intricate attempts of modern therapies. Brain tumour initiating cells (BTICs) are at the source of the initiation, progression, and therapy resistance of heterogenous mass of glioblastoma and are responsible for post-therapy tumour recurrence. BTICs share properties with normal neural stem cells (NSCs), including ability to self-renew and give rise to differentiated progeny. Previously, our lab established that the levels of an atypical cell cycle protein, SPY1 (RINGO; gene *SPDYA*) are elevated in malignant human glioma and its upregulation correlates with poor prognosis of patients with GBM. Spy1 activates Cyclin Dependent Kinases (CDK) non canonically and has been demonstrated to override protective cell cycle checkpoints. SPY1 regulates symmetric division of BTICs in subsets of high-grade glioma leading to aberrant expansion of those aggressive populations of cells. We hypothesize that selective targeting of SPY1-CDKs can be a potential therapeutic intervention to enhance the treatment success in GBM patients.

Methods:

My research project focuses on dissecting the mechanisms behind SPY1-mediated effects and further validation of SPY1 as a potential therapeutic target in GBM. The objectives of my study will allow for evaluation of BTIC biology in face of SPY1 depletion and functional assessment utilizing GBM patient-derived, three-dimensional spheroids *in vitro* using drug treatment response screens (e.g. standard of care, CDK inhibitors) and *in vivo* models including zebrafish and mouse patient derived xenograft (PDX) screening platform.

Results:

We are establishing an elaborate panel of GBM patient-derived cultures which have been evaluated using transcriptomics and are transduced with shRNA vs. control constructs targeting *SPDYA*. Functional *in vitro* assay and drug response signature is established using the panel of Spy1 KD cultures and compared to transcriptomic profiles. Combination of Spy1 KD with selected aberrant changes is then tested for tumour formation using a syngeneic GL261 mouse glioma model in which Spy1 depletion significantly delays tumour initiation and decreases tumour burden.

Conclusions:

Spy1 levels are elevated in human glioma and correlate with poor prognosis and data *in vitro* supports the utility of targeting the Spy1 mechanism clinically. In this work we will conduct a pre-clinical assessment of the utility of targeting Spy1 in GBM and will identify a signature for patients that are the best candidates for the early testing of this response. This work will also be critical to optimize the potential of positive response when moving into clinical testing. The combination of platforms which will be used in this study will help in detailed examination of changes in the heterogeneous GBM population that will provide valuable insight into the changes that can occur in GBM biology during targeted and combination therapy.

Title: Activation of a viral mimicry response inhibits colitis-associated cancer

F. Larsen^{1,2}, W. Down², H. J. Good^{1,2}, A. E. Shin^{1,2}, M. Derouet², L. Zhang², P. Shoostari¹, C. Castellani¹, S. Asfaha^{1,2}

¹Department of Pathology and Laboratory Medicine, Western University, London, ON

²Department of Medicine, Western University, London, ON

Introduction: Almost half of the human genome is comprised of transposable elements (TEs). In homeostasis, these elements are repressed by epigenetic mechanisms such as DNA methylation. Interestingly, it was recently shown that re-expression of these elements by DNA hypomethylating agents inhibits tumor growth by activation of an interferon response (viral mimicry response). The role that re-expression of TEs plays during colitis and cancer initiation, however, is not well understood. Thus, we aim to investigate whether activation of viral mimicry inhibits colitis-associated cancer initiation.

Methods: We first examined the RNA expression of TEs and interferon response genes during acute colitis in WT mice administered 2.5% dextran sodium sulfate (DSS) in the drinking water for 5 days. To examine the effects of viral mimicry on cancer initiation, we used our previously described colitis-associated cancer (CAC) mouse model in which tumors arise from DCLK1+ cells following loss of the tumor suppressor adenomatous polyposis coli (APC) (*Dclk1/Apc^{fl/fl}*) and induction of colitis. *Dclk1/Apc^{fl/fl}* mice were treated with three doses of tamoxifen followed by DSS. Mice were then treated with 6 doses of 5-AZA-2'-deoxycytidine (5-AZA) versus vehicle and tumor number assessed. To induce viral mimicry specifically in the DCLK1+ cells, we crossed *Dclk1/Apc^{fl/fl}* mice to *Dnmt1^{fl/fl}* mice. This allowed us to knockout (KO) the DNA methyltransferase DNMT1 in DCLK1+ cells. Similarly, these mice were treated with tamoxifen and DSS and tumor number assessed. We performed DNA methylation analysis using the Infinium Mouse Methylation BeadChip Array and RNA expression analysis of TEs and interferon response genes on colonic tissues from 5-AZA versus vehicle treated mice. To test whether inhibition of viral mimicry affects tumorigenesis, we crossed *Dclk1/Apc^{fl/fl}/Dnmt1^{fl/fl}* mice to MAVS-KO mice and compared tumor number. Similarly, we treated WT or MAVS-KO mice with 10 mg/kg azoxymethane and DSS followed by 5-AZA or vehicle. To examine the role of viral mimicry specifically in epithelial cells, we compared DCLK1+ cell lineage tracing in 5-AZA treated or DNMT1-KO colonic organoids from MAVS-KO vs MAVS+/+ mice. Finally, we performed RNA expression analysis of TEs and interferon response genes using a patient RNA-seq dataset of control versus colitis and colitis-associated dysplasia colonic samples.

Results: DSS colitis was associated with re-expression of TEs and interferon signaling. 5-AZA or DNMT1-KO led to DNA hypomethylation and upregulation of TEs and interferons. Activation of a viral mimicry response by DNMT1-KO or 5-AZA significantly reduced tumor number. KO of the type I interferon response gene, MAVS, reversed the antitumor effect observed with DNMT1-KO or 5-AZA. MAVS-KO was further associated with increased stem cell lineage tracing capacity of DCLK1+ cells in vitro. Correlating with our observations in mice, we found that TE and interferon expression was significantly decreased in patients with dysplasia when compared to patients with active colitis.

Discussion: Our findings demonstrate that activation of viral mimicry by DNA hypomethylation reduces tumorigenesis. Inhibiting the viral mimicry response by MAVS-KO reverses this effect and further promotes tumorigenesis. Taken together, these data suggest that a reduced viral mimicry response may contribute to the development of colitis-associated dysplasia in humans.

Investigating the Therapeutic Potential of Naporafenib in Anaplastic Thyroid Carcinoma

Harrison Pan^{1,2}, Amir Karimi^{1,2}, Peter Zeng^{1,2}, Mushfiq Shaikh², John Barrett², Anthony Nichols²

¹Department of Pathology and Laboratory Medicine, Schulich School of Medicine and Dentistry,

²Department of Otolaryngology – Head and Neck Surgery, London Health Science Centre

Introduction: The incidence rate of thyroid cancer has significantly increased over the past few decades. The vast majority of these cases are papillary thyroid carcinoma typically with a positive prognosis; in contrast, anaplastic thyroid carcinoma (ATC) is a rare and highly aggressive subtype with an almost 100% mortality rate. Recent approval of RAF inhibitor (dabrafenib) and MEK inhibitor (trametinib) for a subset of ATC patients with *BRAF* V600E mutation has transformed the treatment landscape. Besides the standard treatment, naporafenib, a type II pan-RAFi, has emerged as an effective anti-tumour agent based on the data from our patient-driven xenograft models. Our research group is interested in characterizing the anti-tumour efficacy of naporafenib and elucidating its effect on tumour microenvironment using an immunocompetent mouse model.

Methods: To determine the drug sensitivity of ATC cells, we assessed naporafenib's cell line-specific IC50 by performing dose-response experiments on both human and murine ATC cell lines. Based on the results, we selected two naporafenib-sensitive human cell lines ASH3 (*BRAF*^{WT}) and SW1736(*BRAF*^{V600E}) for a 24-hour naporafenib treatment followed by a reverse phase protein array (RPPA) assay to examine changes in key protein pathways. We then injected murine ATC cell line TBP-3743 into immunocompetent B6129SF1/J mice to test the anti-tumour efficacy of naporafenib. Tumour volumes were measured daily as the primary parameter to evaluate its anti-tumour effects. After the tumour volumes reached the humane endpoint, we harvested the murine tumours and isolated the total RNA from the samples which were then sent for a bulk RNA sequencing analysis.

Results: The human ATC cell lines demonstrated varying levels of sensitivity to naporafenib while the murine cell lines were deemed sensitive to our drug of interest. The RPPA results suggested differential phosphorylation of CRAF, a member of the RAF family, in both cell lines following naporafenib treatment. The results of our syngeneic murine model showed that naporafenib inhibited murine tumour growth compared to the control group. According to the bulk RNA sequencing results, the naporafenib-treated murine tumours appeared to be more inflamed as we observed increased expressions of immune cell-related signatures in the tumour microenvironment.

Discussion: ATC is an uncommon yet fatal cancer that preferentially affects the elderly. Unfortunately, clinical and translational investigations have been dampened by its rarity. Our collective work suggests that naporafenib can control tumour growth by inhibiting *BRAF*^{V600E} in the MAPK signaling pathway, promoting a compensatory increase in phosphorylation of CRAF. Finally, our *in vivo* results demonstrated that naporafenib was able to stabilize murine ATC progression as well as recruiting immune cells into the tumour microenvironment, suggesting its potential to be administered in combination with immunotherapy agents as a future therapeutic strategy.

The role of IKZF3 and its induced degradation by lenalidomide in chronic lymphocytic leukemia.

Maria F. Uribe Estrada and Rodney DeKoter

Department of Microbiology & Immunology Western University

Introduction: Chronic lymphocytic leukemia (CLL) is a rare blood cancer that increases in frequency with age. CLL involves transformation of mature B cells with dysregulated signaling pathways involving the B-cell receptor (BCR). IKZF3 is a transcription factor also known as Aiolos that regulates genes involved in lymphocyte development. Studies have revealed that mutations and overexpression of IKZF3 play a crucial role in CLL. An IKZF3 L162R “hotspot” driver mutation was found in 3% of all CLL cases, causing B cell neoplasia and altering BCR signaling. Lenalidomide, an immunomodulatory drug (IMiD), specifically targets IKZF3 for proteasomal degradation. Lenalidomide acts as a molecular glue, binding IKZF3 to the ubiquitin ligase complex. Through its binding to the substrate receptor CRBN, lenalidomide induces conformational changes, modulating its substrate specificity. The central hypothesis of this project is that overexpression of the IKZF3 L162R mutation will alter gene expression in a manner promoting chronic lymphocytic leukemia, and that lenalidomide-induced degradation of IKZF3 L162R will restore the dysregulated signaling pathways.

Methods: The initial step in our experimental procedure involves cloning the wild-type (WT) IKZF3 gene into an ampicillin resistant plasmid. Subsequently, site-directed mutagenesis was performed to introduce specific amino acid changes (L162R, Q147H, H196Y) into the IKZF3 sequence. The mutated plasmids were ligated into the lentiviral vector PLVX IRES PURO, which contains a puromycin resistance gene. Transient transfection using HEK293T cells was performed to produce lentiviral particles. Next, REH human leukemia cells were infected with these constructs through spin infection. After infection, the REH cells were selected using puromycin. After successful selection of the infected REH cells, the cells will be treated with lenalidomide to study its effects. Lenalidomide treatment will be carried out by culturing the cells in a medium containing the desired concentration of lenalidomide for a specified period.

Results: REH cells effectively degrade IKZF3 in response to lenalidomide treatment, highlighting the potential of this drug in targeting IKZF3 in leukemia cells. We expressed IKZF3 in the leukemia cell line REH following lentiviral transduction. Next, changes in gene expression and cell signaling will be determined.

Discussion: Understanding the molecular mechanisms of IKZF3 mutants in leukemia cells and lenalidomide-induced IKZF3 degradation is essential for developing targeted molecular therapies in blood cancers. This work will help rationalize the use of lenalidomide for treatment of CLL.

Expression of c-Met receptor for tumor-specific near-infrared imaging in human and canine non-small cell lung cancer

Ann S. Ram^{1*}, Jim Petrik¹, Geoffrey A. Wood², Samuel Workenhe³, and Michelle L. Oblak³

¹Department of Biomedical Sciences, Ontario Veterinary College, University of Guelph

²Department of Pathobiology, Ontario Veterinary College, University of Guelph

³ Department of Clinical Studies, Ontario Veterinary College, University of Guelph

Introduction: Non-small cell lung cancer (NSCLC) is the most prevalent subtype of lung cancer and surgical resection is the initial standard of care. Similarly, canines with spontaneous pulmonary carcinoma have comparable disease presentation as non-smoker NSCLC patients and require surgery as the primary treatment. To prolong patient survival and maximize preservation of healthy tissue, intraoperative guidance is necessary to delineate malignant and healthy tissue. Recently, near-infrared (NIR) imaging has been utilized to improve intraoperative tumor bed imaging with high efficacy, however there is a lack of specific tumor targeted NIR imaging agents for NSCLC. We aim to utilize overexpressed receptors in NSCLC to develop an NIR imaging probe that can provide reliable surgical resection guidance. As canines are good models for human lung cancer, we will translate this technique in canine cancer patients to human lung cancer patients as well. We hypothesize that the hepatocyte growth factor receptor (c-Met) will be overexpressed in NSCLC cells and tissues compared to normal lung cells and tissues.

Methods: Three human NSCLC cell lines (A549, NCI-H1975, and NCI-H358), three canine lung adenocarcinoma cell lines (CLAC, HDC, and LuBi), and a normal human small airway epithelial cell line were used. Western blots were performed, and membranes were probed with a c-Met primary antibody. Cells were also seeded in chamber slides for immunofluorescence. ImageLab software was used to quantify protein expression. Slides were assessed by confocal microscopy and analyzed on ImageJ. All experiments were done in triplicate. To further validate the receptor target, immunohistochemistry of tumor and paired normal NSCLC tissues was performed on a human and canine tissue microarray.

Results: Based on protein densitometric analysis, c-Met was significantly overexpressed in human NSCLC cells compared to normal cells ($p < 0.005$) with a fold-change of at least 4. In canine lung cancer cells, c-Met was expressed at similar levels to A549, where there was no significant difference between the canine cell lines and A549 ($p = 0.1028$). Microscopy confirmed overexpression in human and canine lung cancer cells and showed c-Met localization in the membrane and cytoplasm. Relative to normal tissue, c-Met has a higher expression in lung tumor tissue ($p < 0.005$) and this observation was conserved between the two species.

Discussion: These results depict that c-Met may be an optimal imaging target for NSCLC due to the overexpression and distribution of c-Met receptors in tumor tissue compared to normal tissue. Future aims of this study consist of utilizing the c-Met receptor as a target for a novel tumor-specific imaging probe and to evaluate it in vitro and in vivo models of NSCLC.

The resistance of triple-negative breast cancer to anti-PD1 treatment is a result of changes in biochemical signalling of tumor cells in response to the treatment and the intrinsic heterogeneity of different tumor cells

Quan Quach¹, Owen Hovey¹, Shanshan Zhong¹, Tomonori Kaneko¹, Shawn Li¹

¹Department of Biochemistry, Western University

Introduction: Immune cells play an important role in recognizing and eliminating invading pathogens, dying cells, and cancer cells. To prevent damages caused by excessive immune response, ligand-receptor pairs called immune checkpoints are naturally expressed on antigen-presenting cells and cytotoxic cells, particularly cytotoxic T lymphocytes (CTLs), after activation. An example of these immune checkpoint receptors and ligands is PD-1 and PD-L1. Tumor cells often upregulate PD-L1 to engage with PD-1 on CTLs and suppress their cytotoxic functions. Immune checkpoint inhibitors (ICIs) were developed to disrupt the interaction between immune checkpoint receptors and ligands, thereby reactivating CTLs to eliminate cancerous cells. However, ICIs did not demonstrate great results in clinical trials with triple-negative breast cancer (TNBC) patients because of both acquired and intrinsic resistance. This study aims to unfold the underlying mechanisms of both acquired and intrinsic resistance to anti-PD1 treatment in TNBC. I hypothesize that the differences in proteome and phosphoproteome of TNBC cells demonstrating different sensitivity to anti-PD1 treatment will reveal proteins or kinases responsible for their resistant status.

Methods: To understand the mechanisms of resistance to anti-PD1 treatment in TNBC, we used three TNBC cell lines, 4T1, 4T1-DR3 (DR3), and EMT6, as our main research model. EMT6 was shown to be more sensitive to anti-PD1 treatment than 4T1, while DR3 has been developed from 4T1 to be more resistant to the treatment. The proteomics and phosphoproteomics of these cell lines were analyzed thoroughly to determine the differentially expressed and activated proteins or kinases that are likely responsible for their different sensitivity to anti-PD1 treatment. Syngeneic mouse model will also be used to validate the role of the identified protein targets and deepen our knowledge about the interaction between tumor cells and stromal cells.

Results: Proteomic and kinase-substrate enrichment analysis revealed that compared to 4T1, the more resistant cell line DR3 showed a statistically significant increase in IGF1R expression and activity, which led to the activation of PI3K-AKT-mTOR pathway and the increased exocytosis of GLUT4 for glucose uptake. However, IGF1R expression in EMT6 was not significantly lower than that of 4T1. PI3K-AKT-mTOR pathway was also upregulated in EMT6, which contradicted the role of IGF1R in promoting resistance to anti-PD1. Further proteomic and gene set enrichment analysis unveiled that compared to 4T1 and DR3, EMT6 had a higher expression level of proteins involved in antigen presentation such as TAP1/2, ERp57, and B2m, and a more significant response to IFN- γ and IFN- α , indicating that EMT6 was more immunogenic and sensitive to immune cell killing. The difference in mechanism of acquired (DR3 versus 4T1) and intrinsic (4T1 versus EMT6) resistance to anti-PD1 highlights the dynamic change of tumor biochemical signalling overtime and the intrinsic characteristics of tumor cells.

Conclusions: Compared to 4T1, DR3 is more resistant to anti-PD1 treatment due to the increase in IGF1R, while EMT6 is more sensitive because of its immunogenicity and IFN- γ / α -sensitivity. Targeting IGF1R with inhibitors or improving the immunogenicity and response of tumor cells to cytotoxic molecules secreted by CTLs would potentially alleviate their resistance to anti-PD1 treatment.

Examining the Unfolded Protein Response in Radiation Resistance of Pancreatic Ductal Adenocarcinoma

Ye Shen^{1,2}, Emilie Jaune-Pons^{1,2}, Eugene Wong^{3,4,5}, Christopher Pin^{1,2,5,6}

Departments of ¹Physiology and Pharmacology, ³Physics & Astronomy, ⁴Medical Biophysics, ⁵Oncology, and ⁶Paediatrics, Schulich School of Medicine and Dentistry, University of Western Ontario, ²Verspeeten Family Cancer Center, London, Ontario, Canada

Introduction: Pancreatic ductal adenocarcinoma (PDAC) is one of the deadliest malignancies, with a five-year survival rate of around 12%. Eighty percent of patients undergo chemo and radiation therapy as they are not candidates for curative surgery. Despite advances in these treatment modalities, the prognosis remains poor. Radiation therapy, while offering a potential avenue for local control and down staging, is often limited by the inherently resistant nature of PDAC. One potential mechanism underlying this resistance is the unfolded protein response (UPR) which is highly active in PDAC, driven by the tumor's rapid growth and the nutrient and oxygen-deprived tumor microenvironment. UPR is a cellular signaling pathway that is activated in response to the accumulation of unfolded or misfolded proteins in the endoplasmic reticulum upon cellular stress. This pathway is also associated with cancer progression and therapeutic resistance. Understanding the role of UPR in PDAC may lead to the development of novel strategies to enhance the efficacy of radiation therapy. Therefore, we hypothesize that high levels of UPR signaling pathways promotes radioresistance in PDAC cells.

Methods: Three patient-derived 2D PDAC lines (PDAC021T, PDAC001T, and PDAC013T) were seeded in 12 well plates with 60,000 cells per well. 24 hours post-seeding, cells were irradiated with increasing amounts of radiation (0 - 6 Gy). Cell proliferation, measured as cell number and confluency, was monitored using an IncuCyte system to determine the radioresponse of cell lines. Immunofluorescence of γ -H2AX was performed 24 h and 72 h post-irradiation to assess the extent of DNA damage repair. To evaluate UPR activity, we performed RT-qPCR and western blot on UPR signaling mediators for each cell line 24hr after 4 Gy radiation. We focused mostly on the PERK pathway, examining phosphor (p) eIF2 α , ATF3, ATF4 and CHOP, and also examined BiP/GRP78, which can repress all arms of the UPR.

Results: Cell proliferation analysis revealed distinct radioresponse profiles among the three PDAC cell lines, with PDAC021T displaying radioresistance, PDAC013T showing radiation sensitivity, and PDAC001T exhibiting an intermediate response. We observed increased DNA damage repair in all the cell lines following radiation exposure, as indicated by an elevated number of γ -H2AX foci. Preliminary data on UPR signaling showed high levels of (p) eIF2 α even in untreated cells but no difference in the mRNA or protein levels in PDAC021T and PDAC001T treated with 4 Gy radiation compared to controls. Conversely, PDAC013T showed increased CHOP mRNA expression after radiation consistent with increased apoptosis.

Discussion: Our data shows diversity in the radioresponse of cell lines, reflecting an inherent heterogeneity between PDAC patients. To assess the impact of radiation therapy-induced DNA damage, we will quantify γ -H2AX foci under each condition, which will provide insights into the DNA repair capacity of cancer cells. To further elucidate the mechanisms underlying radioresistance in specific cell lines, future experiments will modify UPR activation by combining UPR inhibitors with radiation and translating this work to 3D cultures. Understanding the role of UPR will be crucial for developing targeted strategies to overcome radiation resistance and improve treatment outcomes in PDAC.

#76 – Mahsa Rahimi - WITHDRAWN

Netrin signaling supports spheroid dormancy and metastatic spread in HGSOc

Komila Zakirova^{1,2,3}, James MacDonald^{1,2,3}, Daniel Passos^{1,2,3}, and Frederick Dick^{1,2,3}

¹Department of Pathology and Laboratory Medicine, Western University

²London Regional Cancer Program, London, Ontario, Canada

³Children's Health Research Institute

Introduction: Metastasis in high-grade serous ovarian cancer (HGSOc) is confined to the peritoneal cavity, where cancer cells form multicellular clumps known as spheroids. Spheroids enter dormancy by stopping growth and can go undetected during surgical debulking and persist after chemotherapy. Spheroids are the primary source of residual disease relapse in patients with HGSOc. We identified Netrin signaling as crucial for dormant spheroid survival. Netrins are a family of secreted molecules that guide nervous system development. Although previously linked to various cancers, their role in HGSOc pathobiology remains unexplored.

Methods: We showed that overexpression of Netrin-1 or -3 ligands enhanced spheroid formation *in vitro*. Xenograft experiments in mice revealed that overexpressing Netrin-1 and -3 leads to increased metastatic dissemination *in vivo*. In contrast, inhibition of Netrin signaling through genetic deletion of UNC5 receptors showed significantly prolonged disease-free survival in xenografted mice compared to the control group.

Results: MEK and ERK emerged as downstream targets of Netrin-mediated cell survival in dormant conditions. The viability of HGSOc dormant spheroids was greatly compromised by MEK inhibitors. Similarly, knockout of UNC5 family of receptors blocked ERK activation and inhibited Netrin-mediated survival of spheroids. These results indicate that Netrins signal through UNC5 receptors to activate ERK to support dormant cell survival. Moreover, treatment of xenografted mice with the MEK inhibitor Trametinib resulted in reduced metastasis and significantly fewer spheroids recovered from the peritoneum compared to the vehicle-treated group.

Significance: Understanding spheroid dormancy is key to preventing ovarian cancer recurrence. Our findings indicate Netrin signaling has a central role in metastatic dissemination of dormant HGSOc spheroids and is a promising target for the development of more effective treatment strategies for patients.

Influence of breast cancer-derived extracellular vesicles on lung metastasis

Urvi Patel¹, Braeden Medeiros¹, Austyn Roseborough¹, David Goodale³ and Alison L. Allan^{1,2,3,4}

Department of ¹Anatomy and Cell Biology and ²Oncology, Schulich School of Medicine and Dentistry, Western University; ³London Regional Cancer Program, London Health Sciences Centre; and ⁴London Health Sciences Centre Research Institute, London ON, Canada.

Introduction: Breast cancer is a prominent cause of cancer diagnosis and death in women worldwide. The triple negative (TN) subtype has the poorest prognosis due to its lack of receptor expression and limited treatment options. It is highly aggressive and metastatic in nature, with an increased tendency to metastasize to the lung. Previous studies in our lab have demonstrated that extracellular vesicles (EVs) from the primary breast tumour can help to establish a pre-metastatic niche at the lung. These EVs can deliver cargo to the lung to induce changes that facilitate metastasis such as remodelling of the extracellular matrix and altering soluble components of the lung microenvironment. There is also evidence suggesting that tumor-derived EVs can influence metastatic processes such as angiogenesis (the formation of vasculature) to support tumor growth and dissemination by regulating proliferation and migration of endothelial cells at the primary site and distant secondary sites. Therefore, we hypothesized that TN breast cancer-derived EVs contain cargo that induce molecular and functional changes in the lung microenvironment, and that therapeutic inhibition of EV production/release reduces metastatic properties in TN cells.

Methods: Breast cancer-derived EVs were isolated using ultracentrifugation and size exclusion chromatography from different breast cancer models, including non-malignant breast epithelial cells (MCF10A) and TN breast cancer cells (SUM159, MDA-MB-231, 231-LM2, 231-BoM). Breast cancer-derived EVs were validated using immunoblotting for EV markers, nanoflow cytometry and electron microscopy. To inhibit EV production/release, TN (SUM159, MDA-MB-231, 231-LM2) cells were treated with tipifarnib or vehicle control and assessed using *in vitro* and *in vivo* assays of metastasis.

Results: An initial comparison between EV isolation methods showed that ultracentrifugation yielded higher recovery of EVs than size exclusion chromatography. Breast cancer-derived EVs were positive for the EV markers CD9, CD63, and TSG101 and negative for non-EV controls including TGF β 1 and β -tubulin. We observed variability in EV release between cell lines, with MCF10A and SUM159 cells demonstrating the lowest EV yield with reduced EV marker expression and relative abundance of particles. Treatment of TN breast cancer cells with tipifarnib resulted in an inhibition of EV release *in vitro* and reduced lung metastasis *in vivo* relative to vehicle control. Ongoing work is focused on assessing the influence of tipifarnib on specific metastatic behaviours including proliferation, migration and invasion.

Conclusions: The variability in EV number demonstrates the heterogeneity between breast cancer cells isolated from different patients and highlights the importance of exploring multiple cell line models for EV studies. This study uses multiple cell lines to determine the role of breast cancer-derived EVs in forming the lung pre-metastatic niche. By understanding the factors mediating lung metastasis, a foundation can be constructed for the development of new biomarkers and/or therapies. Moreover, this work explores the inhibition of production/release of EVs from the primary breast tumor to determine whether that can hinder pre-metastatic niche formation and delay metastasis. The fundamentals discovered through this study may ultimately lead to opportunities to improve TN patient outcomes.

Elucidating the target space of CK2 inhibitors CX-4945 and SGC-CK2-1 using thermal proteome profile-PISA in combination with label-free DIA

Daniel Menyhart¹, Owen F. J. Hovey¹, Tyler T. Cooper¹, Laszlo Gyenis¹, Gilles A. Lajoie¹, David W. Litchfield^{1,2}

¹Department of Biochemistry, Schulich School of Medicine & Dentistry, Western University, London, ON, Canada

²Department of Oncology, Schulich School of Medicine & Dentistry, Western University, London, ON, Canada

Introduction: In malignant cells, signalling networks are often perturbed in a manner that is advantageous to growth. Protein kinase CK2 is a constitutively active kinase with a role in the modulation of numerous cellular processes. Due to its roles in proliferative signalling and the negative regulation of apoptosis, CK2 is considered a pro-survival kinase. Consequently, CK2 is upregulated in a wide variety of cancers wherein its expression is predictive of poor prognosis. Given that kinases are key nodes within signalling networks, targeted inhibition of kinases is promising for the treatment of malignancy. Several CK2-directed inhibitors have been developed for targeted therapy and for use as chemical probes in research settings. However, target-space deconvolution of CK2 inhibitors is typically limited to one (incomplete) protein family in kinome-wide assays. Furthermore, the off-target space of inhibitors in cells is poorly recapitulated using *in vitro* assays. There is a need to further screen CK2 compounds *in situ* to determine their selectivity. Here we use a TPP-PISA (Thermal Proteome Profiling-Proteome Integral Solubility Alteration) approach in cells of diverse lineage to deconvolute the full target space of CX-4945, a CK2 inhibitor in clinical trials, and SGC-CK2-1, a highly selective chemical probe for CK2. We examined the performance of this approach by also utilizing U2OS (osteosarcoma) cells engineered to express a variant of CK2 that is resistant to both inhibitors.

Methods: U2OS cells were previously engineered to stably express wild-type (WT) or inhibitor-resistant (V66A/H160D/I174A) CSNK2A1 under the control of tetracycline. U2OS cells were induced for exogenous CK2 expression for 48 hours. Cells were then treated with either CX-4945, SGC-CK2-1, or DMSO (vehicle) at ~80-90% confluency for 30 minutes prior to harvest. Samples were then split into equivalent volumes and heated at 50, 53 and 56°C for 4 minutes using a thermocycler. Split samples were consolidated back into one. To remove insoluble proteins, centrifugation was performed for 30 minutes at 20,000xG. Samples were reduced and alkylated, prior to being prepared by protein aggregation protocol. Following sequential digestion using Lys-C and Trypsin, and desalting, samples were analyzed using liquid chromatography-mass spectrometry by gas-phase fractionation and data-independent acquisition. Results were analyzed using DIA-NN and R.

Results: In traditional TPP, several points along the melting curve must be measured to find shifts in melting temperature induced by small-molecule binding. In the PISA variation, a small number of temperatures are chosen close to the melting point of the majority of the proteome. The difference in area under this melting curve was determined to well approximate the shift in melting temperature of TPP while also increasing the assay throughput. Here we apply this established method to CK2 inhibitors. Preliminary results of this study are being collected.

Conclusions: We are still collecting data and it is too early to come to definitive conclusions. By elucidating the target space of CX-4945, the mechanism of action of this clinical inhibitor can be better understood. Understanding the target space of SGC-CK2-1 will inform researchers of confounding effects in other protein families.

Characterization of histone deacetylase inhibitor (HDACi) activity on ovarian clear cell carcinoma (OCCC) cell line spheroids

Sylvia Cheng⁴, Bart Kolendowski^{1,2}, Yudith R. Valdes^{1,2}, Trevor G. Shepherd^{1,2,3,5,6}, Gabriel E. DiMattia^{1,2,4,6}

¹*The Mary & John Knight Translational Ovarian Cancer Research Unit, Verspeeten Family Cancer Centre, London Ontario Canada;* ²*LHSC Research Institute, London Health Sciences Centre, London, Ontario, Canada;* ³*Departments of* ³*Anatomy and Cell Biology,* ⁴*Biochemistry,* ⁵*Obstetrics & Gynaecology, and* ⁶*Oncology, Schulich School of Medicine and Dentistry, Western University, London, Ontario, Canada*

Introduction: OCCC is a rare histotype of epithelial ovarian cancer (EOC) with poorer prognosis compared to other EOC histotypes due to resistance to first-line chemotherapeutics, Carboplatin and Paclitaxel. Chemoresistance is due to a unique molecular and genetic profile, as well as intra-peritoneal metastasis through the formation of multicellular cancer aggregates, named spheroids, which attach to peritoneal surfaces to form secondary lesions. Therefore, finding effective therapeutics for OCCC spheroids that target the molecular characteristics of this subtype is key to improving patient outcome. There is interest in targeting the OCCC epigenome as ~50% of OCCC lesions carry truncating mutations in AT-rich interaction domain containing protein 1A (ARID1A). ARID1A loss is associated with changes to global H3K27Ac distribution and histone deacetylase (HDAC) activity, contributing to cancer progression. As such, HDACi's are being investigated for ARID1A-mutant cancers. We aim to determine how HDACi disturbs the OCCC spheroid epigenome and how these changes alter spheroid formation and viability to determine the potential of HDACi's as targeted therapy for OCCC.

Methods: Non-adherent, ultra-low attachment (ULA) plates allowed OCCC cell lines to autonomously form multicellular aggregates, or 3D avascular tumourspheres, that better recapitulate patient tumour morphology relative to traditional 2D culture. Human OCCC cell lines cultured in ULA were treated with HDACi's Entinostat (ENT) and ACY1215 (ACY) and subject to spheroid reattachment, IC50 determination, trypan blue cell counting, and whole cell and acid-extracted nuclear histone lysate collection.

Results: Both ENT and ACY treatment increased H3K27Ac levels in both adherent and spheroid OCCC cells in all cell lines tested. The IC50 of ENT was lower than ACY in both KOC-7c and 105C OCCC cell lines, determined using both bulk cell viability and colony forming abilities. KOC-7c spheroids were sensitive to both inhibitors and had a dose-dependent reduction in spheroid cell viability. 105C spheroids displayed increased cell viability and live cell counts when treated with low micromolar concentrations of ENT and ACY due to a short-term protection from detachment-associated apoptosis.

Conclusions: These findings suggest that HDACi's can alter the epigenome of OCCC cell line spheroids, but OCCC spheroids display varying response to HDACi based on their spheroid characteristics.

Understanding How Hypoxia Alters the Breast Cancer Proteome in the Context of Molecular Subtype and Metastatic Organotropism

David Susman¹, Daniel Menyhart², Laszlo Gyenis², David Litchfield², Alison Allan^{1,3,4,5}

Department of ¹Anatomy & Cell Biology, ²Biochemistry and ³Oncology, Western University; ⁴London Regional Cancer Program, London Health Sciences Centre; and ⁵Lawson Health Research Institute, London ON, Canada.

Introduction: Breast cancer is the leading cause of cancer and the second highest cause of cancer mortalities in Canadian women. There are four molecular subtypes categorized by receptor expression which include Luminal A (ER+ PR± HER2-), Luminal B (ER+ PR± HER2±), HER2-positive (ER-PR- HER2+), and Triple-negative (TN). When breast cancers metastasize or spread from their original site, they become harder to treat. These metastatic cancers account for 90% of breast cancer mortalities. The “seed and soil” hypothesis, proposed by Stephen Paget, predicts that a cancer cell (seed) will only spread to an organ (soil) that promotes its growth. Previous work shows that hypoxic growth conditions increase breast cancer aggressiveness and metastatic potential, in part through stimulating the release of breast cancer-derived extracellular vesicles (EVs). These EVs contain molecular cargo such as proteins and nucleic acids that can modify tissues to create a pro-metastatic environment called a premetastatic niche (PMN). However, few studies have investigated the hypoxic breast cancer proteome in the context of differences between molecular subtypes or metastatic organotropism.

Hypothesis: Hypoxia uniquely modifies the proteomes of different types of breast cancer in a manner that contributes to subtype aggressiveness and metastatic potential.

Methods: MCF10A (breast epithelia), SUM159 (TN), MDA-MB-231 (lung metastasizing TN), MDA-MB-231 LM2 (lung metastasizing TN), MDA-MB-231 BoM (bone metastasizing TN), and MCF7 (Luminal A) cells were exposed to both normoxic and hypoxic conditions for 48h. Proteomic analyses were completed using a Tandem Mass Tagging (TMT) mass spectrometry approach.

Results: GSEA analysis determined enrichment of 23 biological hallmarks upregulated in hypoxic proteomes across 5 different cell lines that contribute to cancer survival and metastasis. KEGG and GO Biological Process analyses revealed variations in hypoxic responses in MCF10A relative to TN breast cancers, and MCF7 relative to SUM159 cancers that contribute to subtype-associated aggressiveness. Further, STRING analysis revealed enrichment of hypoxic proteins that contribute to EV formation. Integrins $\alpha 2$, $\alpha 3$, and $\beta 1$ were also preferentially upregulated under hypoxic conditions and may contribute to EV-associated bone tropism. In total, 8 hypoxia-enriched clinically significant proteins (P4HA1, P4HA2, ERG1, TRXR1, TSP1, MPRI, MCP, SPSY) were identified only in TN breast cancers that may serve as potential therapeutic targets.

Conclusions: Formation of hypoxic tumors is a natural progression of cancer expansion. Here we show that hypoxia stimulates increased subtype-specific and organotropic aggressiveness in breast cancer and activates mechanisms that promote cancer survival and metastatic behavior. Additionally, our data suggests that under hypoxic conditions EVs likely play an important role in these processes. Our identification of hypoxia-specific therapeutic targets may permit the development of treatments in the future that can limit TN aggressiveness conferred by the hypoxic tumor microenvironment.

Assessing the impact of microbiome modulation on immunotherapy response in melanoma

Authors: Kelly J Baines¹, Rene Figueredo², John Lenehan^{2,4}, Saman Maleki Vareki^{1,2,3,4}

Affiliations: ¹ Department of Pathology and Laboratory Medicine, Western University, ² Department of Oncology, Western University, ³ Department of Medical Biophysics Western University, ⁴ Verspeeten Family Cancer Centre, Lawson Health Research Institute

Introduction: In 2022, melanoma was projected to account for approximately 9,000 new cancer diagnoses in Canadians and roughly 1,200 deaths, with disproportionately higher mortality in males than in females. Contributing to patient demise is the fact that nearly 50% of advanced melanoma patients receiving anti-programmed death-1 (anti-PD-1) immunotherapies experience therapeutic resistance. Profiling of gut microbiome composition has linked specific gut bacteria with improved response to immune checkpoint inhibitors (e.g., anti-PD-1), however it remains undetermined if specific bacteria play a prominent role in the determination of PD-1 response.

Methods: To further our understanding of the importance of the microbiome and how it interacts with the host's immune response during cancer therapeutic interventions, we have collected stool samples from healthy donors and patients with advanced melanoma (stage III/IV). Samples were collected from responder patients that have received anti-PD1 alone or in combination with anti-cytotoxic T-lymphocyte-associated protein 4 (CTLA4) and have demonstrated a durable radiographic response (partial or complete response according to RECIST 1.1 criteria) for at least six months or two consecutive imaging assessments (responders). To determine if FMT from healthy donors or anti-PD-1 responders is superior in sensitizing resistant tumors to anti-PD-1 therapy, the microbiomes of 20 healthy donors (10 male and 10 female) and 20 responder patient donors (10 male and 10 female) will be engrafted into 50 avator mice, each. Two weeks after FMT, stool will be collected from mice for 16s rRNA and metagenomics analysis. Following FMT, these animals will be inoculated with B16F10 melanoma cells and subsequently administered anti-PD-1 treatment. Tumor growth will be measured daily, and at endpoint the tumor microenvironment will be compared across microbiome sources via flow cytometry analysis of isolated tumor infiltrating lymphocytes.

Conclusions: With the results from this study, we will be able to determine the immunomodulatory properties of each microbiome source on the immune profile within melanoma tumors and their response to immunotherapy, as well as the impact of donor sex on microbial engraftment.

The role of 5-lipoxygenase expressing immune cells in colitis-associated colorectal cancer

Pallister M^{1,2}, Mani Murugan VM^{1,3}, Zhang L¹, Derouet MF¹, and Asfaha S¹

¹Department of Medicine, Schulich School of Medicine & Dentistry, Western University, Canada,

²Department of Physiology and Pharmacology, Schulich School of Medicine & Dentistry, Western University, Canada, ³Department of Pathology and Laboratory Medicine, Schulich School of Medicine & Dentistry, Western University, Canada

Introduction: Colorectal cancer (CRC) is the fourth most common cancer diagnosis in Canada, accounting for 11% of cancer-deaths in 2023. Individuals suffering from inflammatory bowel disease (IBD) have a 20% higher risk of developing CRC. During IBD, colonic immune cells recruit peripheral myeloid cells to the inflamed colon, promoting inflammation and disease progression. Previously, our lab has identified a subset of bone-marrow derived macrophages which can give rise to colitis-associated CRC (CAC) by inducing stemness in colonic epithelial cells. To further study the role of myeloid cells in CAC, we generated the 5LOeGFP-DTR-CreERT2 mouse model. 5-lipoxygenase (5LO) is a proinflammatory enzyme involved in producing chemotactic leukotrienes, which is expressed by macrophages, neutrophils, and monocytes. In our mice, transgene-expressing cells are identified by GFP expression while the diphtheria toxin receptor (DTR) allows for the conditional ablation of 5LO+ cells using diphtheria toxin (DT). With the 5LOeGFP-DTR-CreERT2 model, we plan to test if **5LO-expressing immune cells increase colitis severity and CAC tumor development through increased myeloid cell infiltration.**

Methods: The 5LO transgene is also expressed by intestinal and cardiac cells in our model, requiring bone marrow transplant (BMT) from 5LOeGFP-DTR-CreERT2 donors into pre-irradiated C57Bl/6J recipients. **For colitis experiments,** BMT mice are administered 2.5% DSS in drinking water to induce colitis. Mice receive DT (1000 ng i.p) or vehicle every 72h starting one day before DSS. Colonic tissues are harvested during peak inflammation for analysis by H&E staining and the myeloperoxidase (MPO) assay to assess disease severity. Fluorescent microscopy and flow cytometry are also performed to assess colonic immune cell infiltration. **For CAC initiation experiments,** BMT mice are administered a single dose of AOM (10 mg/kg i.p) followed by 2.5% DSS to induce CAC. To target tumor initiation, mice receive DT (1000 ng i.p) or vehicle once a week for 5 weeks post-DSS. Colonic tissue is harvested at the experimental endpoint to assess tumor burden, crypt dysplasia, and immune cell infiltration as previously described. **For CAC progression experiments,** AOM/DSS BMT mice receive DT (1000 ng i.p) or vehicle once a week from weeks 6 to 10 post-DSS to target the transition from adenoma to carcinoma. Analysis of colonic tissue is identical to CAC initiation experiments.

Results: We expect DT ablation of 5LO+ immune cells during DSS-induced colitis to prevent loss of crypt architecture and reduce MPO activity (inflammation) by decreasing colonic myeloid cell infiltration. Similarly, we anticipate that 5LO+ immune cell ablation during CAC initiation and progression will reduce tumor burden (size and number) and crypt dysplasia.

Conclusion: Uncovering cellular mechanisms contributing to CAC is critical for the development of cancer treatments. With this project, we hope to improve our understanding of how inflammation predisposes cancer and to potentially identify novel therapeutic targets against CAC.

Hiding in plain sight: Suppression of IL-18 proinflammatory signaling by human papillomavirus E7 in head and neck cancer.

Andris M. Evans¹, Wyatt Anderson¹, Joe S. Mymryk^{1,2,3}.

Department of Microbiology and Immunology¹, Otolaryngology², Oncology³, Western University, Canada

Introduction: The incidence of human papillomavirus-positive (HPV+) head and neck squamous cell carcinoma (HNSCC) is rapidly increasing, such that the incidence of men with HPV+ HNSCC has surpassed that of women with cervical cancer. Despite generally favourable treatment outcomes for HPV+ compared to HPV-negative HNSCC, roughly 30% of patients still succumb to the disease. Additionally, many survivors experience lifelong treatment-related sequelae. Improved understanding of the effects of HPV in HNSCC is required for the development of effective therapies with fewer adverse consequences. HPV+ HNSCCs retain expression of the E6 and E7 viral oncoproteins, which are critical for tumour growth, survival, and avoidance of the immune system. To aid in viral immune evasion, E7 can disrupt the methylation of several host gene promoters that interfere with HPV infection. One potential target of E7 is IL-18, a pro-inflammatory cytokine with a critically important role in epithelial barrier function. IL-18 activity is antagonized by the soluble IL-18 binding protein (IL-18BP).

Methods and Results: Our analysis of RNA-sequencing data from the HNSCC cohort of The Cancer Genome Atlas shows increased *IL18BP* and reduced *IL18* mRNA levels in HPV+ HNSCC compared to HPV- HNSCC and normal adjacent tissues. This suggests a concerted antagonism of the IL-18 pathway by E7. Higher levels of methylation also exist at CpG sites in the *IL18* promoter in HPV+ HNSCC. These observations indicate a possible mechanism for transcriptional repression of *IL18* in HPV+ HNSCC. Luciferase reporter assays demonstrate that HPV16 E7 expression alone can repress IL-18 transcription *in vitro*. Using a panel of point mutants for HPV16 E7, we have identified specific surface-exposed amino acid residues that appear necessary for IL-18 repression. Although HPV16 accounts for approximately 80% of HPV+ HNSCC, we also tested this activity in other oncogenic and non oncogenic HPV types. Our analysis identifies that this repression of IL-18 transcription is generally conserved across E7 from most HPVs, but not all.

Discussion: Future experiments will further investigate the mechanism by which IL-18 is repressed by E7 in the context of HPV+ HNSCC. As E7 is consistently retained in HPV+ HNSCC, this novel viral immune evasion mechanism may also impact the immune response within HPV+ HNSCC tumours. This insight provides valuable information for the development of future therapies for targeted reactivation of the immune response to HPV+ HNSCC.

Dynamic epigenetic changes in human ovarian clear cell cancer spheroid formation and viability.

Kolendowski, B^{1,2}, Ramos Valdes Y^{1,2}, Peck, M³, Pin C⁷, Shepherd TG^{1,2,4,5,6}, DiMattia GE^{1,2,3,4}

¹ Mary & John Knight Translational Ovarian Cancer Research Unit, London Regional Cancer Program, London, ON N6A 5W9, Canada; ² LHSC Research Institute, London, ON, Canada; ³ Department of Biochemistry, Western University; ⁴ Department of Oncology, Western University; ⁵ Department of Anatomy & Cell Biology, Western University; ⁶ Department of Obstetrics & Gynaecology, Western University; ⁷ Department of Physiology and Pharmacology, Western University

Introduction: Acceleration of ovarian cancer disease severity occurs when cancer cells dissociate from the primary tumor and disperse through fluid in the peritoneal cavity, adhere to other peritoneal surfaces, and form metastatic lesions. Cancer cells that are shed from the primary tumor can aggregate into 3-dimensional “spheroids”, which enhance cancer cell viability by avoiding anoikis. We hypothesize that spheroid formation is concomitant with rapid epigenetic changes which control gene transcription critical for survival. Delineating specific epigenetic modifications that occur during spheroid formation correlated with changes in transcription will reveal epigenetic mechanisms critical to OCCC metastasis and potentially identify therapeutic targets.

Methods: We used acid-extraction of histones from isolated nuclei from both monolayer and spheroid cultures of 12 human OCCC cell lines. Histone marks associated with transcriptional activation and repression were interrogated using western blot (H3K4me1/2/3 and H3K27Ac/me3). ChIP-Seq using an antibody targeting H3K27Ac (with a drosophila spike-in normalization strategy), in conjunction with RNA-Seq and an assay probing the global genomic DNA methylation landscape was performed on 105C and KOC-7C cell lines. These cell lines demonstrate similar monolayer proliferation rates but drastically divergent proliferation rates when maintained as spheroids. ATAC-Seq analysis will further characterize genome-wide dynamics.

Results: Many of the OCCC cell lines we surveyed show a decrease in H3K27Ac when maintained as 3-day spheroids. ChIP-Seq analyses using H3K27Ac antibody revealed that when placed in suspension the 105C cell line undergoes both a global loss of H3K27Ac and a redistribution of the mark, relative to the KOC-7C cell line. Using a paired RNA-Seq experiment along with GSEA analysis we observed that changes in H3K27Ac are concomitant with changes in the transcription of genes driving pathways that are differentially regulated between the two cell lines when maintained as spheroids. Importantly, these pathways are critical to modulating cell division and proliferation and can explain differences in proliferation rates of suspension cultures of KOC-7C and 105C cell lines. By comparing the core enrichment genes involved in the differential regulation of these pathways to our H3K27Ac ChIP-Seq data we find that adjacent H3K27Ac is dysregulated at these gene loci. Analysis of the DNA methylation status (both global and at these sites) is currently ongoing and will provide further insight into the importance of epigenetics in regulating these pathways and by extension the differences in phenotype observed.

Conclusions: By surveying the response of 12 cell lines maintained as spheroids we have identified H3K27Ac changes that occur in many of these cell lines. ChIP-Seq in conjunction with RNA-Seq revealed pathways that are differentially regulated when OCCC cell lines and are likely responsible for the differences in proliferation observed between the cell lines. H3K27Ac dysregulation at core enrichment genes was also observed. Further investigations delineating the impact of H3K27Ac disruption revealed differential impact on the lines. Additional investigation into the global DNA methylation and chromatin accessibility landscape are ongoing and may provide a potential therapeutic target in a particular subset of OCCC.

Unraveling the Mechanisms Behind ATRX-Driven Astrocytoma Formation

Kasha Y. Mansour^{1,2,4}, Yan Jiang^{2,4}, Ying Xia⁵, John A. Ronald⁵, Qi Zhang⁶ and Nathalie G. Bérubé^{1,2,3,4}

¹Department of Anatomy and Cell Biology, Western University, London ON, Canada; ²Pediatrics and ³Oncology, Western University, London ON, Canada; ⁴Division of Genetics and Development, Children's Health Research Institute, London ON, Canada; ⁵Robarts Research Institute, Western University, London ON, Canada; ⁶Department of Pathology and Laboratory Medicine, Western University, London ON, Canada.

Background: Astrocytomas are a form of glioma that originate from the astrocytes in the brain or spinal cord. Although the prognosis depends on age and grade of the tumour, the median survival of stage 3 astrocytoma is only 23 months and drops to 12-14 months for stage 4 astrocytoma. In the central nervous system, astrocytes and oligodendrocytes arise from a common precursor cell, whose developmental fate is controlled by the expression of various basic helix-loop-helix factors. Astrocytomas can be distinguished from other gliomas due to the presence of several characteristic mutations in the genes encoding isocitrate dehydrogenase 1 (IDH1) and tumour protein 53 (TP53). Astrocytomas with mutations in these two genes often also carry mutations in the alpha-thalassemia intellectual disability X-linked (ATRX) gene, which encodes a chromatin remodelling protein. We previously reported a mouse model in which ATRX is ablated perinatally in oligodendrocyte progenitor cells (OPCs) and observed that ATRX-null OPCs revert to a more primitive state with the ability to differentiate into astrocytes rather than oligodendrocytes, in vivo and in primary mixed glial cultures. Based on these findings, we hypothesize that OPCs could in some cases be the cell of origin of mutant ATRX/TP53 astrocytomas. We predict that loss of ATRX and TP53 in OPCs will drive astrogenesis and promote tumour-initiating events, leading to the development of astrocytomas in male and female mice.

Methods: We created a genetic mouse model of inducible Cre-dependent ATRX and TP53 ablation, and tdTomato expression (a red fluorescent marker) specifically in Sox10+ OPCs. Survival of double KO mice will be compared to single KO and control mice. Tumours will be dissected, sectioned, and histology will be assessed by H&E and immunohistochemical analysis of astrocyte (GFAP), oligodendrocyte (Olig2) and proliferation (Ki67) markers. Primary mixed glial cultures will also be generated from the brains of neonatal mice of various genotypes. The tdTomato+ (Cre+) cells will be evaluated for proliferation, cell death and for markers of astrocytes and oligodendrocytes using flow cytometry. Fluorescence activated cell sorting will then be used to isolate TdTomato-expressing cells to obtain a pure population of cells for RNA-seq and ATAC-seq to identify changes in the transcriptome and in chromatin accessibility, respectively.

Results: The first cohorts of double KO mice reach end of life starting at 7 months of age up to 15 months. They harbour tdTomato-positive masses in the brain and extending from peripheral nerve sheaths. The brains and the tumours were stained with hematoxylin and eosin, and preliminary immunohistochemistry staining revealed that the masses appear to be GFAP+. Primary mixed glial cultures have also been established and preliminary results will be presented.

Discussion: We have confirmed that the loss of ATRX along with p53 leads to the development of tumours, both in the brain and in the periphery. Preliminary results indicating that the cells may be astrocytic in origin, suggesting that OPCs could be the cell of origin of ATRX/TP53 mutant astrocytomas. This will provide a model system that more closely mimics the disease in patients that can be used to gain insight into the mechanisms governing gliomagenesis.

Investigating Pannexin 1 as a target for glioblastoma multiforme

Rehanna Kanji¹, Danielle Johnston¹, Carlijn Van Kessel¹, Katelyn Hunter¹, Andrew Deweyert¹, Matthew Hebb^{2,3}, and Silvia Penuela^{1,3}.

¹Department of Anatomy and Cell Biology, Schulich School of Medicine and Dentistry. The University of Western Ontario, London, ON, Canada, ²Department of Clinical Neurological Sciences, Schulich School of Medicine and Dentistry. The University of Western Ontario, London, ON, Canada, ³Department of Oncology; Division of Experimental Oncology, Schulich School of Medicine and Dentistry. The University of Western Ontario, ON, Canada.

Introduction: Glioblastoma multiforme (GBM) is the most common malignant brain tumor in the central nervous system (CNS). Despite surgical resection, chemotherapy, and radiation therapy, GBM tumors always recur and the median survival time is only 14 months which highlights the need for new therapeutic interventions. The purpose of this study is to investigate the role of Pannexin 1 (PANX1) in GBM and the effects of its inhibition on tumorigenic properties. PANX1 is a channel forming glycoprotein that allows for the passage of ions and metabolites. Its canonical function is to release ATP at the cell surface which participates in both paracrine and autocrine signaling. We have seen that PANX1 is upregulated in patient derived GBM cells relative to glial cells. Thus, there is strong evidence to suggest an oncogenic role of PANX1 in GBM however, PANX1 function and the effect of its inhibition in GBM is not well understood.

Methods: Patient derived GBM tumor fragments and patient-matched brain were embedded in paraffin and used for immunohistochemical staining of PANX1. Five patient derived GBM cell lines were immunoblotted for PANX1 and GBM17 was chosen as a representative cell line. Probenecid (PBN) and Spironolactone (SPIR) are Health Canada approved drugs that can cross the blood brain barrier and have been repurposed as blockers of PANX1. The blockers were used to determine the effect of PANX1 inhibition on malignant properties of GBM17. PANX1 expression and inhibition was also studied in the rat glioma cell line F98 to determine the potential of F98 cells to be employed for a syngeneic allograft to study PANX1 inhibition.

Results: Preliminary results show that PANX1 expression is diffuse in the tumor microenvironment, with presence observed in regions of high cellularity and vascularization. Immunofluorescence staining of PANX1 in GBM17 reveals an intracellular localization. Live cell imaging revealed that PBN and SPIR reduce GBM17 growth and migration and do not affect PANX1 expression or localization, as expected. PANX1 is also expressed in F98s with an intracellular localization and its growth was significantly reduced with SPIR however not with PBN.

Conclusions: We demonstrate that PANX1 is upregulated in GBM and that its inhibition using pharmacological blockers reduced patient derived GBM cell growth and migration. This provides evidence warranting F98 syngeneic allografts to study the effects of PANX1 inhibition *in-vivo*. Overall, our study warrants further investigation into PANX1 as a potential therapeutic target for GBM.

The role of circHUWE1 in prostate cancer

Danielle Taray-Matheson^{1,4}, Hong Diao⁴, Allison McLoughlin^{1,4}, and Weiping Min¹⁻⁴

¹ Pathology and Laboratory Medicine, Schulich School of Medicine & Dentistry, Western University, Canada, ² Surgery, Schulich School of Medicine & Dentistry, Western University, Canada, ³ Oncology Schulich School of Medicine & Dentistry, Western University, Canada, ⁴ Matthew Mailing Centre, London Health Sciences Centre, Canada

Introduction: Prostate cancer (PCa) is the most common type of cancer and third leading cause of cancer mortality in Canadian men. PCa is typically manageable if detected early; however, some patients develop a more aggressive phenotype that is resistant to current therapeutics, highlighting a need for continued research to develop more effective treatment options. We have previously shown that circular RNA HUWE1 (circHUWE1) is upregulated in highly metastatic PCa cells; however, the specific role circHUWE1 plays in PCa is unknown. We aim to assess the role of circHUWE1 in PCa cell proliferation, migration, and invasion, and elucidate the molecular mechanism by which circHUWE1 may modulate PCa pathogenesis.

Methods: PC3 cells were transfected with circHUWE1 siRNA to perform loss-of-function experiments. Cell proliferation, migration, and invasion were assessed using CCK-8, scratch, and transwell assays, respectively. Expression of epithelial-to-mesenchymal transition (EMT)-related molecules was assessed using qPCR and western blot. Cell death and cell cycle were assessed using flow cytometry. Online binding prediction software were used to determine RNA binding proteins and microRNAs that may potentially interact with circHUWE1. An RNA pull-down assay was conducted to pull-down circHUWE1 complexes. qPCR and western blot will be performed to determine the potential binding partners of circHUWE1. Co-transfections will be conducted to confirm the relationship between circHUWE1 and its target molecules.

Results: Knockdown of circHUWE1 significantly reduced PC3 cell proliferation (Fig. 1A) and migration (Fig. 1B-C) but did not affect cell invasion (Fig 1D). A significant reduction in vimentin protein expression was observed in cells transfected with circHUWE1 siRNA compared to control cells, suggesting circHUWE1 promotes EMT in PC3 cells. Transfection with circHUWE1 siRNA did not affect cell death or cell cycle phase relative to control cells. No changes in HUWE1 expression were seen in cells transfected with circHUWE1 siRNA, indicating circHUWE1 likely exerts its effects through a mechanism other than altering linear gene expression. Knockdown of circHUWE1 significantly reduced MAPK1 and RAC1 mRNA expression, suggesting circHUWE1 may be exerting its effects through these molecules.

Discussion: Understanding the role and mechanism of circHUWE1 in PCa progression may contribute to the development of targeted therapeutics to prevent tumour metastasis and improve outcomes for patients with metastatic disease.

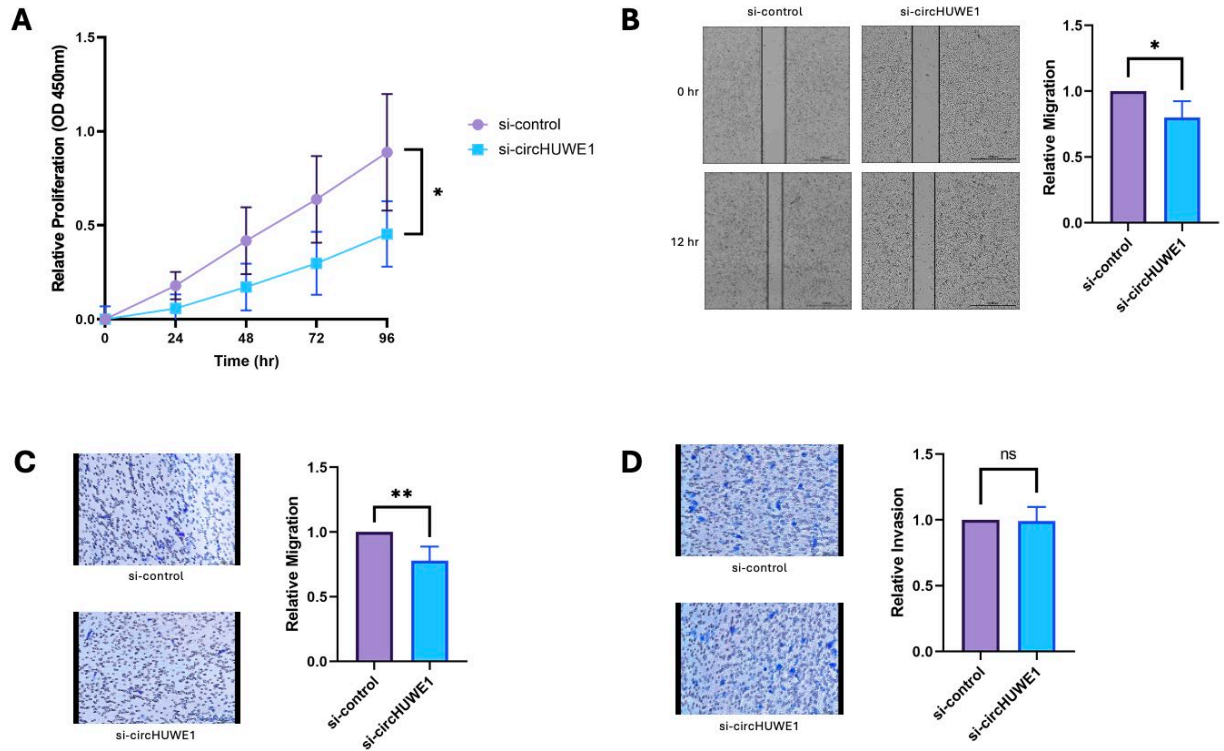


Figure 1. Knockdown of circHUWE1 reduces prostate cancer cell proliferation and migration.

PC3 cells were transfected with control siRNA or circHUWE1 siRNA. A) Proliferation was assessed using a CCK8 assay. Absorbance (OD 450 nm) was measured every 24 hours using a spectrophotometer. B) Migration was assessed using a scratch assay 12 hours post-scratch. Scale bar = 1000 μ m. C) Migration was assessed using a transwell assay. Migrated cells were stained with 0.1% crystal violet and counted after 24 hours. Scale bar = 80 μ m. D) Invasion was assessed using a transwell assay coated with Matrigel. Invaded cells were stained with 0.1% crystal violet and counted after 24 hours. Scale bar = 80 μ m. * p <0.05, ** p <0.01

Preventing Alloimmune Rejection After Heart Transplantation Using Circular RNA ZMIZ1-Engineered Dendritic Cells

Kevin Vytlingam^{1,5}, Serina Chahal^{2,5}, Dr. Weiping Min^{1,3-5}, and Dr. Xiufen Zheng¹⁻⁵

¹ Pathology and Laboratory Medicine, Schulich School of Medicine & Dentistry, Western University, ² Microbiology and Immunology, Schulich School of Medicine & Dentistry, Western University, ³ Surgery, Schulich School of Medicine & Dentistry, Western University, ⁴ Oncology, Schulich School of Medicine & Dentistry, Western University, ⁵ Lawson Health Research Institute, London Health Sciences Centre

Introduction: Alloimmune rejection is a vital concern after organ transplantation. As a result, transplant patients require lifelong immunosuppression, which can lead to toxicity, infections, and cancer. For this reason, new interventions to induce donor antigen-specific immune tolerance are required. Dendritic cells (DCs) play an important role in determining whether a transplanted organ is tolerated. Tolerogenic DCs (Tol-DCs) promote allograft tolerance by preventing T cell activation and stimulating regulatory T cell (Treg) generation. Immunosuppressive agents have been shown to generate Tol-DCs in vitro; however, new molecules to optimize Tol-DC induction should be investigated. Circular RNAs (circRNA) could be an ideal candidate for DC immunomodulation because they have many reported regulatory functions, such as sequestering microRNA and stabilizing protein interactions. Previous microarray data from our lab found an upregulation of circular RNA ZMIZ1 (circZMIZ1) in Tol-DCs. For this reason, we hypothesize that circZMIZ1 is immunosuppressive, and thus, overexpressing circZMIZ1 in DCs will promote a tolerogenic phenotype, conducive to improving allograft tolerance after heart transplantation.

Methods: We will overexpress circZMIZ1 in DCs and assess its effect on DC phenotype based on the expression of co-stimulatory molecules and both pro- or anti-inflammatory cytokines via flow cytometry. We will assess T cell activation and Treg generation using mixed lymphocytic reactions. We will employ a mouse heart transplant model and treat transplant recipient mice with circZMIZ1-engineered DC vaccines prior to heart transplantation. We will monitor graft survival time and examine histopathological features of the graft at endpoint.

Results: We expect to see increased Tol-DCs and immunosuppressive cytokines after circZMIZ1 overexpression in DCs. We also expect to see reduced T cell activation and increased Treg generation, all contributing to increased allograft tolerance. After heart transplantation, we expect to see increased graft survival time and decreased graft injury, inflammatory infiltrate, and fibrosis.

Discussion: Investigating circRNA as a modulator of DC phenotype and immunogenicity could contribute to the development of robust Tol-DC vaccines for preventing alloimmune rejection after organ transplantation.

Drafting the 2023-2028 Strategic Plan for the Western Centre for Translational Cancer Research

Justine Bandola¹, Josh Foster¹, Ivan Ristic¹, Unnati Yagnik¹

The University of Western Ontario¹

Introduction: The Centre for Translational Cancer Research (CTCR) was founded in 2010 and is a collaboration among several leading institutions in London, Ontario. It aims to expedite the transfer of lab discoveries to clinical settings, enhancing cancer research and treatment. The CTCR's approach includes interdisciplinary collaborations and advanced technology to focus on early detection, novel therapies, and improving care across Southwestern Ontario. The strategic planning project involved conducting interviews, analyzing surveys, and facilitating a retreat to shape the CTCR's future strategies. These efforts aim to expand research and partnerships, furthering the CTCR's impact on cancer care.

Methods: To synthesize the strategic plan, we used three approaches. The first was a survey to gather CTCR members' opinions on several key topics such as trainee engagement. The next approach was conducting external stakeholder interviews to receive their opinions on how the CTCR should approach future initiatives. The final approach was a virtual retreat hosted by the CTCR. Our group's role was to analyze the results from all three of the approaches and extract common themes that related to key future priorities. This strategic plan conveys the vision of the CTCR and the initiatives that they can undertake in the future.

Results: We created a strategic plan and identified six strategic outcomes for the CTCR to follow in the next 5 years to help guide with its impact. The six strategic outcomes are leadership and governance, building partnerships, enhancing value and visibility, creating patient-centric research opportunities, supporting translational research groups, and engagement with membership (Fig. 1). For each main outcome we outlined actions that would help achieve them.

Discussion: With this strategic plan we aim to support the CTCR, its members, trainees, patients, and the research community in London. To formulate our strategic plan, we compared our main strategic outcomes to those found in the plans of external organizations such as CIHR, OICR and UHN. Over the last eight months, we have identified that the CTCR is still in its early stages of development. By implementing some of the key initiatives outlined in the strategic plan, it has the potential to establish itself as a larger organization in the future. We believe the strategic plan document helps in this process, benefiting cancer patients in London, Southwestern Ontario, and beyond. Future initiatives include creating digital platforms and public campaigns to extend the CTCR's impact, although developing success metrics remains a challenge. A proposed initiative is building a website to streamline resources and feedback. This project could be challenging due to the vast amount of coordination and time required to complete it, but it promises significant benefits for research connectivity and efficiency.



Figure 1. Western Centre for Translational Cancer Research (CTCR) 2023-2028 strategic plan outline. The new strategic plan identifies 6 strategic goals, which aim to enhance the CTCR’s impact on translational cancer research. Under each strategic goal includes an example of an action time that helps fulfill the goal.

Quantitative phosphoproteomics implicates regulation of protein kinase CK2-dependent phosphorylation by peptidyl-prolyl isomerase Pin1 during mitosis

Scott E. Roffey¹, Kun Ping Lu¹, Xiao Zhen Zhou², and David W. Litchfield^{1,3}

¹Department of Biochemistry, Schulich School of Medicine & Dentistry, Western University, London, Ontario, Canada, N6A 5C1.

²Department of Pathology and Laboratory Medicine, Schulich School of Medicine & Dentistry, Western University, London, Ontario, Canada, N6A 5C1.

³Department of Oncology, Schulich School of Medicine & Dentistry, Western University, London, Ontario, Canada, N6A 5C1.

Introduction: Protein kinase CK2 (CK2, formerly casein kinase 2) is a family of serine/threonine kinases that are involved in many cellular processes and have been implicated in numerous human malignancies. Interestingly, no single mechanism describes how CK2 is regulated, leading CK2 to be labelled a constitutively active kinase. But how can a constitutively active kinase regulate biological processes that require careful control? Previous studies have determined that phosphorylation of specific CK2 substrates can be regulated by extrinsic protein-protein interactions, including those with the peptidyl-prolyl isomerase Pin1, which has been shown to modulate CK2 activity during mitosis and is frequently upregulated in human cancers. However, no systematic studies have been performed to date to further elucidate the role of Pin1 in regulating CK2 activity in this stage of the cell cycle.

Methods: Human cervical adenocarcinoma (HeLa) cells were subjected to stable isotope labelling of amino acids in cell culture (SILAC) labelling with Light (K0, R0), Medium (K4, R6) or Heavy (K8, R10) amino acids. Cells were then synchronized at the G1/S checkpoint with a double-thymidine block, released into the cell cycle for 8 hours, and treated with Taxol for 4 hours to arrest cells in mitosis while being simultaneously treated with 5 μ M Sulfoxon (Medium) or 5 μ M SGC-CK2-1 (Heavy) to inhibit Pin1 or CK2, respectively. Light cells were treated with an equal volume of DMSO. Proteomic and phosphoproteomic analyses were subsequently performed using a Orbitrap Fusion Lumos mass spectrometer. MaxQuant was then used for identification and quantification, followed by downstream analysis and visualization with Perseus and R. Mitotic Pin1-regulated CK2 substrates were identified by comparing differentially regulated phosphosites between Sulfoxon- and SGC-CK2-1-treated cells.

Results: Treatment of mitotic HeLa cells with Sulfoxon (Pin1 inhibitor) or SGC-CK2-1 (CK2 inhibitor) resulted in differential phosphorylation of 237 and 807 phosphosites, respectively. Bioinformatics tools revealed that CK2 and Pin1 participate in numerous biological processes which are essential for cell division. Furthermore, 10 candidate CK2 substrates were identified that may be regulated by Pin1 – including 6 that are preferentially phosphorylated during mitosis.

Discussion: This study explores the intricate signaling changes in response to the phosphorylation-dependent interaction between CK2 and Pin1, providing insight into how a constitutively-active kinase may be regulated during cell division, and what may cause its aberrant signaling that is commonly observed in human cancers.

The effects of EZH2 inhibition on colitis-associated colorectal cancer

G. Leung^{1,2}, F. Larsen^{1,2}, M. Derouet¹, L. Zhang¹, S. Asfaha¹

¹Department of Medicine, Schulich School of Medicine & Dentistry, Western University, Canada

²Department of Pathology and Laboratory Medicine, Schulich School of Medicine & Dentistry, Western University, Canada

Introduction: Colorectal cancer is the second leading cause of cancer death in Canada. Inflammatory bowel disease (IBD) is a major risk factor, leading to colitis-associated colorectal cancer (CAC). We previously generated a CAC model in which quiescent colonic DCLK1+ tuft cells transform into cancer-initiating cells following truncation of the tumor suppressor gene APC and colitis. Epigenetic changes during inflammation are proposed to contribute to transformation. Interestingly, enhancer of zeste homolog 2 (EZH2), a histone methyltransferase involved in epigenetic regulation, is upregulated in colorectal cancer. EZH2 generates repressive H3K27me3 marks, and loss of EZH2 results in re-expression of endogenous retroviruses (ERV), reducing tumor growth. Thus, in this study we aim to test the hypothesis that EZH2 inhibition decreases colitis-associated tumorigenesis by activating a viral mimicry response.

Methods: Two murine models of CAC were used in this study. In the first model, a single dose of AOM (10 mg/kg i.p) followed by 2.5% DSS in drinking water was used to induce CAC. In a second model, *Dclk1^{CreERT2};Apc^{ff};R26TdTom* mice were treated with three doses of tamoxifen (6 mg) followed by 2.5% DSS. To test the effects of pharmacological EZH2 inhibition on CAC, mice treated with AOM/DSS or *Dclk1^{CreERT2};Apc^{ff};R26TdTom* mice were administered five doses of vehicle or the EZH2 inhibitor GSK343 (10 mg/kg i.p) one week following DSS. Tumor burden, tumor H&E histology, western blot for H3K27me3, and RT-qPCR for ERV and interferon gene expression were assessed at experimental endpoints. To assess the effects of EZH2 knockout on CAC, *Dclk1^{CreERT2};Apc^{ff};Ezh2^{ASET/ASET};R26TdTom* mice were treated with tamoxifen (6 mg) followed by 2.5% DSS and analysed as described above. To assess the effects of inhibiting EZH2 on stemness of DCLK1+ cells, colonic organoids from *Dclk1^{CreERT2};Apc^{ff};R26TdTom* mice were treated with 4-OH-tamoxifen and cultured in the presence or absence of the EZH2 inhibitor EPZ-6438, IL1- β , or the combination of IL-1 β and EPZ-6438. Microscopy images were taken to analyze the extent of lineage tracing 2 and 4 days after 4-OH-tamoxifen treatment.

Results: There were no significant differences in the tumor burden of AOM/DSS treated mice administered GSK343 versus vehicle. In *Dclk1^{CreERT2};Apc^{ff};R26TdTom* mice treated with GSK343 and *Dclk1^{CreERT2};Apc^{ff};Ezh2^{ASET/ASET};R26TdTom* mice, we anticipate reduced tumor burden and H3K27me3 levels coinciding with increased expression of ERVs and IFN genes. Finally, *Dclk1^{CreERT2};Apc^{ff};R26TdTom* organoids treated with the combination of EPZ and IL1- β showed less Dclk1+ cell lineage tracing versus organoids treated with IL1- β alone.

Conclusions: While the AOM/DSS mouse model of CAC suggests that EZH2 inhibition may not affect colonic tumor initiation, we plan to validate this observation with a second model of CAC and additional EZH2 histone methyltransferase inhibitors. Our murine colonic organoid experiments suggest that EZH2 inhibition may decrease stemness of DCLK1+ cells.

Title: **Antibody-drug conjugates with SH2 bases payload in combating with breast tumor drug resistance**

Author list: Yan Feng¹, Tomonori Kaneko¹, ShanShan Zhong¹, Owen Hovey¹ and Shawn S.-C. Li¹

¹ Department of Biochemistry, Western University, London, Ontario, Canada

Introduction

Breast cancer is a type of cancer that has the phenotype to over-express human epidermal receptor 2 (HER2), a growth receptor overexpressed in most breast cancers. The traditional chemo treatment will cause an increase in the tolerance of the specific drug. In recent years, antibody-drug conjugates (ADCs) have a growing class as new cancer chemotherapeutics with more specific targets for breast cancer cells. The clinical potential is huge as an increase of approved ADCs by the U.S. Food and Drug Administration (FDA). However, the traditional ADCs still rely on small chemical toxins to treat cancer cells; this still has an issue of increase of drug tolerance. Here, we have replaced the traditional small molecules with a triple-point mutant Src Homology 2 (SH2) domain called 'superbinder', which could bind pY-containing peptides with much stronger affinity. Hence, it can block any growth receptor and lead to cell apoptosis.

Method

The pCDNA3 plasmid containing human IgG antibody FC domain was transfected in HEK-293T cell, and the antibody purification used the protein A column. The SH2 domain was designed to have a free cysteine at the N-terminal. Hence, maleimide containing SMCC linker can react with SH2 through the free cysteine. The other end of the linker is N-hydroxysuccinimide ester, which can react with any amines on amino acid in antibodies. The linked SH2-FC will be purified through size exclusion column. All linked SH2-FC will be tested further by adding a protein green tracker. Where can be transmembrane with the incubation with 4T1 cell, by image under fluorescent microscopy.

Results

SH2 domains have been purified and validated on SDS-PAGE. The antibody FC domain was transfected in HEK 293 cells and purified by the IgA protein column. The SH2 was successfully fully linked to the FC domain by the N-acetyl linker SMCC. The linked SH2-FC was purified by size-exclusion column flowed validation through SDS-PAGE. Those purified SH2-FC have been tested for transcellular efficiency and show that after incubation with the 4T1 cell line for 2h, FC-SH2 can transmembrane.

Conclusion

The new development of SH2 domain-based ADC has shown that it can be an entire of cytoplasmic. This is a big improvement to the traditional small molecule payload. That shows that any protein or peptide can be linked to an antibody for specific targeting of cancer cells. The SH2 domain to inhibit tumour growth has yet to be tested. Since the 'super

binder' has a high affinity for phosphopeptide, it has a good potential to block cell signalling, thereby making it a good candidate for a new ADC.

Identification of rare *DPYD* variants and association with severe 5-fluorouracil toxicity in a patient cohort using whole-exome sequencing

Elizabeth Cui¹, Samantha Medwid², Ute I Schwarz^{1,2}, Richard B Kim^{2,3,4}

¹Department of Physiology and Pharmacology, Western University, London, Canada,

²Department of Medicine, Western University, London, Canada, ³London Health Sciences Centre, London, Canada, ⁴Lawson Health Research Institute, London, Canada

Introduction: 5-fluorouracil (5-FU) is a common chemotherapeutic. However, up to 30% of 5-FU-treated patients experience severe toxicity during treatment. The main enzyme responsible for 5-FU clearance is dihydropyrimidine dehydrogenase (DPD; gene *DPYD*), and single nucleotide variants (SNVs) that impair DPD function reduce 5-FU clearance leading to toxicity. Currently, pre-emptive *DPYD* genetic testing and 5-FU dose-reductions are recommended for 4 well-studied SNVs, however these SNVs exist primarily in Caucasians and account for only a fraction of toxicities.

Objectives: Hundreds of *DPYD* SNVs have been identified, but for the vast majority, particularly rare (minor allelic frequency <1%) and non-Caucasian ethnicity-specific SNVs, effects on DPD activity and 5-FU toxicity have not been investigated.

Methods: To study the association between rare *DPYD* SNVs and 5-FU toxicity, we retrospectively identified SNVs via whole-exome sequencing (WES) in a cohort of 336 cancer patients from the London Regional Cancer Program.

Results: We identified 370 SNVs in *DPYD* including 15 rare SNVs, 10 of which are unique (9 missense, 1 synonymous). Rare SNV carriers made up 8.8% of patients that experienced early severe 5-FU toxicity, and only 3.1% of patients that did not. Patients carrying common SNVs (c.85A>T, c.496A>G, c.1601A>G, c.1627C>T, c.2194C>T; MAF>1%) did not have increased risk of early severe toxicity, whereas carriers of rare SNVs trended to greater toxicity risk than noncarriers (OR = 2.793, CI 0.9424 to 8.097; p=0.0566).

Conclusions: Thus, rare but not common *DPYD* SNVs potentially contribute to toxicity, and more comprehensive screening measures that capture rare and ethnicity-specific SNVs may be necessary to reduce 5-FU toxicity risk.

Keywords: fluoropyrimidines, *DPYD*, toxicity, pharmacogenetics, Next-Generation sequencing

Title: Investigating the Role of Spy1 in Mediating Senescence in Glioblastoma
Stephanie Dinescu¹, Dorota Lubanska², Lisa Porter²

¹University of Windsor, ²St. Joseph's Health Care London, ²Henry Ford Hospital

Introduction: Glioblastoma (GBM) is the most frequent and aggressive primary malignant brain tumour. The heterogeneity of GBM renders it resistant to standard-of-care treatment and contributes to the high rate of tumour recurrence. An emerging area of research in the study of GBM explores cellular senescence, a prolonged state of cell cycle arrest triggered by various stressors. Spy1 is a cyclin-like protein elevated in glioblastoma. Spy1 activates cyclin-dependent kinases (CDKs) and overrides cell-cycle checkpoints, avoiding conditions that would normally cause cell cycle arrest. Spy1 has also been shown to override reprogramming-induced senescence by suppressing critical senescence-inducing CDK inhibitors (CKIs), contributing to increased and uncontrolled cell proliferation. Thus, Spy1 may play a role in GBM tumour formation by helping cancerous cells evade senescence and promoting their re-entry into the cell cycle.

Methods: Using *in vitro* and *ex vivo* systems, this project explores the influence of Spy1 on senescence in GBM and assesses whether Spy1 targeting can enhance the effect of therapies targeting senescent cells, known as senolytics. Endogenous levels of Spy1 in GBM cells induced into senescence were first assessed. Senescent markers were evaluated through staining and quantification of senescent cells, alongside analyzing the transcriptional expression of these markers. Next, Spy1 was knocked down in GBM cell lines and the levels of senescence were compared to the control. These assessments were also replicated in Spy1-knockdown GBM cell lines subjected to Temozolomide (TMZ) the conventional treatment for GBM. Finally, senolytics were administered to these cell lines, and the levels of cell death were compared between the Spy1 knockdown and control conditions.

Results: Spy1 has been shown to be involved in regulating cellular senescence of GBM. We have demonstrated that endogenous levels of Spy1 increase during naturally occurring oxidative-stress induced senescence as well as during therapy-induced senescence with TMZ. Additionally, Spy1 knockdown contributes to increased senescence levels in GBM, whereas Spy1 overexpression shows the opposite effect. GBM cells induced into senescence were also sorted into senescent and non-senescent cell populations. Spy1 gene expression was found to be altered in each of these subsets. Lastly, we found that when senolytic treatment is combined with targeting Spy1 in GBM cells induced into senescence with TMZ, it increases cell death.

Discussion: We have demonstrated that targeting Spy1 leads to an increase in the number of senescent cells, and importantly, these senescent populations can be effectively eliminated using senolytics. Further investigations are needed to determine the optimal timing and duration for administering the TMZ, Spy1-targeting, and senolytic therapies. Future studies should also explore these therapeutic combinations in an *in vivo* setting. Continued research into Spy1 and its involvement in GBM senescence of GBM may open new avenues for the development of personalized treatments aimed at preventing the onset and progression of GBM.

Use of synthetic protein secreting CHO cells for protein purification of Fc3TSR in the treatment of advanced stage ovarian and pancreatic cancer

Aitken. C¹, Garlisi. B², Lauks. S³, and Petrik. J¹
^{1,2,3}University of Guelph, Guelph, ON Canada

Introduction: Ovarian and pancreatic cancer have become two of the most lethal cancers worldwide. Due to the advanced stages at the time of diagnoses, initial treatment usually consists of surgical resection of the primary tumor, and multiple rounds of maximum tolerated dose chemotherapy. Targeted therapies that inhibit signal transduction pathways have been advancing in cancer research to increase systemic therapy options. A major target of interest is angiogenesis, in which the tumor initiates a program that stimulates new blood vessel formation to meet the tumors metabolic needs. To target this pathway, we have developed a fusion protein (Fc3TSR) which is derived from the potent anti-angiogenic factor thrombospondin-1. Fc3TSR has multi modal effects against tumor progression. Fc3TSR has shown promising effects in both pancreatic and ovarian murine models as a single agent, and in combination with chemotherapy and immune checkpoint inhibitors. The proposed mechanisms of this new targeted treatment are its pro-apoptotic activation pathways in tumor cells and normalization of the tumor vasculature, enhancing tumor perfusion. In this project, we seek to expand the use of Fc3TSR through the use of genetically manufactured Chinese Hamster Ovarian (CHO) cells which release the protein into its microenvironment. This project aims to study these cells and their target protein secreting capabilities *in vitro*, and the ability to purify Fc3TSR for scale up experiments *in vivo*.

Methods: We used genetically manufactured CHO cells with an inserted coding sequence for Fc3TSR. These cells were cultured, and serum starved for three days, after which serum free media was collected and ran through the purification process using protein A IgG spin trap columns. 0.88 mg/mL of purified Fc3TSR (F3R) was collected and used for comparison with our original manufactured Fc3TSR in our *in vivo* advanced stage pancreatic and ovarian cancer model. At end point of each model, tumors were collected, and weighed for further analysis.

Results: Fc3TSR was able to induce tumor regression in both ovarian and pancreatic murine models, both displaying significant differences in tumor weights compared to PBS controls ($p < 0.001$). Mice treated with purified F3R displayed even smaller tumor weights compared to PBS and Fc3TSR. Secondary metastatic tumors were also analyzed in both models, and significant differences were observed between the three groups. F3R had significantly decreased the number of metastatic lesions in both models.

Discussion: The preliminary data of purified F3R from the modified cell line indicates a potential increase in potency of Fc3TSR derived from cell secretions, compared to systemic injection of the protein. Possible rationale behind this could be a result of differences in the length or size of F3R released by these cells, increasing both half-life and functional receptor dimerization for downstream signalling. Due to Fc3TSR's multimodal nature, further analysis of this projects applications requires comparing various cellular markers of the tumor such as proliferation, apoptosis, and vessel maturation. If F3R provides an increased therapeutic effect, this opens opportunities for the use of manufactured cells in both the production and in cell therapy applications.

ROLE OF *IKZF3* AS A DRIVER MUTATION IN B CELL ACUTE LYMPHOBLASTIC LEUKEMIA

Heidi Rysan¹, Bruno Rodrigues de Oliveira¹, James Iansavitchous¹, Wei Cen Wang¹, Rodney P. DeKoter¹.

¹Department of Microbiology and Immunology, Schulich School of Medicine & Dentistry, University of Western Ontario, London, Ontario, Canada.

Introduction: B cell acute lymphoblastic leukemia (B-ALL) involves the acquisition of primary and secondary driver mutations that cooperate to promote cancer development. Using the Mb1-Cre Δ PB mouse model, we have shown that deletion of the E26-transformation-specific transcription factors PU.1 and Spi-B leads to the development of B-ALL. Using whole-exome sequencing, we identified secondary mutations in the transcription factor *Ikzf3*. The H195Y *Ikzf3* mutation is located in a zinc finger domain within the DNA binding region. Therefore, we hypothesized that ectopic expression of H195Y would result in altered gene expression, leading to pro-leukemic changes in precursor B cells.

Methodology: To determine the role of H195Y in B-ALL, we used retroviral vectors encoding wild-type and H195Y *Ikzf3* to infect primary pre-leukemic B cells isolated from the bone marrow of Mb1-Cre Δ PB mice. Changes in gene expression were then measured in infected cells by RT-qPCR. To measure interactions between IKZF3 and target gene promoters, luciferase reporter assays were performed by co-transfecting uninfected cells with wild-type or H195Y *Ikzf3* and gene promoters fused to the firefly luciferase gene. Site-directed mutagenesis was then performed to determine if mutating IKZF3 binding sites would affect luciferase activity.

Results: RT-qPCR revealed that cells infected with H195Y had increased expression of target genes such as *Igll1*. Cells transfected with H195Y had increased *Igll1*-driven expression of firefly luciferase, and mutating IKZF3 binding sites significantly reduced this activity.

Conclusions: In cells expressing H195Y, increased *Igll1* expression and *Igll1*-driven expression of firefly luciferase indicate that H195Y IKZF3 transcriptionally activates this gene. Reduced luciferase activity following mutations to IKZF3 binding sites suggests that *Igll1*-driven expression of firefly luciferase is due to direct binding of H195Y IKZF3 to the *Igll1* promoter. These effects were not observed in cells expressing wild-type IKZF3, suggesting that H195Y alters IKZF3 activity.

Funding: This work was supported by the Leukemia & Lymphoma Society of Canada, the Canadian Institutes of Health Research, and the Natural Sciences and Engineering Research Council of Canada.

Thank you to our Silver Sponsors

abbvie



Thank you to our Bronze Sponsors

